Western Graduate&PostdoctoralStudies

Western University
Scholarship@Western

Electronic Thesis and Dissertation Repository

10-5-2017 10:30 AM

# Investigating The Functional Relationships Of RND Efflux Pumps In Methicillin Resistant Staphylococcus Aureus

Jamie N. Halucha
*The University of Western Ontario*

Supervisor
McGavin, Martin J.
*The University of Western Ontario*

Graduate Program in Microbiology and Immunology
A thesis submitted in partial fulfillment of the requirements for the degree in Master of Science
© Jamie N. Halucha 2017

Follow this and additional works at: https://ir.lib.uwo.ca/etd

Part of the Medicine and Health Sciences Commons

## Recommended Citation

Halucha, Jamie N., "Investigating The Functional Relationships Of RND Efflux Pumps In Methicillin Resistant Staphylococcus Aureus" (2017). *Electronic Thesis and Dissertation Repository*. 4936.
https://ir.lib.uwo.ca/etd/4936

This Dissertation/Thesis is brought to you for free and open access by Scholarship@Western. It has been accepted for inclusion in Electronic Thesis and Dissertation Repository by an authorized administrator of Scholarship@Western. For more information, please contact wlswadmin@uwo.ca.

# Abstract

The RND superfamily of efflux pumps plays vital roles in the intrinsic defense mechanisms of bacterial pathogens. The Staphylococci have two genes encoding RND efflux pumps; *farE*, which promotes efflux of antimicrobial fatty acids, and an uncharacterized gene we have named *femT*. Although RND pumps are known to play roles in physiological function and antimicrobial resistance, the function of FemT, and the relationship between FemT and FarE in Staphylococci have not been identified. Using established assays, we have tested the phenotype of a *femT* deletion mutant. Here, we show that this mutant is more susceptible to lysostaphin, vancomycin and oxacillin, and grows faster in Mueller-Hinton broth. Most notably, when evaluating the relationship between these transporters, inducible expression of FarE in fatty acids was abolished in FemT-deficient mutants. These findings suggest an interplay between the two transporters, and cumulatively, represent the first description of both systems operating in *S. aureus*.

**Keywords:** Staphylococci, USA300, MRSA, RND protein, redundancy, efflux pumps, antimicrobial lipids, FarE

# Co-Authorship Statement

James Schneider contributed to work undertaken in this thesis through his creation of the original USA300Δ*farER* strain and the USA300 pGY*farE::lux* strain.

# Acknowledgments

I would first like to acknowledge all members, past and present, of the McGavin lab for their help, friendship, and support throughout the course of my research. Each of them have played a significant role in easing my transition into the lab, and I am truly grateful for every experience we have shared. Notably, I would like to acknowledge Heba Alnaseri for her tremendous encouragement, support, and direction both inside and outside of the lab; it is impossible to thank her enough. I would also like to thank my friends and family who have always been there for me. There are no words to describe my gratitude for their constant encouragement and support for everything I have chosen to pursue, and for reinforcing the importance of continuing my education.

I would also like to thank the donors that have contributed to the awards and scholarships provided by the Department of Microbiology and Immunology. Specifically, Dr. RGE Murray for his generous donation towards the Graduate Scholarship in Microbiology and Immunology, and Dr. FW Luney for his generous donation towards the Graduate Entrance Scholarship and the Graduate Travel Award in Microbiology and Immunology. As a recipient of these prestigious awards, I am sincerely grateful for your kindness and support.

Thank you to my advisory committee members, Dr. David Heinrichs and Dr. Jimmy Dikeakos, for their advice and participation on my committee. Their helpful suggestions and constructive feedback have been instrumental for the completion of this thesis.

Finally, I would like to extend my sincere gratitude and thanks to my supervisor, Dr. Martin McGavin, whose patience, guidance, and encouragement have been invaluable to me throughout the course of this thesis. His support has been instrumental in the successful completion of this research project. I am truly thankful for his time and for giving me the confidence to succeed.

# Table of Contents

**Abstract** .......... i

**Co-Authorship Statement** .......... ii

**Acknowledgments** .......... iii

**Table of Contents** .......... iiv

**List of Tables** .......... viii

**List of Figures** .......... iix

**List of Abbreviations** .......... x

**List of Units** .......... xiii

**1 Introduction** .......... 1

1.1 Overview of *Staphylococcus aureus* .......... 1

1.1.1 Background .......... 1

1.1.2 Pathogenesis .......... 2

1.1.3 Cell Wall Biology .......... 3

1.1.4 Emergence of Antibiotic Resistance .......... 6

1.1.5 Origins of Strain USA300 .......... 7

1.2 USA300 Virulence .......... 8

1.2.1 Spread of USA300 .......... 8

1.2.2 Unique Genomic Contents .......... 8

1.2.3 Virulence Factors .......... 10

1.2.4 Invasion of Skin Innate Immune Defenses .......... 12

1.2.5 Resistance to Antimicrobial Fatty Acids .......... 14

1.3 The RND Superfamily .......... 15

1.3.1 Features .......... 15

1.3.2 Structure-function analysis of AcrB in *E. coli* ........ 16

1.3.3 Function in Gram-positive Bacteria and Mycobacteria ........ 20

1.3.4 Function in *S. aureus* ........ 22

1.4 Hypothesis and Research Objectives ........ 25

**2 Materials and Methods** ........ 26

2.1 Storage and Growth of Strains ........ 26

2.2 DNA Methodology ........ 29

2.2.1 Plasmid Isolation from *E. coli* ........ 29

2.2.2 Plasmid Isolation from *S. aureus* ........ 29

2.2.3 Chromosomal DNA Isolation from *S. aureus* ........ 29

2.2.4 Restriction Enzyme Digestions ........ 30

2.2.5 DNA Ligations ........ 30

2.2.6 Agarose Gel Electrophoresis ........ 31

2.2.7 DNA Isolation from Agarose Gels ........ 31

2.2.8 Polymerase Chain Reaction (PCR) ........ 31

2.2.9 Nucleotide Sequencing ........ 32

2.2.10 Computer Analyses ........ 32

2.3 Transformation Methodologies ........ 34

2.3.1 Preparation of Transformation Competent *E. coli* ........ 34

2.3.2 Transformation of Competent *E. coli* ........ 34

2.3.3 Preparation of Transformation Competent *S. aureus* ........ 34

2.3.4 Transformation of Competent *S. aureus* ........ 35

2.4 Mutagenesis and DNA Cloning Methods ........ 35

2.4.1 Generation of an In-Frame Mutation ........ 35

2.4.2 Construction of pGY*lux* Reporter Strains ........ 39

2.4.3 Construction of pET28 Recombinant Plasmids ........ 39
2.4.4 Complementation of Mutants ........ 40
2.5 Protein Methodologies ........ 40
2.5.1 SDS-PAGE ........ 40
2.5.2 Expression and Purification of Recombinant FemT and FarE ........ 40
2.5.3 Western Blot ........ 41
2.6 Experimental Methodologies ........ 43
2.6.1 Growth Analysis ........ 43
2.6.2 Bactericidal Assays ........ 43
2.6.3 Luciferase Assays ........ 43
2.6.4 Lysis Assays ........ 44
2.6.5 Antibiotic Susceptibility Assays ........ 44
2.6.6 Statistical Analysis ........ 45
**3 Results** ........ 46
3.1 Evaluation of the Role of FemT in Cell Wall Synthesis ........ 46
3.1.1 Deletion of the *femT* locus ........ 46
3.1.2 Deletion of *femT* improves growth of USA300 in Mueller-Hinton broth ........ 49
3.1.3 USA300Δ*femT* is more susceptible to lysostaphin ........ 51
3.1.4 Deletion of *femT* slightly increases sensitivity of USA300 to select antibiotics ........ 53
3.2 Evaluation of Substrate Redundancy between FemT and FarE ........ 56
3.2.1 *femT* expression is not upregulated in USA300Δ*farER* ........ 56
3.2.2 *farE* exhibits loss of inducible expression in USA300Δ*femT* ........ 58
3.2.3 USA300Δ*femT* is more susceptible to killing by bactericidal concentration of linoleic acid ........ 60
3.2.4 Failure to express *farER* is responsible for increased sensitivity of *femT* deficient strains to killing by linoleic acid ........ 62

**4 Discussion** ........................................................................................................ 64

**5 References** ........................................................................................................ 72

Curriculum Vitae ........................................................................................................ 87

# List of Tables

**Table 2.1** Strains and plasmids used in this study ........................................................................ 27

**Table 2.2** Oligonucleotides used in this study .................................................................................. 33

**Table 3.1** Resistance profiles of *S. aureus* strains USA300, USA300Δ*farER*, USA300Δ*femT*, and USA300Δ*farER-femT* .......................................................................................................... 55

# List of Figures

**Figure 1.1** Overview of peptidoglycan synthesis in *S. aureus*. .................................................... 5

**Figure 1.2** Secondary structure of the AcrB monomer in *E. coli* ............................................... 19

**Figure 1.3** Structures of AcrB, FemT, and FarE efflux pumps.................................................. 24

**Figure 2.1** Genetic organization of the *femT* region for pKOR1 markerless mutagenesis .......... 37

**Figure 2.2** Construction of *femT* mutant using pKOR1 markerless mutagenesis ........................ 38

**Figure 3.1** Confirmation of *femT* deletion ..................................................................... 48

**Figure 3.2** Growth analysis of USA300 and RND pump mutants in TSB, BHI, MHB, and RPMI .......................................................................................................................... 50

**Figure 3.3** Deletion of *femT* increases sensitivity of USA300 to lysostaphin ............................ 52

**Figure 3.4** E-test results for determination of antibiotic sensitivity........................................... 55

**Figure 3.5** Assay of *femT* expression in E. coli, USA300, and USA300Δ*farER* ......................... 57

**Figure 3.6** *farE* loses inducible expression in USA300Δ*femT*.................................................. 59

**Figure 3.7** Sensitivity of USA300 and USA300Δ*femT* to the bactericidal activity of linoleic acid .......................................................................................................................... 61

**Figure 3.8** Sensitivity of USA300Δ*farER-femT* to killing by linoleic acid occurs in a *farER*-dependent manner ....................................................................................................... 63

# List of Abbreviations

| | |
|---|---|
| AA | Arachidonic acid |
| ACME | Arginine catabolic mobile element |
| ADAM | A disintegrin and metalloproteinase |
| Amp | Ampicillin |
| aTc | Anhydrotetracycline |
| ATP | Adenosine triphosphate |
| BHI | Brain-heart infusion |
| BLAST | Basic Local Alignment Search Tool |
| BSA | Bovine serum albumin |
| CA-MRSA | Community-associated MRSA |
| Cm | Chloramphenicol |
| DMSO | Dimethyl sulfoxide |
| DNA | Deoxyribonucleic acid |
| E-test | Epsilometer test |
| EDTA | Ethylenediamine tetra-acetic acid |
| ESH | Eukaryotic sterol homeostasis |
| FAME | Fatty acid-modifying enzyme |
| GlcNAc | N-acetylglucosamine |
| $Gly_5$ | Pentaglycine |
| HA-MRSA | Healthcare-associated MRSA |
| HAE | Hydrophobe/amphiphile efflux |
| HME | Heavy metal efflux |
| IPTG | Isopropyl-β-D-thiogalactopyranoside |
| Km | Kanamycin |

| | |
|---|---|
| LA | Linoleic acid |
| LB | Luria-Bertani |
| MFP | Membrane fusion protein |
| MGE | Mobile genetic element |
| MHB | Mueller-Hinton broth |
| MIC | Minimum inhibitory concentration |
| MLST | Multilocus sequence typing |
| MMDAG | Minierimycolyl diacylglycerol |
| MmpL | Mycobacterial membrane protein large |
| MmpS | Mycobacterial membrane protein small |
| MRSA | Methicillin-resistant *Staphylococcus aureus* |
| MurNAc | N-acetylmuramic acid |
| NCBI | National Center for Biotechnology Information |
| NEB | New England Biolabs |
| NFE | Nodulation factor exporter |
| NO | Nitric oxide |
| NOS | Nitric oxide synthase |
| OD | Optical density |
| $OD_{595}$ | Optical density (determined at 595 nm) |
| $OD_{600}$ | Optical density (determined at 600 nm) |
| OMF | Outer membrane factor |
| PAGE | Polyacrylamide gel electrophoresis |
| PBP | Penicillin binding protein |
| PBS | Phosphate-buffered saline |
| PBS-T | PBS containing tween20 |

| | |
|---|---|
| PCR | Polymerase chain reaction |
| PFGE | Pulsed-field gel electrophoresis |
| PSM | Phenol-soluble modulin |
| PVL | Panton-Valentine Leukocidin |
| RND | Resistance-nodulation-division |
| RPMI | Roswell Park Memorial Institute |
| SCCmec | Staphylococcal cassette chromosome mec |
| SDS | Sodium dodecyl sulfate |
| SPC | Staphylococcal proteolytic cascade |
| SSTI | Skin and soft tissue infections |
| Tet | Tetracycline |
| TM | Transmembrane |
| TSA | Tryptic soy agar |
| TSB | Tryptic soy broth |
| UV | Ultraviolet |
| v/v | Volume/volume |
| w/v | Weight/volume |
| WTA | Wall teichoic acid |

# List of Units

| | |
|---|---|
| b | Nucleotide base |
| bp | Nucleotide base pair |
| °C | Degrees Celsius |
| CFU | Colony forming units |
| Da | Dalton |
| F | Farad |
| g | Gram |
| × g | Gravitational force |
| k | Kilo |
| L | Litre |
| µ | Micro ($10^{-6}$) |
| m | Milli ($10^{-3}$) |
| M | Molar (1 mol/L) |
| n | Nano ($10^{-9}$) |
| OD | Optical density |
| Ω | Ohm |
| psi | Pounds per square inch |
| RLU | Relative light units |
| rpm | Revolutions per minute |
| V | Volt |

# 1 Introduction

## 1.1 Overview of *Staphylococcus aureus*

### 1.1.1 Background

Staphylococci are Gram positive, spherical bacteria that are distinguished microscopically by their characteristic organization into clusters. The *Staphylococcus* genus includes at least 40 species, most of which are harmless and reside normally on the skin and mucous membranes of humans and other organisms. Although members of the staphylococci are commensal, benign colonization can be the starting point for disease, transmission, and selection of new microbial traits. Therefore, bacteria in this category can be identified as pathobionts, as they exhibit duality of behavior from commensal to pathogen (1). This is especially true for the most pathogenic of the staphylococci, *Staphylococcus aureus*.

Carriage of *S. aureus* as a commensal appears to play a significant role in the epidemiology and pathogenesis of infection. As part of the normal flora, *S. aureus* asymptomatically colonizes skin and mucous membranes, with the anterior nares being the most consistent area from which this organism can be isolated (2). Over time, three patterns of carriage can be distinguished: roughly 20% of people are persistent carriers, 60% are intermittent carriers, and approximately 20% almost never carry *S. aureus* (3). Although the presence of *S. aureus* as a commensal is asymptomatic, carriage has been identified as a risk factor for the development of *S. aureus* infections.

The identification of *S. aureus* as a pathogen began with its discovery in 1880 by Scottish surgeon Alexander Ogston, who first observed the bacterium while microscopically examining a pus sample removed from the leg of a patient (4). Ogston hypothesized that acute abscesses were caused by micrococci and, after injecting pus from infected abscesses into healthy animals, could demonstrate that new abscesses formed, followed by signs of septicemia and death (5). In 1882, what Ogston described as micrococci were named *Staphylococcus* due to their spherical, cocci shape and growth in masses that mimic the appearance of a bunch of grapes (6). Two years later, Anton J. Rosenbach coined the term *Staphylococcus aureus*, from the Latin word ‘aurum’, meaning gold, owing to their distinctive gold hue on agar medium (7). The pigment molecule staphyloxanthin has since been attributed to this characteristic gold colour, and is an important contributor to the remarkable virulence of *S. aureus* and its ability to cope with environmental stresses by acting as an antioxidant that helps evade death by reactive oxygen species produced by the host immune system (8). In addition to its microscopic appearance and production of staphyloxanthin, *S. aureus* can also be distinguished by the production of the major virulence factor coagulase, a protein that binds prothrombin and facilitates the conversion of fibrinogen to fibrin, causing clot formation in plasma (9). Traditionally, staphylococci were divided into two groups based on their ability to produce coagulase, with the coagulase-positive staphylococci constituting the most pathogenic species; however, this classification can be misleading as it has been discovered that some *S. aureus* strains are coagulase-negative (10). These characteristics, combined with a large arsenal of virulence factors, have made *S. aureus* capable of causing a wide variety of diseases and syndromes.

### 1.1.2 Pathogenesis

The success of *S. aureus* as a pathogen and its ability to cause such a wide range of infections are the result of its extensive virulence factors, and initial exposure of *S. aureus* to host tissues beyond the skin and mucosal surfaces is thought to trigger upregulation of virulence genes (11). Carriage of *S. aureus* provides a reservoir from which bacteria can be introduced when host defenses are breached, whether by open wound inoculation, insertion of an indwelling catheter, surgery, or viral-mediated damage in the mucosa of the respiratory tract. Therefore, colonization of the skin and anterior nares by *S. aureus* is a common precursor to infection (12). Multiple studies have confirmed this finding, with a substantial proportion of *S. aureus* infections appearing to be of endogenous origin, as they originate from the strain present in the nasal mucosa (12, 13). If a host is not colonized with *S. aureus* asymptomatically via carriage as a commensal, colonization with *S. aureus* can occur due to transmission among individuals in health care and community settings.

When encountering the body surfaces, *S. aureus* cells first interact with and adhere to epithelial surfaces on the skin and mucosa. The presence of adherent bacterial cells is sensed by epithelial surface receptors that recognize microbial components derived from the bacterial cell wall, including wall teichoic acid, lipoteichoic acid, peptidoglycan, and lipoproteins (15). Once the host-pathogen interface has been breached and infection is established, *S. aureus* can cause skin and soft tissue infections, the most common being abscesses. Pyogenic bacterial abscesses can form in deeper tissues, such as underlying muscle, and bacteria can disseminate to form abscesses at distal sites and affect virtually any internal organ system (16). Abscess formation and tissue invasion is mediated by a range of secreted and cell surface factors, such as proteases, lipases, elastases, and hemolysins, that enable *S. aureus* to degrade host cells and tissues, seize nutrients, and spread to other sites of the body (17). Regulation of these secreted factors plays a central role in pathogenesis, and their expression during the different stages of infection is critical to the success of *S. aureus* as a pathogen (18, 19). In addition to abscess formation, *S. aureus* can form biofilms on host and prosthetic surfaces, enabling the cells to persist via evasion of host defenses and antimicrobial molecules (20). *S. aureus* is also capable of producing septic shock by interacting with and activating the host immune system and coagulation pathways. In some *S. aureus* strains, this is due to the production of superantigens, which cause non-specific activation of T-cells resulting in polyclonal T cell activation and massive cytokine release (21). Apart from this activity, superantigens can also cause symptoms that are characteristic of infection, such as emesis, which occurs in cases of food poisoning. In addition to these characteristics, it is now firmly established that *S. aureus* can survive and even replicate both inside and outside many mammalian cell types, including macrophages (22, 23). These features represent important strategies by which *S. aureus* circumvents innate immune function to promote bacterial dissemination.

### 1.1.3 Cell Wall Biology

The cell wall of a microorganism is critical for providing protection, support, and shape, but it also plays an important role in infectivity and pathogenicity. The cell wall of *S. aureus* shows the typical features of gram-positive bacterial cell walls, composed of a thick layer of peptidoglycan, teichoic acids, and wall-associated surface proteins (24). Stress-bearing peptidoglycan is the main structural component of the cell wall and acts as a continuous macromolecular cover surrounding the cytoplasmic membrane to protect the cell from rupture (25). The two basic structural features of this giant macromolecule are linear glycan chains interlinked with short peptide bridges. The glycan chains are composed of alternating units of N-acetylglucosamine (GlcNAc) and N-acetylmuramic acid (MurNAc), and the carboxyl group of each MurNAc residue is substituted by a short stem peptide subunit. The formation of the three-dimensional structure of peptidoglycan is ensured by cross-linking between the peptide subunit of one chain to that of a neighboring chain.

It is a distinctive feature of staphylococci that the degree of cross-linking, which is determined as a ratio of bridged peptides to the total amount of all peptide ends, is extremely high, on the order of 80 to 90%, compared to 50% cross-linking in the walls of bacilli (26–28).

The characteristic stem peptide branching off the MurNAc unit is synthesized in *S. aureus* by three non-ribosomal peptidyl-transferases; FemX, FemA, and FemB. Using Gly-tRNA as a donor, and the peptidoglycan precursor lipid II as a substrate, they add five glycine residues in a sequential fashion to form the pentaglycine ($Gly_5$) interpeptide (29). Cross-linking of adjacent peptidoglycan strands and anchoring of surface proteins, contributing to the virulence of *S. aureus*, occurs via this $Gly_5$-interpeptide structure (30). An incomplete $Gly_5$ interpeptide leads to aberrant growth, requiring compensatory mutations to guarantee survival, while a complete lack is lethal (31–33). Importantly, antibiotic resistant *S. aureus* depend on the correct formation of the peptidoglycan precursor, including a complete $Gly_5$ chain, for high-level resistance (34). After transport across the cytoplasmic membrane, the peptidoglycan precursor is incorporated into the existing cell wall by the penicillin binding proteins (PBPs), which are enzymes that catalyze transglycosylation of the sugar moiety and transpeptidation of the $Gly_5$ chain. Since bacterial cell wall synthesis is essential to growth, cell division, and maintaining cellular structure, it has been an attractive target for antibiotics. For example, β-lactam antibiotics act by inhibiting the synthesis of peptidoglycan, specifically by targeting the transpeptidation reaction catalyzed by the PBPs. Synthesis of peptidoglycan and the major constituents of the *S. aureus* cell wall are summarized in Figure 1.1.

Wall teichoic acids (WTAs) are another component of the staphylococcal cell wall known to contribute to cell morphology and division. WTA polymers play numerous, varied roles in the cell wall owing to their location, abundance, and polyanionic nature (35). *S. aureus* mutants lacking these polymers exhibit numerous morphological abnormalities, including a non-uniform thickening of the peptidoglycan, increased cell size, and defects in septal positioning and number (36, 37). In addition, WTAs and their attached substituents contribute to cell surface charge and hydrophobicity, which in turn affects binding of extracellular molecules and plays a role in protection. For example, WTA-deficient cells are more susceptible to antimicrobial fatty acids, presumably because the hydrophobic fatty acids can penetrate the less hydrophilic mutant cell wall more easily, and bind to the cell membrane where they can elicit their antibacterial effects (38). Additionally, blocking WTA synthesis renders *S. aureus* sensitive to β-lactam antibiotics (39).

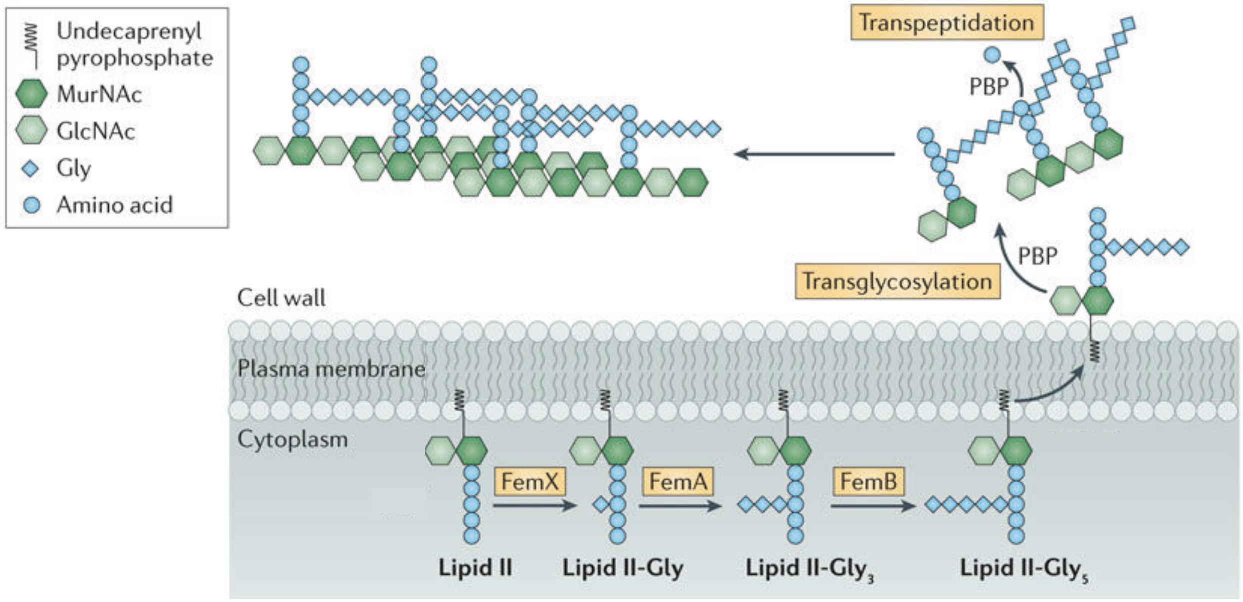
Undecaprenyl pyrophosphate
MurNAc
GlcNAc
Gly
Amino acid
Transpeptidation
PBP
PBP
Transglycosylation
Cell wall
Plasma membrane
Cytoplasm
FemX
FemA
FemB
Lipid II
Lipid II-Gly
Lipid II-Gly$_3$
Lipid II-Gly$_5$

**Figure 1.1 Overview of peptidoglycan synthesis in *S. aureus*.** The process begins in the cytoplasm, where the Lipid II precursor is formed. A peptide crossbridge of five glycine residues is added at the third amino acid by the non-ribosomal peptidyl-transferases FemX, FemA, and FemB. Lipid II-Gly$_5$ is then flipped to the external side of the cell membrane, where it is incorporated into nascent peptidoglycan by penicillin binding proteins (PBPs). PBPs catalyze transglycosylation and transpeptidation reactions, resulting in the respective polymerization and crosslinking of the glycan strands via flexible peptides. Figure adapted from Pinho *et al.* (40).

### 1.1.4 Emergence of Antibiotic Resistance

The combination of virulence factors and staggering rates of antibiotic resistance of *S. aureus* has led to its classification of a 'superbug'. During the Second World War, Fleming's discovery of penicillin was a revolutionary event, providing an effective antibiotic for the treatment of *S. aureus* infections. Penicillin is a member of the β-lactam family, which is a class of broad-spectrum antibiotics that prevent cell wall biosynthesis by binding to and inhibiting PBPs. Yet, only a few years after its introduction into clinical practice, penicillin resistance was encountered in hospitals and, within a decade, had become a significant problem in the community (41). In 1944, Kirby was the first to demonstrate that penicillin was inactivated by penicillin-resistant strains of *S. aureus*, and soon after, Bondi and Dietz identified the specific role of the penicillinase enzyme in penicillin resistance (42, 43). To overcome penicillin resistance, penicillinase-resistant antibiotics were developed, and methicillin was the first to be produced. Methicillin is a narrow-spectrum antibiotic also part of the β-lactam family, however, the first methicillin-resistant *S. aureus* (MRSA) were discovered in the same year methicillin reached the market (44).

Although the basis of methicillin resistance was not identified until more than 20 years later, it was known that the resistance mechanism was different from penicillinase, as there was no drug inactivation (41). After examining the PBP patterns of methicillin resistant staphylococci, an additional PBP was discovered that conferred resistance to methicillin and all available β-lactam antibiotics (45). Whereas non-resistant *S. aureus* normally employ three PBPs, PBPs 1, 2, and 3, to catalyze cross-linking of peptidoglycan, MRSA have an additional PBP, named PBP2a, which is encoded by *mecA* and confers resistance to methicillin. The *mecA* gene is carried by large (32–60 kb) sections of chromosomally inserted DNA, which has been termed the staphylococcal cassette chromosome *mec* (SCC*mec*), likely acquired through horizontal gene transfer from *Staphylococcus epidermidis* (46). Although the mechanism of gene acquisition is not known, two genes, *ccrA* and *ccrB*, present on the SCC*mec* have been shown to code for recombinase proteins, which are responsible for site-specific excision and insertion into the chromosome (47). During the onset of MRSA emergence, isolates were largely restricted to hospitals in large urban centres; however, throughout the last few decades, there has been a larger spread of MRSA into smaller hospitals and even into the community, referred to as healthcare-associated MRSA (HA-MRSA) and community-associated MRSA (CA-MRSA), respectively. One of the major strains attributing to the epidemic wave of CA-MRSA in North America is the USA300 clone. Although USA300 isolates were initially resistant only to β-lactam antibiotics, mediated by *mecA*, and macrolides, mediated by *msrA*, they have broadened their resistance profiles considerably over the last 5 years. This includes additional resistance to clindamycin, due to the acquisition of *ermA* and *ermC*, and tetracycline, due to the acquisition of *tetK* and *tetM*, as well as resistance to mupirocin, fluoroquinolones, vancomycin, and, in some cases, to daptomycin (48–51).

### 1.1.5 Origins of Strain USA300

The increasing prevalence of strain USA300 in the community is of special concern to the medical establishment. Perhaps the most notable and well-documented epidemic of CA-MRSA has been in the United States, and is attributed to the USA300 strain. The name USA300 describes one of many MRSA strains identified in the United States through genomic DNA examination of pulsed-field gel electrophoresis (PFGE) patterns (52). The strain emerged within *S. aureus* multilocus sequence typing (MLST) clonal complex 8, which is the presumptive ancestor of the first MRSA strain, and carried SCC*mec* (53). MRSA PFGE type USA300 differs from its ancestor strain by at least 20 genes, a significant number of which are potentially mobile elements (49). The most characteristic genes of USA300 are the Panton-Valentine Leukocidin (PVL) genes and the arginine catabolic mobile element (ACME).

Infections caused by USA300 were first noted in a Mississippi state prison in 1999 where 59 inmates were infected (54). The infections associated with colonization included moderate to severe skin and soft tissue infections (SSTIs) and more invasive infections, including necrotizing pneumonia, fasciitis, and bone and joint infections. During the next few years after the first outbreak, further outbreaks appeared in which infected individuals had no link to healthcare systems. These outbreaks occurred among prisoners, children, and athletes. Although there were no ascertainable links between the various outbreaks, the PFGE patterns of the isolates recovered from all the involved individuals were mostly type USA300 (48). Since then, USA300 has become one of the most commonly isolated strain types recovered in community settings.

## 1.2 USA300 Virulence

### 1.2.1 Spread of USA300

Investigations of CA-MRSA outbreaks in prisons, athletic quarters, daycares, and military recruits have all contributed to our understanding of the development and spread of MRSA infections. Investigations of various outbreaks identified several critical risk factors contributing to the spread of infection, including sharing towels and razors, frequent skin to skin contact, unattended skin abrasions, and lack of attention to cleaning of environmental surfaces and athletic equipment (55). In addition, the high rate of antibiotic use among individuals has acted as a selective factor for MRSA disease. Thus, USA300 is well adapted to spread and cause infections in the community and healthcare settings.

International and intercontinental spread of epidemic *S. aureus* strains, including MRSA type USA300, is not a new phenomenon, but is arguably being facilitated by increasing volumes of international travel and migration. Within a few years of its first description, USA300 SSTIs have been reported in 36 countries on five continents (56). Furthermore, autochthonous acquisition has been documented in Canada, 10 European countries, Colombia, Trinidad and Tobago, Israel, Japan, and Samoa (56). The sustained spread of CA-MRSA may, in principle, be due to the total number of infections and direct transmission from infected patients, and thus to infectivity or virulence. However, CA-MRSA may also show increased transmissibility and colonization characteristics due to acquisition of virulence factors encoded by unique genomic contents.

### 1.2.2 Unique Genomic Contents

Many different lineages of CA-MRSA cause outbreaks and invasive infections, but in North America, none are as prevalent as the epidemic strain USA300. These clones have acquired many genes in the form of mobile genetic elements (MGE) that may confer a selective advantage over other CA-MRSA strains. The USA300 chromosome can be divided into a core component, consisting of gene regions shared by all strains of *S. aureus*, and an accessory component, which includes gene regions that are absent in closely related strains. Virtually all unique genes in USA300 cluster in five novel allotypes of MGEs that encode virulence or resistance determinants, and the capacity of USA300 to cause severe disease is attributable to one or more of these elements.

The first genetic element is known as SCC*mec*, which encodes the *mecA* gene and is located on a MGE. There are currently eight recognized types of SCC*mec*, with types I, II, and III containing additional drug resistance determinants, and types IV, V, VI, and VII harboring resistance only to β-lactams through the *mecA* gene (57). In the absence of antibiotic pressure, the SCC*mec* element is thought to reduce the biological fitness of MRSA (58). However, strains of CA-MRSA such as USA300 carry the type IV allotype of SCC*mec*, which is smaller than the other types, and therefore, may impose less of a fitness cost (59). Thus, it is thought that harboring SCC*mecIV*, as opposed to other SCC*mec* types, imparts CA-MRSA with an advantage in its ability to cause infection in healthy individuals.

Adjacent to the SCC*mec* element of USA300 is the pathogenicity island ACME, which is the largest genomic region distinguishing USA300 from other *S. aureus* strains, and the physical linkage between these two elements suggests that selection for pathogenicity and selection for antibiotic resistance are interconnected (59). Evidence has indicated that the initial assembly of the ACME locus originated in *S. epidermidis* or other coagulase negative staphylococci, and was acquired by USA300 through a single horizontal gene transfer (60). ACME encodes a complete arginine deiminase pathway, which converts L-arginine to carbon dioxide, ATP, and ammonia. Although the functional relevance of ACME to infection and disease remains unclear, the ACME element has been suggested to promote survival of USA300 on human skin and persistence within cutaneous abscesses (61). The ACME locus is composed of at least 33 putative genes and two operons, referred to as *opp* and *arc* (60). The *opp* operon encodes an oligopeptide permease or metal transporter, and homologous genes have been implicated in virulence of *Streptococcus pyogenes* (62). The *arc* operon encodes genes thought to be involved in arginine catabolism, and have been implicated in USA300 survival in acidic environments that mimic human skin (61). Host arginine feeds multiple pathways during a typical immune response; initially, macrophages in infected tissue primarily consume arginine via nitric oxide synthase (NOS) enzymes to generate nitric oxide (NO) (63, 64). However, over time, the host response shifts away from NO production and towards an anti-inflammatory phase, where macrophages redirect arginine consumption towards the production of ornithine, which can be further converted to polyamines (61, 63, 64). Consequently, since ACME-*arc* promotes long-term survival of USA300 in acidic environments such as the skin, it indirectly drives excessive production of host polyamines, which are uniquely toxic to *S. aureus*. To mitigate this, ACME also encodes the spermidine acetyltransferase SpeG, a polyamine-resistance enzyme that is essential for combating excess host polyamines in a murine SSTI model (61).

In addition to SCC*mec* and ACME, USA300 contains a novel staphylococcal pathogenicity island, SaPI5, that encodes two enterotoxins. These enterotoxins are closely related to enterotoxins SEQ and SEK, which are pyrogenic toxin superantigens belonging to the HA-MRSA clone COL. Since the SaPI5 enterotoxins of USA300 share more than 98% identity in amino acid sequences to those in COL, these molecular variants probably stimulate a similar subset of T cells (65). The fourth genetic element present in USA300 is prophage ϕSA2usa, which harbours the genes that encode PVL, a pore-forming toxin that induces polymorphonuclear cell death by apoptosis. PVL is strongly associated with invasive disease and virulence of USA300 and other CA-MRSA strains (66). The fifth genetic element of USA300 is prophage ϕSa3usa, encoding staphylokinase and a chemotaxis inhibiting protein (65). Staphylokinase is a potent plasminogen activator that could facilitate bacterial spreading, and the chemotaxis-inhibiting protein is an anti-inflammatory agent that inhibits C5a-dependent recruitment of neutrophils (67). These five genetic elements of USA300 most likely account for phenotypes of interest, as they carry known virulence factors and resistance determinants that could allow for success of USA300 in colonization and pathogenesis.

### 1.2.3 Virulence Factors

In addition to possessing antibiotic resistance, USA300 is more virulent and causes more severe disease than other CA-MRSA strains due to high expression of genomic virulence determinants. In animals, USA300 has exhibited enhanced production of dermonecrotic lesions in skin abscess models when compared to other MRSA clones, and USA300 was more lethal in a rat model of pneumonia compared with a USA400 isolate (53, 68, 69). Within abscesses, *S. aureus* reduces its expression of adhesion proteins and produces large amounts of toxins, immune evasion factors, and tissue degrading enzymes, all of which contribute to the remarkable pathogenicity of USA300.

The success of CA-MRSA infection depends mostly on efficient evasion of attacks by human host defenses, for which *S. aureus* has developed many different strategies. The most crucial strategy that allows USA300 to invade human hosts is likely the production of toxins that kill human leukocytes, especially neutrophils, as they represent the main leukocyte type responsible for the elimination of bacterial pathogens (11). Many *S. aureus* toxins and virulence determinants are encoded on MGEs, including the leukolytic toxins, collectively called leucocidins, and are the toxins responsible for destroying neutrophils after uptake. Most work has been performed on PVL, owing to the initially strong epidemiological correlation with CA-MRSA infections (70). PVL is a two-component exotoxin that forms pores in the membranes of leukocytes, causing their lysis. PVL has also been indicated to activate leukocytes to release pro-inflammatory cytokines, including IL-8, which drive inflammation (71). Although this attracts immune cells to the site of infection, a strong inflammatory effect may lead to tissue destruction and exacerbation of infection, even in the absence of leukocyte lysis. Epidemiological and clinical reports indicate a strong correlation between PVL production and severe SSTIs, as well as necrotizing pneumonia and fasciitis (72). Thus, PVL is significantly correlated with invasive CA-MRSA disease.

Another pore-forming leukocyte toxin, α-toxin, also known as α-hemolysin, has been well described as a virulence factor in many *S. aureus* strains, including USA300. Unlike PVL, secreted α-toxin does not lyse neutrophils, but instead lyses other immune cells such as macrophages and lymphocytes. At lower concentrations, α-toxin forms a complex with a protein belonging to a disintegrin and metalloproteinase (ADAM) family, which allows it to form a pore in the membrane and cause apoptosis (73). At higher concentrations, α-toxin non-specifically absorbs into cellular membranes and causes the release of calcium ions and subsequent cell necrosis (74). The secretion of α-toxin is an important determinant of virulence in CA-MRSA models, and is consistently expressed at higher levels in USA300 compared to less pathogenic strains of *S. aureus* (75). Additional virulence factors that are also expressed at higher levels in USA300 include the phenol-soluble modulins (PSMs), which have potent leukocidal and chemotactic properties, and are able to recruit, activate and lyse human neutrophils (76).

Strains of *S. aureus* also express several secreted proteases that mediate the breakdown of host tissue, specifically fibrotic tissue synthesized to confine lesions containing *S. aureus*. As with α-toxin and PSMs, USA300 clones are also known to excrete proteases in excess, potentially limiting the ability of the host to control minor SSTIs (77). These secreted proteases have been identified as important contributors to virulence through cleavage of specific host proteins, and *S. aureus* possesses several major secreted proteolytic enzymes. These include the serine protease SspA, the cysteine protease SspB, the metalloprotease Aur, and six serine-like proteases that are SspA homologues (SplABCDEF) (78). SspB, for example, can degrade human fibronectin, fibrinogen, and kininogen, and may therefore contribute to the ability of *S. aureus* to disseminate (79). Secreted proteases can also cleave the heavy chains of all human immunoglobulin classes, and elastin, which aids in tissue evasion (80, 81). In addition to their interaction with the host, extracellular proteases are also capable of modulating the stability of self-derived virulence determinants. Specifically, SspA was shown to cleave surface proteins, including fibronectin-binding protein and surface protein A (82, 83). As a result, the cleavage of these proteins by proteases is thought to affect the transition from an adhesive to an invasive phenotype. Several of the *S. aureus* proteases are expressed as inactive pro-enzymes that can be activated in a sequence known as the staphylococcal proteolytic cascade (SPC) pathway. The SPC pathway is induced in response to unsaturated free fatty acids, such as those encountered on the skin or in infected abscess tissue, and thus, acts as an environmental signal-response pathway for *S. aureus* to survive in these conditions with increased virulence (84). Similarly, it has also been suggested that extracellular proteases can cleave secreted toxins to regulate the abundance of virulence factors, depending on the specific niche encountered within the host (85). The over-production of toxins and proteases, in combination with the ability of *S. aureus* to sense changes in the environment, confers the selective advantage that explains the overwhelming success of the USA300 strain.

### 1.2.4 Invasion of Skin Innate Immune Defenses

Bacterial strains that cause epidemics, such as USA300, commonly combine extraordinary virulence with efficient colonization. The skin provides a formidable barrier to infection, yet recent evidence suggests an ability of USA300 to colonize the skin at higher rates than other strains (86). To successfully colonize, this clone must be able to evade host defense mechanisms, and the first line of defenses encountered are those belonging to the innate immune system. The innate immune system harbors a multitude of different receptor systems and cells that are constantly prepared to sense and eliminate invading microbial pathogens. When encountering the host, *S. aureus* cells interact with and adhere to epithelial surfaces on the skin and mucosa. Most of the defensive functions of the epidermis localize to the stratum corneum, the outermost layer, which limits pathogen colonization through its low water content, acidic pH, resident microflora, and secretions of polyamines and antimicrobial lipids (87, 88). Sweating and drying of the skin also means considerable changes in osmolarity, salt concentration and mechanical stress. Polyamines, notably putrescine, spermidine, and spermine, are synthesized from L-arginine and their secretion facilitates countless cellular functions, including wound healing and inflammation (87). Interestingly, most *S. aureus* clones are sensitive to exogenous polyamines in culture, except for USA300 (65). USA300 is notably capable of growing despite the presence of polyamines due to *speG*, encoded by the ACME cassette (86).

Another key physical feature preventing bacterial colonization of the skin is its acidic pH, which is the result of many factors including the secretions of lactic acid, amino acids, and fatty acids (89). The naturally low pH of skin and sweat (pH ~ 4.5-5.9) is well below the optimal pH of many bacteria, including *S. aureus*, and it has long been documented that patients with a higher natural skin pH are more susceptible to infections (90). Remarkably, USA300 is again capable of tolerating these acidic conditions due to the acquisition of ACME, which increases the production of ammonia from L-arginine catabolism, thereby countering the acidic stress (61). The constitutive activity of ACME drives ammonia production regardless of the presence of glucose or oxygen, a unique feature of ACME that sets it apart from the arginine deiminase system encoded in the chromosome of all *S. aureus* strains (61). Thus, through ACME, USA300 is better able to resist the acidic environment of the skin, implying a unique colonization advantage for this strain.

Sebum, a liquid phase lipid mixture secreted from the sebaceous glands of the skin, is another important aspect of skin innate immune defenses, consisting of approximately 28% free fatty acids, 32% triglycerides, 25% wax esters, and 11% squalene (91, 92). These free fatty acids contribute to most of the antimicrobial activity of the sebum, with the saturated fatty acid lauric acid, and the unsaturated fatty acid sapienic acid, being the most notable (91). The importance of sapienic acid as an innate defense mechanism is evident in atopic dermatitis, where the skin is deficient in this fatty acid, and there is a near 100% recovery of *S. aureus* from the skin of atopic dermatitis patients (93). Similarly, nasal secretions also contain antimicrobial fatty acids, primarily linoleic acid (LA), arachidonic acid (AA), and palmitoleic acid or their corresponding cholesterol esters, and infected abscess tissue also contains abundant antimicrobial fatty acids (94–96). Consequently, *S. aureus* is exposed to antimicrobial fatty acids not only during colonization, but also during infection, and thus it is likely that *S. aureus* has evolved mechanisms of intrinsic resistance.

### 1.2.5 Resistance to Antimicrobial Fatty Acids

The human skin is rich in antimicrobial fatty acids produced by the sebaceous glands, and there is increasing evidence that *S. aureus* produces dedicated proteins that protect against the antibacterial activity of fatty acids. The heme coordinating surface protein, iron surface determinant A (IsdA), *S. aureus* surface protein F (SasF), and teichoic acids have all been implicated to contribute to fatty acid resistance (38, 97, 98). Recently, an efflux pump in *S. aureus* USA300 has also been characterized to play a role in mediating resistance to LA and AA specifically (99).

Although different mechanisms have been put forward for the bactericidal effects of free fatty acids, in *S. aureus*, the main mechanism appears to be membrane disruption and correspondingly the collapse of energy metabolism, which relies on a proton gradient involving the membrane (100). Recent research has expanded this idea, suggesting that the accumulation of unsaturated free fatty acids that possess surfactant properties, such as palmitoleic acid, disrupt the phospholipid bilayer to such an extent that solutes such as ATP, and even larger proteins, are able to diffuse out (101). Since fatty acids require hydrophobic interactions for their activity, many defense mechanisms employed by *S. aureus* alter the hydrophobicity of the cell wall. One of these mechanisms is IsdA, which renders the cell more hydrophilic via its C-terminal domain, thereby leading to decreased efficiency of fatty acids at gaining access to the cell (97). Similarly, WTAs contribute to resistance by blocking the hydrophobic fatty acids from penetrating the cell wall and binding to the cytoplasmic membrane where their antimicrobial activity is exerted (38). In addition to these cell wall modifiers, *S. aureus* also secretes a fatty acid-modifying enzyme (FAME) that esterifies fatty acids with cholesterol or short-chained alcohols, thereby inactivating them (102).

To combat a wide variety of host compounds, some bacteria also possess efflux pumps, for which fatty acids are known substrates (103). An efflux pump belonging to the resistance-nodulation-division (RND) family of transporters has recently been identified in USA300 to confer resistance to LA and AA that would normally be encountered on the skin or in a tissue abscess (99). This novel gene pair, *farR-farE* (fatty acid resistance), constituting divergently transcribed genes, is the first known description of a dedicated and inducible mechanism of *S. aureus* resistance to antimicrobial fatty acids. The efflux of fatty acids by FarE contributes to the growth of *S. aureus* in the presence of LA, and provides one example of the diversity of substrates transported by efflux pumps. There is now accumulating evidence that certain classes of efflux pumps, such as the RND family, not only confer resistance to drugs used in therapy, but also have a role in the colonization and the survival of bacteria in the host.

## 1.3 The RND Superfamily

### 1.3.1 Features

Found ubiquitously in all domains of life, multidrug efflux transporters have gained recognition as a major contributor to many resistant bacterial infections. Efflux proteins identified to date have been classified into five families, and of these, proteins belonging to the RND superfamily play an important role in the intrinsic resistance of bacterial pathogens and confer resistance to the broadest range of antimicrobial agents (104). Although the importance of the RND family of transporters in drug resistance has made them an attractive target of new therapeutic agents, most knowledge of their structure and function is derived from Gram-negative bacteria and remain poorly understood in Gram-positive bacteria. While efflux pumps are mostly known for their transport of drugs from the cytoplasm, other pump substrates include sugars, lipids, proteins, synthetic compounds, toxic metabolites, and host defense molecules (105). Such a heterogeneous substrate profile allows bacterial efflux pumps to play diverse roles in drug resistance and virulence, and promote key physiological processes (106).

The RND superfamily can be classified into eight recognized phylogenetic families, three of which are largely restricted to Gram-negative bacteria and include the heavy metal efflux (HME), the hydrophobe/amphiphile efflux-1 (HAE-1), and the nodulation factor exporter (NFE) families (107). RND pumps with features comparable to the well characterized AcrA-AcrB-TolC complex from *Escherichia coli* comprise the HAE-1 family, which are characterized for their role in antibiotic resistance (108). Although AcrB belongs to this subfamily, its physiologic function is likely to facilitate efflux of fatty acids that must be replaced due to membrane damage or phospholipid turnover, or to facilitate efflux of host-derived toxic compounds, including fatty acids and bile salts encountered in the intestine (103, 109). Similar functions of AcrB homologs in other species have also been reported, including in *Pseudomonas aeruginosa*, *Neisseria gonorrhoeae*, and *Salmonella typhimurium* (110–112). These observations suggest that bacterial efflux pumps, such as those belonging to the RND superfamily, have the capacity to transport various host-derived antimicrobial compounds and can therefore facilitate the adaptation and survival of bacteria in their ecological and physiological niches. Other phylogenetic families that make up the RND superfamily include (i), the SecDF family, found in both Gram-negative and -positive bacteria as well as archaea; (ii), the hydrophobe/amphiphile efflux-2 (HAE-2) family, restricted to Gram-positives; (iii), the eukaryotic sterol homeostasis (ESH) family; (iv), the hydrophobe/amphiphile efflux-3 (HAE-3) family; and (v), a more recently identified family that includes a probable pigment exporter in Gram-negative bacteria (107, 113). Extensive studies on the representative AcrB pump complex from *E. coli* in recent years have revealed both the structure and functional mechanisms of RND pumps in the efflux of a wide range of agents.

### 1.3.2 Structure-function analysis of AcrB in *E. coli*

Recent cryo-electron microscopy of the AcrA-AcrB-TolC pump structure has provided insight into subunit cooperation and how each of the protein components fit together into an operating machine (114, 115). In Gram-negative bacteria, many of these transporters form multicomponent pumps that span both the inner and outer membranes to efflux substrate out of the cell. The model system for such a pump, the AcrA-AcrB-TolC assembly, comprises the outer-membrane channel TolC, the secondary transporter AcrB located in the inner membrane, and the periplasmic AcrA, which bridges these two integral membrane proteins (114). AcrB, anchored in the inner membrane, is the RND protein component of this complex, while AcrA and TolC are members of the outer membrane factor (OMF) family and membrane fusion protein (MFP) family, respectively (116, 117). The RND proteins of these tripartite complexes function as an energy module with the help of the proton motive force to efflux substrate. These three protein components form a continuous channel across the Gram-negative cell envelope, gathering substrates from the outer leaflet of the inner membrane and periplasm to the cell exterior, with the absence of any component rendering the entire complex non-functional.

Although RND efflux pumps are found in all three domains of life in differing cell envelope architectures, these proteins share a common organization. To date, the five available RND protein structures (AcrB, CusA, MexB, ZneA, and MtrD) reveal that they function as homotrimers, wherein each protomer harbors 12 transmembrane (TM) helices, with N-terminal and C-terminal periplasmic domains inserted between TM1 and TM2, and between TM7 and TM8, respectively

(118–120). AcrB operates as a trimer, rotating through three distinct conformation states of open, binding, and extrusion conformations to facilitate efflux in the presence of its substrate (121). Recent modeling of the tripartite systems shows that, in addition to the AcrB trimer, the assembly comprises an AcrA hexamer and a TolC trimer (114). The AcrB trimer can be divided into a TM domain and an extensive periplasmic domain, comprising a distinct porter domain and a docking domain (122). The porter domain is located closest to the inner membrane and can be subdivided into four subdomains, PN1 and PN2, situated in the N-terminal portion of the protein between TM helices 1 and 2, and subdomains PC1 and PC2, situated in the C-terminal portion between TM helices 7 and 8 (122). These four subdomains meet to form proximal and distal binding pockets, both of which are enriched in aromatic, polar, and charged amino acid residues, forming a hydrophobic interior that interacts with substrates for transport (115). These two pockets might each contribute to the substrate poly-specificity of AcrB, as the pockets appear to have different substrate preferences (115, 122). Substrates may enter AcrB either from the outer leaflet of the cytoplasmic membrane, or from the periplasm, through three open channels, as well as a central cavity between the porter and TM domains (115). A vertical groove on the membrane-exposed surface of the protein, between TM segments 7 and 8, is suggested to provide access for membrane located substrates (117). The upper regions of subdomains PC1 and PC2 of AcrB are involved in defined interactions with specific domains of AcrA protomers (114). Also in the periplasmic domain, AcrB monomers are tightly interlocked and form a closed central pore, with the top of the protein forming a funnel-like structure, collectively called the docking domain, and is thought to dock TolC. The docking domain consists of subdomains DN and DC (Figure 1.2).

Substrate efflux through the transporter is coupled with proton translocation through AcrB, and crystallographic evidence supports a proton pathway involving the TM domains (123). Specifically, asparagine and lysine located in the middle of TM helices 4 and 10 are required. When AcrB protomers are in their open and binding states, the asparagine side chain forms a salt bride with the two lysine residues, and in the extrusion conformation, the salt bridges are broken by internal movement (124). Therefore, protonation and conformational switching are coupled during transport due to structural changes of the protein that influence the environment around the proton pathway. In this way, the proton relay network through the pump provides energy for efflux via the proton motive force.

Increasing numbers of small proteins are being identified to interact with RND proteins but their functions and influences on transport are largely unknown. Small protein binding partners of AcrB, such as the protein known as AcrZ, have been identified to enhance transport activity of AcrB for certain substrates (125). AcrZ folds into a long, largely hydrophobic α-helix that fits into a wide groove located in the TM domain of AcrB (114). Modeling of AcrZ has shown that its N-terminus is positioned in the periplasm, and its C-terminus is in the cytoplasm where it interacts with the hydrophilic surface of AcrB near the membrane (114). However, it is still not clear as to how AcrZ modulates the activity of the transporter for specific substrates. Potential mechanisms could involve conformational changes of the substrate binding pockets, or the organization of lipids near the substrate portal sites (115). Given that the surface of AcrB that interacts with small proteins is conserved among RND family proteins, it seems likely that other RND transporters may similarly be modulated by protein-protein interactions in the membrane.

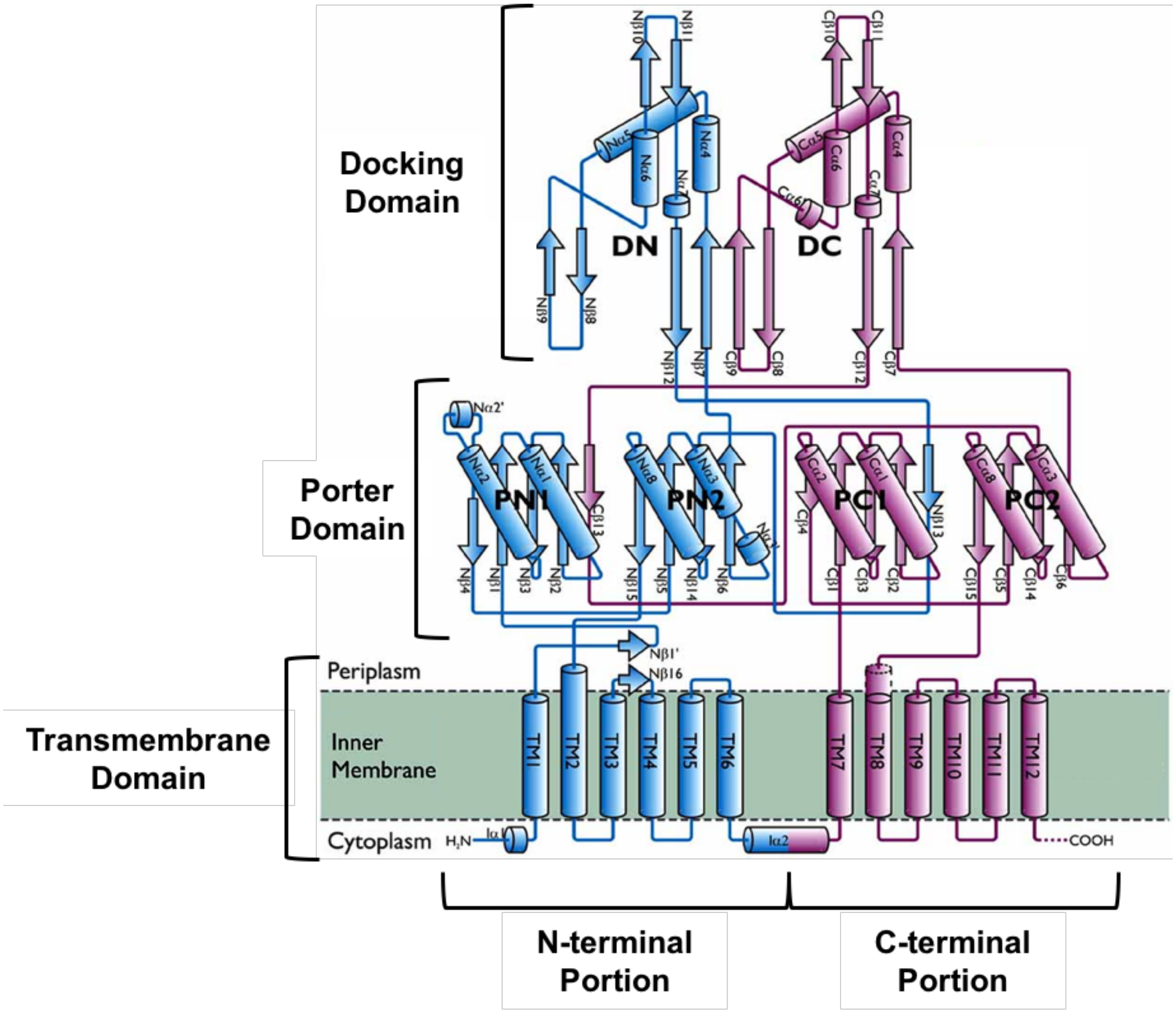
Docking Domain
DN
DC
Nβ10
Nβ11
Cβ10
Cβ11
Nα5
Nα6
Nα4
Nα7
Cα5
Cα6
Cα4
Cα6'
Cα7
Nβ9
Nβ8
Nβ12
Nβ7
Cβ9
Cβ8
Cβ12
Cβ7
Porter Domain
Nα2'
Nα2
Nα1
PN1
Nα8
Nα3
PN2
Nα7'
Cα2
Cα1
PC1
Cα8
Cα3
PC2
Cβ13
Cβ4
Cβ13
Nβ4
Nβ1
Nβ3
Nβ2
Nβ15
Nβ5
Nβ14
Nβ6
Cβ1
Cβ3
Cβ2
Cβ15
Cβ5
Cβ14
Cβ6
Nβ1'
Nβ16
Transmembrane Domain
Periplasm
Inner Membrane
Cytoplasm
H₂N
Iα1
TM1
TM2
TM3
TM4
TM5
TM6
Iα2
TM7
TM8
TM9
TM10
TM11
TM12
COOH
N-terminal Portion
C-terminal Portion

**Figure 1.2 Secondary structure of the AcrB monomer in *E. coli*.** The transmembrane domain of the AcrB monomer consists of 12 TM helices, numbered 1 to 12. The first six helices are located in the N-terminal portion of the protein, and the other six are located in the C-terminal portion. The porter domain consists of four subdomains, PN1, PN2, PC1, and PC2. The docking domain has two subdomains, DN and DC. N, N, C and C are -helices and -sheets of the N-terminal part or the C-terminal part of the periplasmic domain. N-and C-terminal portions are depicted in blue and magenta, respectively. Figure adapted from Seeger *et al.* (126).

### 1.3.3 Function in Gram-positive Bacteria and Mycobacteria

Since Gram-positive bacteria differ in cell wall structure compared to their Gram-negative counterpart, the HAE-2 family of RND efflux pumps in Gram-positive bacteria are more closely related to the ESH family than to the Gram-negative HAE-1 proteins (107, 127). A prototypic member of the ESH family is the Nieman Pick Type C protein NPC1, which binds cholesterol in late endosomes/lysosomes and promotes its transport into the cytosol (128). One member of the Gram-positive HAE-2 family that is also involved in lipid transport is the mycobacterial membrane protein large (MmpL) proteins from *Mycobacterium tuberculosis*, which have been implicated in mediating substrate transport across the mycobacterial membrane, mainly cell wall lipids (129). The *M. tuberculosis* genome possess 15 different genes encoding RND proteins (105), 14 of which belong to the MmpL protein family (130). Recently, three-dimensional molecular modeling of MmpL transporters has revealed that these proteins have homologous structural architecture to other RND superfamily proteins, including AcrB (130). MmpL proteins contain a periplasmic headpiece and a TM region, and form a channel-like arrangement of trimeric structures. According to conserved domain studies, it is evident that the MmpL proteins possess AcrB, ActII, sterol sensing and hopanoid biosynthesis related domains, which signify similarity of the MmpL proteins with the well-known RND superfamily members (130). Using pairwise comparison of MmpL proteins with each other, two common motifs in TM helix 4 and 10 have been identified. More specifically, molecular modeling has shown the contribution of the conserved amino acid pair aspartic acid and tyrosine to the proton relay, substantiated by the fact that they are in the same position as the essential residues involved in the proton relay network of AcrB (124, 131, 132). These amino acids are highly conserved in all MmpL proteins and form an aspartic acid/tyrosine pair within TM helix 10. This amino acid pair, along with one additional aspartic acid residue in TM helix 4, serve as essential elements for the proton relay pathway in MmpL transporters (131). This finding was further supported in studies showing that a tyrosine to phenylalanine mutation in two types of MmpL pumps abolish their function, suggesting the necessity of Tyr-OH mediated proton transport (131).

Since *M. tuberculosis* contains 15 different genes encoding RND proteins, some of these transporters have been found to be redundant, whereby inactivation of one pump causes increased activity of another. Specifically, MmpL4 and MmpL5 have redundant functions in siderophore export, and a double MmpL4/5 mutant cannot be constructed, suggesting that they are essential for siderophore-mediated iron acquisition (133). This is comparable to RND efflux pumps operating in *E. coli* and *Salmonella*, as the antimicrobial susceptibility of deletion mutants and strains with an increased expression of certain RND efflux pumps indicates an overlap or redundancy between the antimicrobials, biocides, dyes and detergents that can be transported by the different RND pumps (134, 135).

Also comparable to RND efflux pumps of Gram-negative bacteria, many MmpL transporters appear to cooperate with smaller accessory proteins called mycobacterial membrane protein small (MmpS), which are involved in scaffolding and are predicted to have only one N-terminal TM domain with an extra-cytoplasmic C-terminus (136). However, unlike most Gram-negative RND transporters, MmpL proteins are not believed to export antibiotics and seem to be much more specific for their substrate, interacting with only one lipid metabolite (136, 137). Furthermore, whereas RND family members from Gram-negative bacteria act purely as efflux pumps, RND transporters in Gram-positive bacteria may also be involved in the synthesis of certain molecules. For example, in *M. tuberculosis*, MmpL8 plays a role in the synthesis of sulfolipid-1, possibly by transporting a precursor of this molecule to the cell surface (136). Indeed, it is believed that MmpL transporters, in conjunction with their MmpS accessory proteins, are responsible for coupling lipid biosynthesis and export, transporting fatty acid and lipid components that are required to produce the lipid rich mycobacterial cell wall, such as monomeromycolyl diacylglycerol (MMDAG), mycolate ester wax, trehalose monomycolate, sulfolipids, and even siderophores (105, 130, 133, 138, 139). Most *mmpL* and *mmpS* genes are located close to genes involved in the synthesis or modification of polyketides, and MmpS proteins may promote interactions between various proteins involved in biosynthetic pathways. These small MmpS TM proteins may promote protein interactions via their extracytoplasmic C-terminal domains, which stabilizes the protein complex and enhances synthesis and export (136). This observation is apparent in some MmpL proteins such as MmpL11, which promotes export of mycolic acids. MmpL11 has two smaller extracytoplasmic domains and a large cytoplasmic C-terminal domain compared to that of AcrB. The large C-terminal cytoplasmic segment is thought to facilitate localization of the protein to the septum of dividing cells, where mycolic acid is being synthesized and exported (140). It is proposed that its extracytoplasmic C-terminal domain facilitates protein interaction in the cytoplasm, a key process for its function. Although MmpS proteins display no similarity to the

MFP family of Gram-negative bacteria, the close association of *mmpS* and *mmpL* genes suggests that MmpS proteins may be the functional homologues of MFPs. Similarly, related HAE-2 transporters ActII-3 in *Streptomyces coelicolor*, and YerP/SwrP in *Bacillus subtilis* are also suggested to couple the synthesis and export of their substrates (141, 142). These observations suggest that microbial RND efflux pumps support physiological processes that are defining traits of a genus or species, and that protein-protein interactions may be essential to their function.

### 1.3.4 Function in *S. aureus*

Most studies on RND pump structure and function focus on those found in Gram-negative bacteria; however, research on RND efflux pumps in Gram-positive bacteria has become increasingly more prevalent. In *S. aureus*, three RND proteins are present: SecDF, FarE, and SAUSA300_2213, which is currently uncharacterized. SecDF is an accessory factor of the conserved Sec protein translocation machinery and belongs to the RND family of multidrug exporters. SecDF has been shown in both *E. coli* and *B. subtilis* to be involved in the export of proteins. In *S. aureus*, lack of SecDF affects cell separation, resistance, and virulence factor expression, suggesting its importance in pathogenesis (143, 144).

Recently, through comparative genome sequencing of *S. aureus* USA300 variants that were selected for enhanced resistance to LA, a regulator of fatty acid resistance, *farR*, and an effector of fatty acid resistance, *farE*, were identified; this is the first description of a dedicated and inducible mechanism of *S. aureus* resistance to antimicrobial fatty acids (99). These genes bear similarity to the *acrR* and *acrB* model in *E. coli*, and protein structural modeling and homology searches indicate that FarR belongs to the TetR/AcrR family of regulators, while FarE belongs to the RND family of multidrug efflux pumps (99). Although AcrB family efflux pumps have been most extensively characterized as mediators of multidrug resistance, the primary function of FarE is to promote efflux of antimicrobial fatty acids that would be encountered during colonization or within a tissue abscess. This is consistent with the belief that members of the AcrB family have evolved to promote efflux of host-derived toxic compounds, including bile salts and fatty acids (99, 103). Although recent studies reveal important observations on the role of FarE in fatty acid efflux, functional redundancy with the third uncharacterized RND transporter in *S. aureus* remains to be investigated.

The SecDF and FarE transporters of *S. aureus* represent two of three RND-family transporters that are conserved among staphylococci. A third conserved RND transporter, SAUSA300_2213, that has not been characterized is adjacent to *femX* (SAUSA300_2214), a gene that is essential for viability of *S. aureus* due to its role in synthesis of the $Gly_5$ cross-bridge structure that is a unique trait of staphylococcal peptidoglycan (29). This arrangement is conserved among staphylococci, implying that SAUSA300_2213 may have a role in transport of this structure, which is assembled on a lipid carrier. Importantly, synthesis of other non-ribosomal peptides/polyketides like FemX is a common trait in the assembly of mycobacterial glycolipid, actinorhodin of *S. coelicolor*, and lipopeptide surfactant of *B. subtilis*, all of which are transported by RND efflux pumps (141, 142). Hence, we refer to SAUSA300_2213 as FemT to denote a predicted role in transport of peptidoglycan precursor, however, the function of FemT and its role in cell wall synthesis remains to be elucidated.

Comparing structural features, AcrB and FemT share a striking alignment of TM segments and extracytoplasmic domains, which were modeled using Phyre2 (145) (Figure 1.3). Phyre2 predicted with 100% confidence that FemT has porter and docking domains similar to AcrB. Moreover, FarE, FemT and AcrB all appear to share high structural conservation in their membrane domain segments. However, FarE has significantly smaller porter domains, and lacks a defined docking domain. These predictions are supported by analyses of MmpL proteins; for example, crystallization of the soluble D2 domain of MmpL11, which resembles the porter domain of AcrB, is significantly smaller (~150 residues) compared to other RND transporters (~300 residues). In addition, MmpL11 lacks a docking domain and contains a large C-terminal cytoplasmic segment (140). Although the functions and structure of RND transporters are being extensively studied in both Gram-negative and Gram positive bacteria, many outstanding questions remain regarding the characterization of this family of transporters in *S. aureus*.

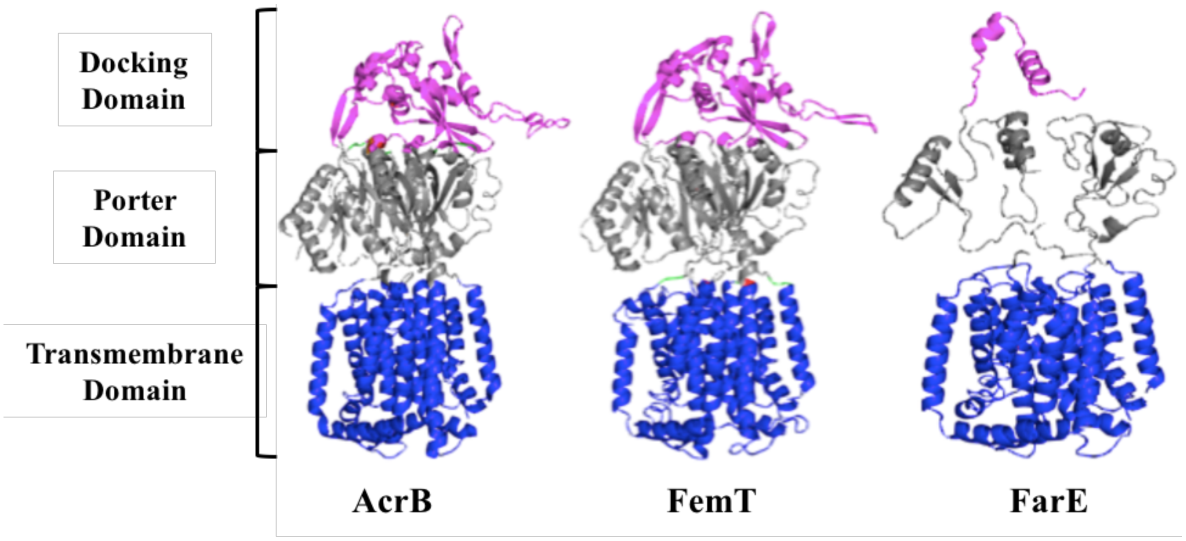
Docking Domain
Porter Domain
Transmembrane Domain
AcrB
FemT
FarE

**Figure 1.3 Structures of AcrB, FemT, and FarE efflux pumps.** AcrB is annotated from its known structure (122) and compared to predicted structures of FemT and FarE, which were modeled using Phyre2 (145). The docking domain, coloured in magenta, the porter domain, in grey, and the transmembrane domain, in blue, are indicated.

## 1.4 Hypothesis and Research Objectives

Although RND pumps are known to play critical roles in physiological function and antimicrobial resistance, the function of FemT, and the relationship between FemT and FarE in staphylococci have not been identified. Thus, the goal of this research was to elucidate the specific role of FemT, and to identify a relationship between FemT and FarE in *S. aureus*. We hypothesized that FemT, which is conserved among staphylococci, plays a role in cell wall synthesis by promoting transport of a peptidoglycan precursor. We further hypothesized that redundancy in substrate efflux may occur between FemT and FarE, as both are RND efflux pumps with implicated roles in physiological processes.

To test this hypothesis, we pursued two different research objectives. The first objective was to evaluate the role and impact of FemT in *S. aureus* by examining the phenotype of a *femT*-deletion mutant. To accomplish this, the FemT-deficient mutant was evaluated for perturbations in growth under various growth and stress conditions. The second objective was to identify a relationship between FemT and FarE transporters in *S. aureus*, specifically by evaluating whether inactivation of one pump caused an increase in expression of the other pump, and assessing the extent of substrate redundancy among these two RND pumps. To achieve this, both *farE* and *femT* expression were examined in a strain deficient in either FemT or FarE, respectively. Overall, this detailed evaluation of the function of both RND efflux pumps operating in *S. aureus* will provide new insight into the biology of staphylococci and further our understanding of this family of proteins in Gram-positive bacteria.

# 2 Materials and Methods

## 2.1 Storage and Growth of Strains

A list of bacterial strains and plasmids that were used or constructed in this study is provided in Table 2.1. Cultures were maintained as frozen stocks (−80°C) in tryptic soy broth (TSB; Difco™) with 20% glycerol. To generate single colonies, *S. aureus* strains were streaked onto tryptic soy agar (TSA; 1.5% Difco™ Agar) plates supplemented, when required, with 10 µg/mL of erythromycin or chloramphenicol for propagation of strains bearing resistance markers. *E. coli* strains were grown on Luria-Bertani (LB; Sigma) agar or in LB broth containing 100 µg/mL ampicillin or 50 µg/mL kanamycin when required. Unless otherwise stated, inoculum cultures were prepared by transferring cells from a single colony into 13-mL polypropylene tubes containing 3 mL of broth supplemented with antibiotic, as required, followed by overnight incubation at 37°C with shaking at 200 rpm.

**Table 2.1** Strains and plasmids used in this study

| Strain or plasmid | Description | Source |
|---|---|---|
| **Strains** | | |
| *S. aureus* | | |
| USA300 | CA-MRSA, wild-type strain cured of resistance plasmids | (84) |
| RN4220 | Restriction endonuclease deficient lab strain, capable of accepting foreign DNA | (146) |
| USA300Δ*farER* | USA300 with markerless deletion of *farE* and *farR* (SAUSA300_2489 and 2490) | (147) |
| USA300Δ*femT* | USA300 with markerless deletion of *femT* (SAUSA300_2213) | This study |
| USA300Δ*farER-femT* | USA300 with markerless deletion of *farE*, *farR*, and *femT* (SAUSA300_2489, 2490, and 2213) | This study |
| USA300 Δ*femT* (pALC*femT*) | USA300 Δ*femT* complemented with native *femT*, cloned in pALC2073, Cm$^R$ | This study |
| USA300 Δ*farER-femT* (pALC*femT*) | USA300 Δ*farER-femT* complemented with native *femT*, cloned in pALC2073, Cm$^R$ | This study |
| USA300 (pALC2073) | USA300 with empty pALC2073 vector, Cm$^R$ | This study |
| *E. coli* | | |
| DH5α | λ$^-$ ϕ80d*lacZ*ΔM15 Δ(*lacZYA-argF*)*U169 recA1 endA1 hsdR17*($r_K^-$ $m_K^-$) *supE44 thi-1 gyrA relA1* | Invitrogen |
| BL21 (DE3) | F$^-$ *ompT gal dcm lon hsdS*$_B$ ($r_B^-$ $m_B^+$) λ (DE3 [*lacI lacUV5*-T7 gene 1 *ind1 sam7 nin5*]) | Novagen |
| **Plasmids** | | |
| pGY*lux* | *E. coli-S. aureus* shuttle vector carrying a promoterless *luxABCDE* operon; Amp$^R$, Cm$^R$ | (148) |
| pGY*farE*::*lux* | *E. coli-S. aureus* shuttle vector carrying a putative *farE* promoter for *luxABCDE* operon; Amp$^R$, Cm$^R$ | (147) |

| | | |
|---|---|---|
| pKOR1 | *E. coli-S. aureus* shuttle vector; contains *xyl-tetO* promoter, expresses antisense *secY* RNA; Amp$^R$, Cm$^R$, Tet$^R$ | (149) |
| pKORΔ*femT* | pKOR1 containing upstream and downstream flanking sequences for deletion of *femT*; Amp$^R$, Cm$^R$, Tet$^R$ | This study |
| pALC2073 | *E. coli-S. aureus* shuttle vector with *xyl*/*tetO* promoter-operator region; Cm$^R$, Tet$^R$ | (150) |
| pALC*femT* | Native *femT* gene cloned in *SacI* site for expression from *xyl*/*tetO* promoter; Cm$^R$, Tet$^R$ | This study |
| pET28a(+) | *E. coli* shuttle vector; overexpression vector for 6xHis-tagged proteins; Km$^R$ | Novagen |
| pET*femT* | *femT* porter domain cloned in *Nhe*I and *BamH*I sites for overexpression of 6xHis-tagged *femT* porter domain; Km$^R$ | This study |
| pET*farE* | *farE* porter domain cloned in *Nde*I and *BamH*I sites for overexpression of 6xHis-tagged *farE* porter domain; Km$^R$ | This study |

Abbreviations: Amp$^R$ – ampicillin resistance; Cm$^R$ – chloramphenicol resistance; Tet$^R$ – tetracycline resistance; Km$^R$ – kanamycin resistance.

## 2.2 DNA Methodology

### 2.2.1 Plasmid Isolation from *E. coli*

Plasmid DNA from *E. coli* strains was isolated using the Presto™ Mini Plasmid Kit (Geneaid) following the instructions provided by the manufacturer. Briefly, 3 mL of *E. coli* culture at stationary phase was pelleted via centrifugation and then resuspended in 200 μL Solution I (50 mM Tris, pH 8.0, 20 mM EDTA, 100 μg/mL RNaseA). Cells were then lysed via the addition of 200 μL Solution II (200 mM NaOH, 1% w/v SDS), and then incubated for 2 minutes until lysate became homogenous. The solution was then neutralized with the addition of 300 μL Solution III (guanidine hydrochloride with acetic acid), and inverted several times until a flocculent precipitate formed. Subsequently, samples were centrifuged for 8 minutes at 14,500 × g to pellet the insoluble precipitate. The supernatant was then transferred to a column and centrifuged for 1 minute. To wash the column, 600 μL of Wash Buffer diluted with absolute ethanol was then added to the column and centrifuged for an additional minute. The column was then centrifuged for 3 minutes to dry and remove any remaining ethanol. Plasmid DNA was then eluted from the column and into a microcentrifuge tube by the addition of 30 μL elution buffer (10 mM Tris-HCl, pH 8.5) to the column, and subsequent centrifugation at 14,500 × g for 2 minutes.

### 2.2.2 Plasmid Isolation from *S. aureus*

Plasmid DNA isolation from *S. aureus* was accomplished following the same protocol as described for *E. coli*, with the following one modification. The pellet of 3 mL *S. aureus* culture at stationary phase was resuspended in 200 μL Solution I with the addition of 50 μg/mL lysostaphin. Cells were then incubated at 37°C for 30 minutes to lyse the cells prior to addition of Solution II.

### 2.2.3 Chromosomal DNA Isolation from *S. aureus*

Chromosomal DNA from *S. aureus* was prepared using the GenElute™ Bacterial Genomic DNA Kit (Sigma) following the instructions provided by the manufacturer. In brief, 1.5 mL of *S. aureus* culture at stationary phase was pelleted via centrifugation and resuspended in 200 μL solution of $2.1 \times 10^6$ units/mL lysozyme (Sigma) supplemented with 50 μg lysostaphin. Cells were then incubated at 37°C for 30 minutes to allow for lysis. After incubation, 20 μL proteinase K and

200 µL Lysis Solution C were added to the cells, which were then vortexed and incubated at 50°C for 10 minutes. Simultaneously, a GenElute Miniprep Binding Column was prepared with the addition of 500 µL Column Preparation Solution and subsequent centrifugation at 13,000 × g. The cell lysate was then prepared for binding by the addition of 200 µL absolute ethanol, followed by 10 seconds of vortex prior to loading into the Binding Column. The column was then centrifuged at 5,000 × g for elution. To wash away protein contaminants, 500 µL of Wash Solution 1 was added to the column, followed by centrifugation at 5,000 × g. Afterwards, the column was loaded with Wash Solution Concentrate (containing 70% ethanol) and centrifuged for 3 minutes at 13,000 × g to dry the column. Genomic DNA was then eluted into a new microcentrifuge tube by the addition of 100 µL elution solution to the column and subsequent centrifugation at 5,000 × g for 1 minute.

### 2.2.4 Restriction Enzyme Digestions

All restriction enzymes used in this study were purchased from New England Biolabs (NEB). Digestions occurred in 25 µL volumes and were incubated for 2-4 hours at 37°C. Digested DNA was cleaned using a GenepHlow™ Gel/PCR Kit (Geneaid) following instructions provided by the manufacturer. Briefly, 125 µL Gel/PCR Buffer was added to each digestion reaction and mixed by vortex. The sample mixture was then added to a DFH Column and centrifuged at 14,500 x g for 1 minute. To wash the column, 600 µL of Wash Buffer diluted with absolute ethanol was added, and contents were centrifuged at 14,500 × g for 1 minute. The column was then centrifuged for 3 minutes to dry and remove any remaining ethanol. DNA was then eluted from the column and into a microcentrifuge tube by the addition of 30 µL elution buffer (10 mM Tris-HCl, pH 8.5) to the column, and subsequent centrifugation at 14,500 × g for 2 minutes.

### 2.2.5 DNA Ligations

DNA ligations were accomplished using T4 DNA ligase purchased from NEB. In brief, DNA fragments were ligated in 20 µL volumes and were incubated at room temperature overnight. Briefly, a 20 µL reaction was composed of 2 µL 10 × T4 DNA ligase reaction buffer, 1 µL T4 DNA ligase ($4 \times 10^5$ units/mL), and a 5:1 molar ratio of insert to vector.

### 2.2.6 Agarose Gel Electrophoresis

Agarose gel electrophoresis was used for separation and visualization of DNA fragments. Agarose gels (0.8% w/v) were prepared using a 1 × TAE buffer (40 mM Tris acetate, 1 mM EDTA) supplemented with 1.5 μg/mL ethidium bromide (Sigma) to allow visualization. To run gels, DNA samples, typically 5 μL, were mixed with 6× loading buffer and added into the well of the gel. Electrophoresis was performed utilizing a BioRad PowerPac 300 set at 120 V and samples were run for 30-40 minutes. A 1 kb ladder (NEB) was utilized to determine DNA fragment size. DNA fragments were visualized using a Syngene G-Box.

### 2.2.7 DNA Isolation from Agarose Gels

To isolate specific DNA fragments from restriction enzyme digestions, fragments were visualized with UV light and extracted from 0.8% w/v agarose gels with razor blades. DNA fragments were then cleaned using a GenepHlow$^{TM}$ Gel/PCR Kit (Geneaid) following instructions provided by the manufacturer. Briefly, DNA fragments were excised from the agarose gel, and gel slices were transferred to a 1.5 mL microcentrifuge tube. Next, 500 μL of Gel/PCR Buffer was added to the tube and mixed by vortex. Samples were then incubated at 55-60°C for 10-15 minutes to completely dissolve the agarose gel slices. Once the dissolved sample cooled to room temperature, the mixture was added to a DFH column and centrifuged at 14,500 × g for 1 minute. Flow-through was discarded and 400 μL W1 Buffer was added to the column and centrifuged for an additional minute. Next, 600 μL Wash Buffer diluted with absolute ethanol was added to the column and contents were centrifuged at 14,500 × g for 1 minute. The column was then centrifuged for an additional 3 minutes to dry and remove any remaining ethanol. DNA was then eluted from the column and into a microcentrifuge tube by the addition of 30 μL elution buffer (10 mM Tris-HCl, pH 8.5), and subsequent centrifugation at 14,500 × g for 2 minutes.

### 2.2.8 Polymerase Chain Reaction (PCR)

PCR reactions occurred in 50 μL volumes following protocols outlined by GenScript. A 50 μL reaction was composed of 5 μL 10 × Taq buffer containing $Mg^{2+}$, 1 μL 10 mM dNTP, 1 μL forward primer (100 μM), 1 μL reverse primer (100 μM), 1 μL template DNA (1-100 ng/μL), 40.5 μL sterile Milli-Q water, and 0.5 μL Taq polymerase (5 units/μL). Oligonucleotides used in this study are listed in Table 2.2. PCRs were carried out utilizing a PTC-100 Programmable Thermal Controller (MJ Research Inc.) optimized for specific primer annealing temperatures and DNA fragment lengths.

### 2.2.9 Nucleotide Sequencing

Nucleotide sequencing was performed at the London Regional Genomics facility of the Robarts Research Institute (London, ON) with samples prepared according to their specifications. In brief, 10 µL DNA (50-150 ng/µL) and 5 µL oligonucleotide primer (20 µM) were combined and sent for analysis.

### 2.2.10 Computer Analyses

Analyses of sequenced DNA and designing of primers were completed with MacVector (MacVector, Inc, Cambridge, United Kingdom). Protein and DNA BLAST searches were accomplished utilizing the National Center for Biotechnology Information (NCBI) website (http://blast.ncbi.nlm.nih.gov/Blast.cgi).

**Table 2.2** Oligonucleotides used in this study

| **Primer Name** | **Sequence**[a] |
|---|---|
| FemTUP_SacII[b] | ggacctccgcggCTTATTCCCTAAAGAAAATTGTAATAGC |
| FemTUP_attB1[c] | *attB1*-CAAAAGACTACATCCAACCACG |
| FemTDW_SacII[b] | ggacctccgcggACACTTGTAGTTGTACCAGT |
| FemTDW_attB2[d] | *attB2*-TGTTCTGTCACTGTTATCCCTTC |
| femT_Del_F2 | GTGAACATGGTGCAACAACTTACG |
| femT_Del_R2 | GTCGGTAATGTCGAAGTGACAGG |
| femT-DEL_For | CGAAGAATCGCTGTAGGTCGTGAC |
| femT-DEL_Rev | TTCCAAACATCACAAAGGCACC |
| pALCfemT_FP[e] | ggttgagtaaaatatttttggagctcGTGAAAGAGGGGGAAGTACTGTG |
| pALCfemT_RP[e] | cggattacatgttgagctcCAGTATTGTTTTATTAACACATCG |
| GYfarE_F[f] | cccggatccTTGTACGGTGTACGAGTGCG |
| GYfarE_R[g] | cccgtcgacCGGTGCATTTGTAGCAAGTG |
| femT::lux_Bam[f] | gattatgtattgaatcagccatggatccAATTAATTGAGCAAGTTAAACC |
| femT::lux_Sal[g] | ctaatttcaatttagcagtcgacTATACACCGCCCAAGA |
| femT_Port F[h] | aacacagctagcTTTGGAGGACCGAGACTAGGCAC |
| femT_Port R[f] | aacacaggatccATCTGATGCACCACCGATATTAACC |
| MMP_pET28_FP[i] | ctgcattaacgcatatgTTTGGAAAAGGT |
| MMP_pET28_RP[f] | cccggatccGTCATTGATAGACATTTAAA |

[a] Lower case denotes 5′ additions. Restriction sequences are underlined.
[b] *Sac*II
[c] *attB1* site for cloning in pKOR1: GGGGACAAGTTTGTACAAAAAAGCAGGCT
[d] *attB2* site for cloning in pKOR1: GGGGACCACTTTGTACAAGAAAGCTGGGT
[e] *Sac*I
[f] *BamH*I
[g] *Sal*I
[h] *Nhe*I
[i] *Nde*I

## 2.3 Transformation Methodologies

### 2.3.1 Preparation of Transformation Competent *E. coli*

Calcium chloride competent *E. coli* DH5α or BL21 (DE3) cells were prepared for transformation following an established lab protocol (151). Briefly, the optical density (OD) of overnight stationary phase DH5α cells was measured at 600 nm wavelength ($OD_{600}$) using a Beckman Coulter spectrophotometer, and the volume equivalent of 0.01 $OD_{600}$ was sub-cultured into 400 mL LB. When this culture reached mid-exponential phase ($OD_{600}$ ~0.5), cells were placed on ice to cool for 20 minutes. The culture was then pelleted at 4,000 × g at 4°C for 10 minutes, and washed through resuspension in 100 mL ice cold 0.1 M $CaCl_2$ containing 15% glycerol (v/v). This mixture was then left on ice for 30 minutes and centrifuged again to pellet cells. After centrifugation, the supernatant was discarded and the pellet was resuspended in 4 mL 0.1 M $CaCl_2$, 15% glycerol (v/v) to aliquot into 100 µL volumes. Competent cells were then flash frozen and placed in a -80°C freezer for storage until future use.

### 2.3.2 Transformation of Competent *E. coli*

Calcium chloride competent *E. coli* DH5α or BL21(DE3) cells were transformed with plasmid prepared via techniques described above. Once prepared, 5 µL plasmid or 10 µL ligation mixture was added to an aliquot of thawed competent *E. coli* cells and incubated on ice for 30 minutes. Subsequently, cells were heat shocked at 42°C for 2 minutes to allow DNA to enter the cells, followed by a 2-minute incubation on ice. Cells then received 900 µL LB containing relevant antibiotics at a 1/10 dilution and left to resuscitate at 37°C. Cells were incubated for 1 hour to allow recovery before plating on LB agar containing selective antibiotics. Plates were grown overnight at 37°C and examined for single colonies the following day.

### 2.3.3 Preparation of Transformation Competent *S. aureus*

Electro-competent *S. aureus* RN4220, USA300, and USA300 derivatives were prepared for transformation utilizing established lab protocols (146). Overnight stationary phase *S. aureus* cells were used to inoculate 400 mL TSB to an $OD_{600}$ of 0.01. When this culture reached mid-exponential phase ($OD_{600}$ ~ 0.5), cells were placed on ice to cool for 10 minutes. The culture was then pelleted at 4,000 × g at 4°C for 10 minutes, and washed through resuspension in 40 mL ice cold 0.5 M sucrose. This mixture was then left on ice for 20 minutes and centrifuged again to pellet cells. After centrifugation, the cell pellet was resuspended in 5 mL 0.5 M sucrose, and centrifuged a second time. The new pellet was then resuspended in 4 mL 0.5 M sucrose and aliquoted into 100 µL volumes. Competent cells were then flash frozen and placed in a -80°C freezer for storage until future use.

### 2.3.4 Transformation of Competent *S. aureus*

Electro-competent *S. aureus* cells were transformed with plasmid extracts prepared from other cells. All recombinant plasmids were first constructed as shuttle vectors in *E. coli* DH5α. The integrity of plasmids isolated from *E. coli* was confirmed by restriction enzyme digestion and nucleotide sequencing of the cloned DNA fragments, as described previously, prior to introduction into *S. aureus* RN4220. Importantly, RN4220, a restriction endonuclease deficient strain, could be transformed with plasmid from *E. coli* and was used as an intermediate host prior to introduction into USA300 and its isogenic variants. To transform competent *S. aureus*, 3 µL of plasmid was added to an aliquot of thawed competent cells and incubated on ice for 30 minutes. The cell mixture was then transferred to a col 2 mm electroporation cuvette (VWR) and electroporated using a Bio-Rad Gene Pulser II, set to 2.5 KV, 200 Ω, and 25 µF. Electroporated cells then received 900 µL TSB containing relevant antibiotics at a 1/10 dilution and left to resuscitate at 37°C. Cells were incubated for 1 hour to allow recovery before plating on TSA containing selective antibiotics. Strains transformed with larger plasmids (>10 kb) were plated with top agar (0.8% agar) to provide a slower introduction to antibiotics. Plates were grown overnight and examined for single colonies the following day.

## 2.4 Mutagenesis and DNA Cloning Methods

### 2.4.1 Generation of an In-Frame Mutation

Deletion of the *femT* gene was generated utilizing the temperature sensitive plasmid pKOR1 (149). This plasmid possesses several important features to allow in-frame deletion of genes, including the *cat* gene to encode chloramphenicol resistance for positive selection, the *attP* sequences to allow recombination with genetic material possessing *attB* sequences, and the *repF* gene to permit replication at 30°C, but not at 42°C. It also possesses a *tetR* and *secY570* cassette to allow for negative selection utilizing anhydrotetracycline (aTc), which drives production of antisense *secY* that inhibits bacterial growth and survival. For construction of a *femT* deletion, two sequences of approximately 1 kb flanking the *femT* gene were amplified with the primers FemTUP_attB1 and FemTUP_SacII for the upstream segment, and FemTDW_SacII and FemTDW_attB2 for the downstream segment (Figure 2.1). Once amplified, the downstream and upstream segments were digested with *Sac*II and ligated to produce a fusion of the upstream and downstream segments flanking *femT*. This 2-kb construct was then cloned into pKOR1 through site-specific recombination between the *attP* and *attB* sites utilizing Gateway® BP Clonase II (Life Technologies) following instructions provided by the manufacturer. In brief, DNA fragments were recombined in a 10 μL reaction volume containing 15-150 ng *attB* product, 1 μL BP Clonase II, 150 ng pKOR1 plasmid, and TE buffer. The reaction was incubated for 4 hours at room temperature, generating pKORΔ*femT*. The plasmid was subsequently transformed into *E. coli* DH5α and after confirmation by *Sac*II digestion and nucleotide sequencing of the cloned fragment, was transformed into *S. aureus* strain RN4220 as described previously. After selection for chloramphenicol resistant colonies at 30°C, plasmid was extracted and transformed into wild-type USA300 and USA300Δ*farER* through electroporation. To promote integration of pKORΔ*femT* into the target gene via homologous recombination, 3 mL cultures were incubated at 32°C for 2 hours, after which the temperature was increased to 42°C. After overnight incubation, cells were plated on TSA supplemented with chloramphenicol and incubated at 42°C to select for integration of the plasmid with the target gene. Single colonies were then selected and grown at 30°C with shaking to allow the plasmid to excise from the chromosome. These cultures were then plated on TSA with aTc (20 μg/mL) to select for colonies cured of the plasmid, as the lethal antisense *secY* on pKOR1 is induced by aTc. Colonies were subsequently screened for sensitivity to chloramphenicol, confirming the removing of the plasmid. Deletion of *femT* in both USA300 and USA300Δ*farER* was confirmed via PCR and nucleotide sequencing. An overview of *femT* mutant construction using pKOR1 is presented in Figure 2.2.

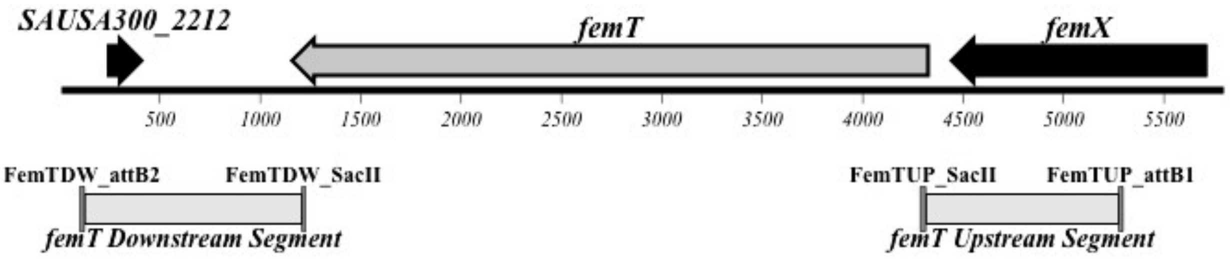
SAUSA300_2212
femT
femX
500
1000
1500
2000
2500
3000
3500
4000
4500
5000
5500
FemTDW_attB2
FemTDW_SacII
femT Downstream Segment
FemTUP_SacII
FemTUP_attB1
femT Upstream Segment

**Figure 2.1 Genetic organization of the *femT* region for pKOR1 markerless mutagenesis.** Map of *femT* (SAUSA300_2213) with primers annotated for pKOR1 mutagenesis. The region between the *femT* upstream and downstream segments are ligated together following SacII digestion. *attB* sites are located on each end of the upstream and downstream segments.

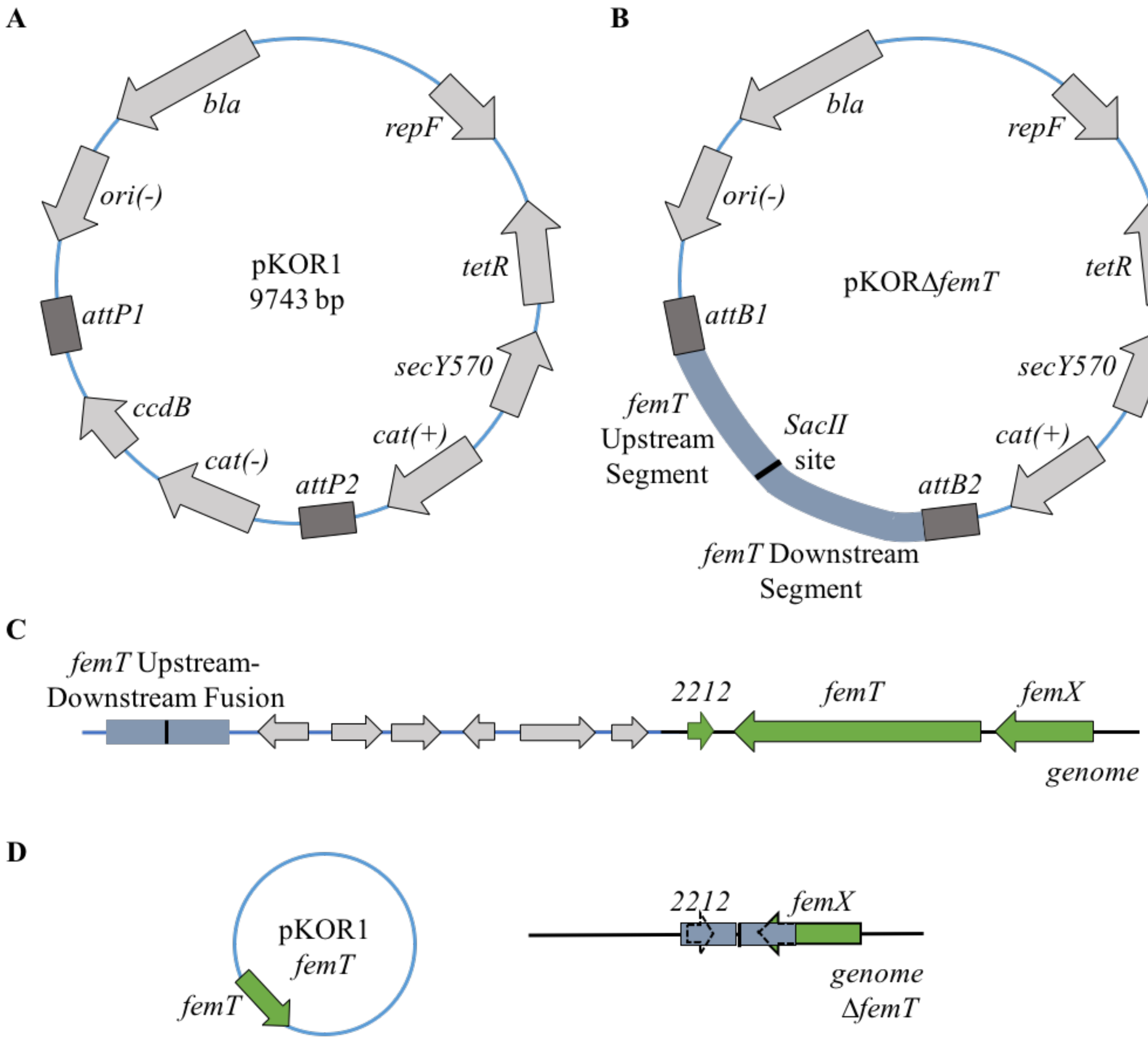
A
bla
repF
ori(-)
pKOR1
9743 bp
tetR
attP1
secY570
ccdB
cat(+)
cat(-)
attP2
B
bla
repF
ori(-)
pKORΔfemT
tetR
attB1
secY570
femT
Upstream
Segment
SacII
site
cat(+)
attB2
femT Downstream
Segment
C
femT Upstream-
Downstream Fusion
2212
femT
femX
genome
D
pKOR1
femT
femT
2212
femX
genome
ΔfemT

**Figure 2.2 Construction of *femT* mutant using pKOR1 markerless mutagenesis.** (A) Map of the pKOR1 plasmid. pKOR1 encodes *repF* (replication gene), *secY570* (N-terminal 570 nucleotides of *secY*), *cat* (chloramphenicol acetyltransferase), *attP* (phage lambda attachment site), *ori(-)* (plasmid replication origin), and *bla* (β-lactamase). *attP* sequences allow recombination with *attB* sequences. (B) Map of pKOR1 with Δ*femT* fusion inserted; not to scale. (C) Hypothetical integration of pKORΔ*femT* into the genome by homologous recombination. Blue and grey shapes represent genes in the pKOR1 plasmid, while the green arrows indicate genes present in the USA300 genome. (D) The pKOR1 plasmid is excised with genomic *femT*, resulting in the deletion of *femT* and the insertion of the upstream-downstream fusion in the genome. Bacteria were then selected for plasmid loss.

### 2.4.2 Construction of pGY*lux* Reporter Strains

To construct pGY*farE::lux* and pGY*femT::lux* reporter strains, where the promoter of *farE* or *femT* drives expression of the luciferase operon, a fragment containing the promoter site of the gene was first amplified. For pGY*farE::lux*, a 396-bp fragment containing the promoter site for *farE* was amplified via PCR with the primers GYfarE_F and GYfarE_R (Table 2.2). For pGY*femT::lux*, the primers femT::lux_Bam and femT::lux_Sal were used to amplify a 276-bp fragment containing the predicted promoter site of *femT*. After PCR amplification, clean up, and digestion with endonucleases *BamH*I and *Sal*I, these segments were ligated into pGY*lux*, which had previously been digested with *BamH*I and *Sal*I. Both recombinant plasmids were first constructed as shuttle vectors in *E. coli* DH5α. The integrity of plasmids isolated from *E. coli* was confirmed by restriction enzyme digestion and nucleotide sequencing of the cloned DNA fragments prior to electroporation into *S. aureus* RN4220 as an intermediate host. From RN4220, the individual plasmids were then introduced, via electroporation, into USA300 or isogenic derivatives as required.

### 2.4.3 Construction of pET28 Recombinant Plasmids

To construct pET*femT* and pET*farE* recombinant plasmids, primers were designed according to the porter domain sequence of *femT*, and the C-terminal cytoplasmic segment of *farE*. For the porter domain of *femT*, a 900-bp fragment was amplified via PCR with the primers femT_Port F and femT_Port R (Table 2.2). For amplification of the C-terminal cytoplasmic domain of *farE*, a 471-bp fragment was amplified using the primers MMP_pET28_FP and MMP_pET28_RP. After PCR amplification, clean up, and digestion with endonucleases *Nhe*I and *BamH*I for *femT*, and *Nde*I and *BamH*I for *farE*, these segments were ligated into pET28a(+), which was digested with the same restriction enzymes, generating the recombinant plasmids pET*femT* and pET*farE*. The *E. coli* strain BL21 (DE3) was used for transformation of both recombinant plasmids. The transformed bacteria were selected by screening the colonies on kanamycin (50 µg/mL) containing media and subsequent plasmid purification. Positive colonies were confirmed by restriction enzyme digestion and nucleotide sequencing.

### 2.4.4 Complementation of Mutants

To restore *femT* in deficient strains, the vector pALC2073 was used. Briefly, PCR conducted with primers pALCfemT_FP and pALCfemT_RP (Table 2.2) was performed to amplify *femT*. This product was then digested with *Sac*I and ligated into the pALC2073 shuttle vector, creating pALC*femT*. After transformation into *E. coli* DH5α, colonies were screened through restriction enzyme digest and sequencing to determine the orientation of the *femT* insert with respect to the *xyl/tetO* promoter. Fragments confirmed in the correct orientation were then electroporated into RN4220 before being introduced into USA300 isogenic derivatives. To induce expression of *femT* from the *xyl/tetO* promoter, 20 ng/mL aTc was added to cultures containing pALC*femT*.

## 2.5 Protein Methodologies

### 2.5.1 SDS-PAGE

Proteins in culture were assessed using sodium dodecyl sulfate polyacrylamide gel electrophoresis (SDS-PAGE) (152). Protein samples were prepared and resuspended in 1 × Laemmli loading buffer (4 × buffer: 240 mM Tris-Cl pH 6.8, 8% w/v SDS, 40% v/v glycerol, 20% β-mercaptoethanol, 0.01% bromophenol blue and milli-Q water). The entire sample and a pre-stained protein ladder (Frogga Bio) were then loaded into a 12% bis-acrylamide gel and run at 100 V for approximately 90 minutes. The separated protein bands were then stained for 18 hours with Coomassie blue stain for visualization, or transferred onto a membrane for Western blotting. Stained gels were then destained with buffer composed of 40% methanol, 10% acetic acid, and 50% $dH_2O$ by volume, and visualized.

### 2.5.2 Expression and Purification of Recombinant FemT and FarE

For purification of FemT and FarE, a single colony of *E. coli* BL21 (DE3) with pET*femT* or pET*farE* was incubated in 30 mL LB, containing 50 µg/mL kanamycin, overnight at 37°C with shaking. The next day, the entire 30 mL culture was added to 1 L LB broth and grown at 37°C with shaking to an $OD_{600}$ of ~0.7. Isopropyl-β-D-thiogalactopyranoside (IPTG) was then added to a final concentration of 0.5 mM for expression of FemT and FarE. The cells were then grown for an additional 18 hours at room temperature with shaking, after which cells were collected via centrifugation at 3,000 × g for 12 minutes at 4°C. The cell pellets were then resuspended in 30 mL binding buffer (10 mM Tris-HCl pH 8.0, 300 mM NaCl, 10 mM imidazole, filter sterilized). The cells were then lysed using a cell disrupter (Constants Systems Ltd.) at 30 psi, and cultures were centrifuged at 4,000 × g for 15 minutes at 4°C. From this point, any remaining cellular debris in the BL21 (DE3) pET*femT* culture was removed by ultracentrifugation at 50,000 × g for 45 minutes at 4°C in a Beckman Coulter Optima® L-900K ultracentrifuge. For BL21 (DE3) cultures containing pET*farE*, the pelleted debris after cell disruption was resuspended in 30 mL buffer B (100 mM $NaH_2PO_4$, 10 mM Tris-Cl, 8 M urea, adjusted to pH 8.0) for denaturing conditions to solubilize inclusion bodies. The pellet was incubated in buffer B for 1 to 2 hours with agitation prior to ultracentrifugation at 50,000 × g for 45 minutes at 4°C in a Beckman Coulter Optima® L-900K ultracentrifuge. After ultracentrifugation, the soluble lysate of both cultures was passed through a 0.45 µM nylon filter (VWR) before being passed through a nickel-loaded 1-mL HisTrap column (GE Healthcare) equilibrated with binding buffer or urea buffer for FemT and FarE samples, respectively. The 6×His-tagged FemT protein was eluted from the column with a gradient of 0.1 M to 0.5 M imidazole. Conversely, FarE protein was eluted from the column with two passes of buffer B adjusted to pH 5.9, and two passes of buffer B adjusted to pH 4.5. Eluted fractions were analyzed via SDS-PAGE on a 12% bis-acrylamide gel run at 100 V for approximately 90 minutes to determine which fractions contained the highest amount of purified protein. FemT fractions eluted with 0.2, 0.3, and 0.4 M imidazole were then combined, and FarE fractions eluted with the second pass of buffer B pH 5.9 and both passes of buffer B pH 4.5 were combined. Combined fractions were then dialyzed overnight at 4°C against 10 mM Tris pH 8.0. Protein purity was then confirmed using SDS-PAGE, described above, and protein concentrations were determined through Bradford assay using the Bio-Rad Protein Assay Dye (Bradford) Reagent Concentrate (5X). Samples were read at absorbance $OD_{595}$ and a standard curve was made for each concentration determination with 1 mg/mL bovine serum albumin (BSA).

### 2.5.3 Western Blot

Rabbit polyclonal antisera recognizing FarE and FemT were generated by ProSci (Poway, CA) with protein prepared as described above. For blots with FemT antisera, single colonies of *S. aureus* USA300 or its isogenic variants were inoculated in 3 mL TSB, supplemented with antibiotics, if necessary, and incubated at 37°C for 8 hours with shaking. Cultures were then sub-cultured into 25 mL TSB at a volume equivalent to 0.01 $OD_{600}$ and incubated at 37°C for 18 hours with shaking. Conversely, for blots with FarE antisera, single colonies of *S. aureus* USA300 or its isogenic variants were inoculated in 3 mL TSB, supplemented with antibiotics, if necessary, and incubated at 37°C for 18 hours with shaking. Cultures were then sub-cultured at a volume equivalent to 0.01 $OD_{600}$ into 25 mL TSB supplemented with 20 µM LA (Sigma) and 0.1% DMSO (v/v) (Sigma), and incubated at 37°C to mid-exponential phase, or an $OD_{600}$ of ~0.5. After incubation, all cultures were harvested by centrifugation at 3,000 × g for 15 minutes, and cells were washed with 1 × PBS to remove residual media. After additional centrifugation, the pellet was resuspended in 3 mL lysis buffer (150 mM NaCl, 5 mM EDTA pH 8.0, 50 mM Tris-HCl pH 8.0, 1% (v/v) Triton X-100, 0.5% (v/v) SDS, 5 µg lysostaphin) and incubated at room temperature for 2 hours with agitation. Samples were then centrifuged at 4,200 × g for 20 minutes and supernatant was collected in a new tube. Protein concentrations were determined through Bradford assay using the Bio-Rad Protein Assay Dye (Bradford) Reagent Concentrate (5X). Samples were read at absorbance $OD_{595}$ and a standard curve was made for each concentration determination with 1 mg/mL BSA. Samples were then aliquoted in volumes equal to 25 µg protein along with 10 µL 1 × Laemmli buffer and mixed by vortexing. This mixture was then incubated at 37°C for 30 minutes and loaded onto a 10% bis-acrylamide gel and separated by SDS-PAGE.

Resulting protein bands on the gel were then transferred onto a FluoroTrans PVDF membrane (PALL Life sciences) in a system submerged in transfer buffer consisting of 200 mL methanol, 14.4 g glycine, and 3.03 g of Tris filled to 1 L with $dH_2O$ (153). The membrane was then incubated overnight with blocking buffer (1 g skim milk powder (EMD) with 20 mL with 1 × PBS). The next day, the membrane was incubated in 25 mL 1 × PBS supplemented with 0.1% tween20 (Sigma) (PBS-T) and 0.5 g skim milk powder with rabbit polyclonal antiserum diluted 1:1000 and incubated for 2 hours at room temperature. After incubation, the membrane was washed three times with PBS-T for 10-minute time periods. The blot was then incubated for another 2 hours at room temperature with secondary antibody, anti-rabbit IgG conjugated to IRDye 800 (Li-Cor Biosciences, Lincoln, NE), at a 1:20000 dilution. After incubation, the blot was washed three time with PBS-T for 10-minute periods, and washed a final time with 1 × PBS for 10 minutes prior to scanning on a Li-Cor Odyssey Infrared Imager (Li-Cor Biosciences) and visualized using Odyssey V3.0 software.

## 2.6 Experimental Methodologies

### 2.6.1 Growth Analysis

To evaluate the effect of different conditions on the growth of *S. aureus* USA300 or its isogenic variants, overnight cultures were inoculated into 25 mL volumes of media at the volume equivalent of 0.01 $OD_{600}$ and supplemented with indicated concentrations of fatty acids or other reagents. Unless otherwise indicated, all growth assays were conducted in 125 mL Pyrex Erlenmeyer flasks and cultures were incubated in a 37°C incubator with orbital shaking at 180 rpm. Measurements of $OD_{600}$ were taken at hourly intervals. Liquid growth media used for analysis included Mueller-Hinton broth (MHB; Sigma), brain-heart infusion (BHI; VWR) broth, and Roswell Park Memorial Institute (RPMI; Gibco) broth. All solutions and media were made using water purified with Milli-Q water purification system (Millipore).

### 2.6.2 Bactericidal Assays

Overnight pre-cultures were inoculated at a volume equivalent to 0.01 $OD_{600}$ into flasks containing 25 mL TSB supplemented with 20 µM LA (Sigma) and 0.1% DMSO (v/v) to ensure fatty acid dissolution. A 5-mM stock solution of LA was produced by diluting pure fatty acids in 5 mL TSB with vigorous vortexing. These cultures were then grown to mid-exponential phase (2-3 hours; $OD_{600}$ ~0.5) and inoculated into 25 mL fresh TSB containing a bactericidal (100 µM) concentration of LA and 0.1% (v/v) DMSO and grown at 37°C with shaking. To determine bactericidal activity, aliquots were withdrawn at hourly intervals, and diluted and plated on TSA at $10^0$ to $10^3$ dilutions with quadruplicate technical replicates. After incubation overnight, colonies were counted and viable CFU/mL counts were determined.

### 2.6.3 Luciferase Assays

Luciferase assays were conducted using growth analysis conditions described above. Cultures harboring pGY*lux*, pGY*femT::lux*, or pGY*farE::lux* plasmids were prepared in triplicate flasks and grown in specified conditions. At indicated time points, aliquots were removed from each culture for $OD_{600}$ measurements, and concurrently, 4 × 200 µL technical replicates were withdrawn from each flask for quantification of luciferase activity. Specifically, each 200 µL aliquot was added to individual wells of a flat-bottom, opaque white 96-well microtiter plate (Greiner Bio-One). The wells were then supplemented with 20 µL 0.1% (v/v) decanal in 40% ethanol, followed by immediate measurement of luminescence utilizing a Biotek Synergy H4 Hybrid Reader, with an integration time of 1 second and a gain of 200. Luminescence background was removed from the relative light unit (RLU) measurements by averaging the technical replicates and subtracting the observed RLU from the promoterless pGY*lux* reporter. These data were then standardized by dividing individual RLU readings with the $OD_{600}$ reading of the culture, producing RLU/$OD_{600}$ measurements.

### 2.6.4 Lysis Assays

Cultures of *S. aureus* USA300 or its isogenic variants were grown in 3 mL TSB overnight at 37°C. Cells were then inoculated at a volume equivalent to 0.01 $OD_{600}$ into flasks containing fresh 25 mL TSB and grown with shaking at 37°C to an $OD_{600}$ of ~1.0. Cells were harvested by centrifugation (4,000 × g; 10 min) and washed twice with phosphate-buffered saline (PBS). The pellet was then resuspended in either 1 × PBS to an $OD_{600}$ of 1.0, used as a control, or in 1 × PBS to an $OD_{600}$ of 1.0 in the presence of a cell wall stressor, including Triton X-100, lysostaphin, or lysozyme. Cultures were then incubated at 37°C with shaking. Cell lysis was measured as a decrease in $OD_{600}$ over time and represented as percent of initial $OD_{600}$, calculated by subtracting individual $OD_{600}$ readings at timely intervals with the initial $OD_{600}$ at time zero.

### 2.6.5 Antibiotic Susceptibility Assays

To evaluate the minimum inhibitory concentration (MIC) of several antibiotics, cultures of USA300 or its isogenic variants were grown in 3 mL MHB overnight at 37°C with shaking. Cells were then inoculated at a volume equivalent to 0.01 $OD_{600}$ into flasks containing fresh 25 mL MHB and grown with shaking at 37°C to an $OD_{600}$ of ~0.5, and turbidity was adjusted so that it was equal to that of a McFarland 0.5 standard. A total of 100 µL of the 0.5 McFarland suspension was plated on a Mueller-Hinton agar plate. When the surface of each plate had dried, one Epsilometer test (E-test) strip was placed in the centre of each plate. Plates were then incubated at 37°C for 24 hours. MICs in µg/mL were read directly from the test strip according to the instructions provided by the manufacturer, where the elliptical zone of inhibition intersected with the MIC scale on the test strip.

### 2.6.6 Statistical Analysis

All data generated by the assays described above were plotted using Graphpad PRISM software, version 6.0f. Significance at specific points was determined using unpaired one-tailed Student's *t*-tests utilizing the statistics portion of Graphpad PRISM.

# 3 Results

## 3.1 Evaluation of the Role of FemT in Cell Wall Synthesis

### 3.1.1 Deletion of the *femT* locus

The first objective of this study was to determine the role of the RND efflux pump encoded by *femT* (SAUSA300_2213). The *femT* gene is 3,168 bp and encodes a protein containing 1,055 amino acids, with a predicted molecular mass of 114.7 kDa. To assess the importance of FemT during growth, a *femT* deletion was constructed in a wildtype USA300 background, generating USA300Δ*femT*, and in a USA300 background with *farER* deleted, producing USA300Δ*farER-femT*, as described in the Materials and Methods section. A diagram of the *femT* locus with indicated primers for PCR screening is illustrated in Figure 3.1A. PCR amplification with the femT_Del_F2 and femT_Del_R2 primers across the *femT* locus of wildtype *S. aureus* USA300 and both mutants, USA300Δ*femT* and USA300Δ*farER-femT*, confirmed the deletion of *femT* in both strains (Figure 3.1B). With these PCR primers, the expected size of wild-type USA300 is 4,070 kb and the size of the product amplified for the *femT* deletions is expected to be 900 kb. In addition, the *femT* mutation was confirmed through nucleotide sequencing using primers further upstream and downstream of the *femT* locus, femT-DEL_For and femT-DEL_Rev. PCR was also used to confirm the deletion of *farER* once USA300Δ*farER-femT* was created. Western blot analysis of USA300, *femT* mutants, and complemented *femT* mutants was also performed with specific antibodies generated against FemT (Figure 3.1C). Membrane fractions of each sample were used for analysis, and 25 ng protein was loaded into each well for detection. Detected FemT protein was of expected size.

A

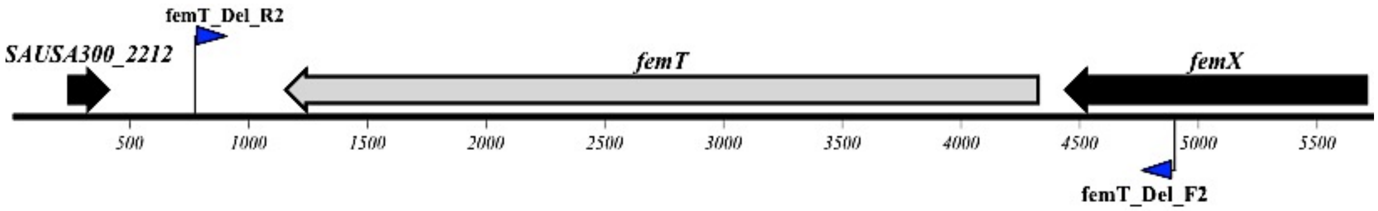
femT_Del_R2
SAUSA300_2212
femT
femX
500
1000
1500
2000
2500
3000
3500
4000
4500
5000
5500
femT_Del_F2

B

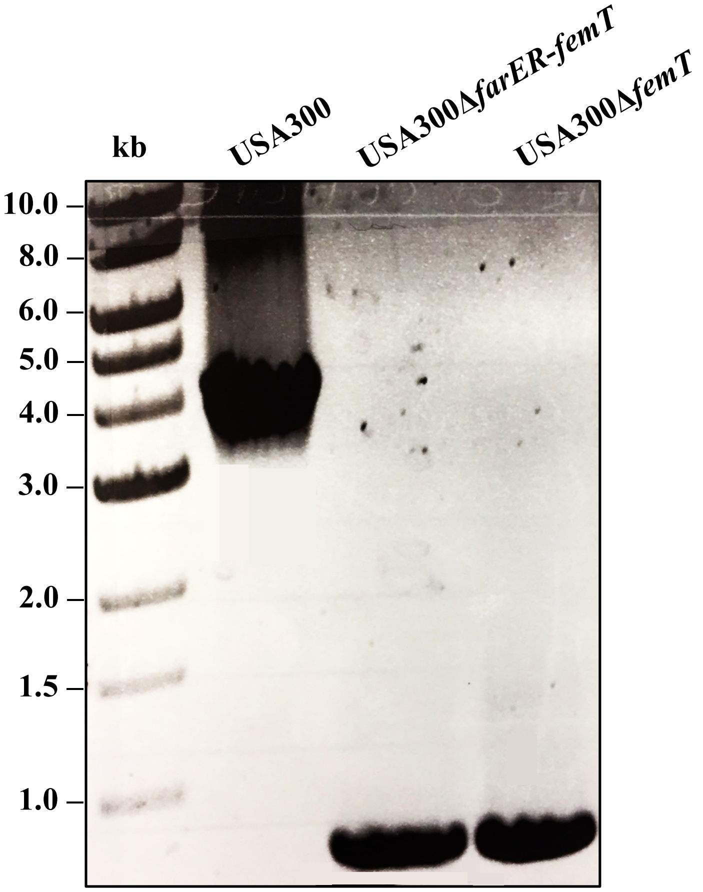
kb
USA300
USA300ΔfarER-femT
USA300ΔfemT
10.0
8.0
6.0
5.0
4.0
3.0
2.0
1.5
1.0

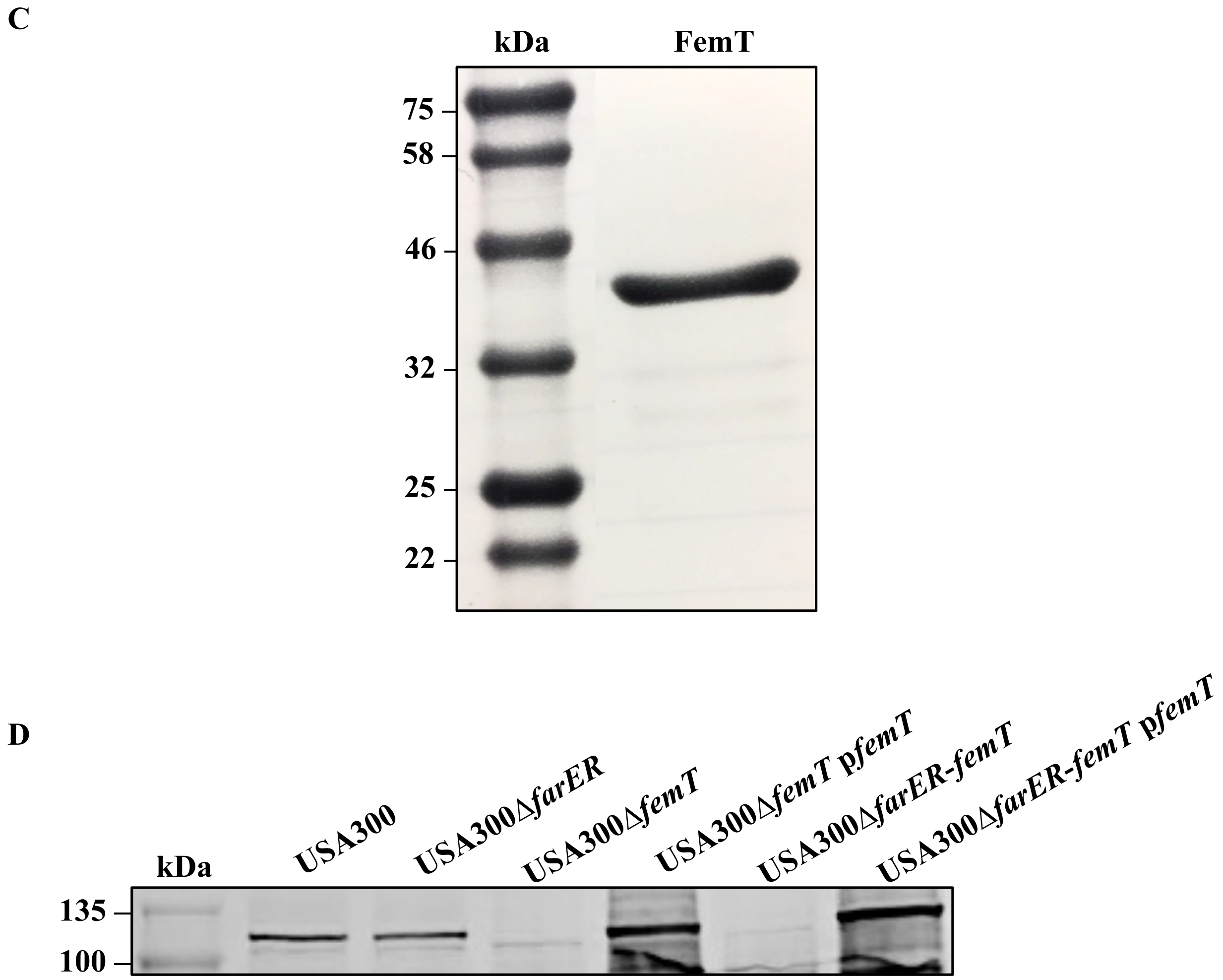
C
kDa
FemT
75
58
46
32
25
22
D
kDa
USA300
USA300Δ*farER*
USA300Δ*femT*
USA300Δ*femT* p*femT*
USA300Δ*farER-femT*
USA300Δ*farER-femT* p*femT*
135
100

**Figure 3.1 Confirmation of femT deletion.** (A) Map of the *femT* locus with primers, indicated by blue arrows, used for PCR amplification. (B) Genomic DNA of wildtype USA300 and the deletion mutants USA300Δ*farER-femT* and USA300Δ*femT* was used as a template for PCR with primers flanking the femT region. (C) SDS-PAGE stained with Coomassie blue for visualization of FemT porter domain used for antibody production. The predicted molecular mass of the FemT porter domain is 42 kDa. (D) Western blot with FemT antisera confirming the deletion and complementation of *femT*. Membrane fractions of each sample were used for detection; 25 µg of protein was loaded into each well. The predicted molecular mass of FemT is 114.7 kDa.

### 3.1.2 Deletion of *femT* improves growth of USA300 in Mueller-Hinton broth

To assess the importance of FemT on the growth of USA300, cultures of USA300 and RND pump mutants USA300Δ*farER*, USA300Δ*femT* and USA300Δ*farER-femT* were grown in different types of media. Specifically, four different types of liquid growth media were chosen for analysis, namely TSB, BHI broth, MHB, and RPMI media. TSB and BHI were chosen as nutritious, general-purpose growth media that are widely used for cultivating *S. aureus*. Conversely, MHB and RPMI media were chosen for comparison as they are more depleted in nutrients. More specifically, both MHB and RPMI lack glucose and contain only free amino acids as a source of protein, compared to TSB and BHI, which both contain glucose and more complex forms of protein such as peptone. Since glucose is not present in MHB and RPMI, *S. aureus* must grow on non-preferred carbon sources to facilitate gluconeogenesis. In addition, much antibiotic work employs Mueller-Hinton medium, and the fatty acid composition of *S. aureus* membrane glycerolipids has shown to be altered when grown in MHB compared to TSB (154). Upon analysis, no difference in growth was observed between USA300 and the three RND pump mutants in TSB, BHI, and RPMI media (Figure 3.2). However, when these strains were cultured in MHB, USA300Δ*femT* appears to reach the logarithmic phase of growth faster than wildtype USA300 and the two other mutants. Therefore, the deletion of *femT* does not affect the growth of USA300 in TSB, BHI, and RPMI, but does, however, improve growth of USA300 in MHB.

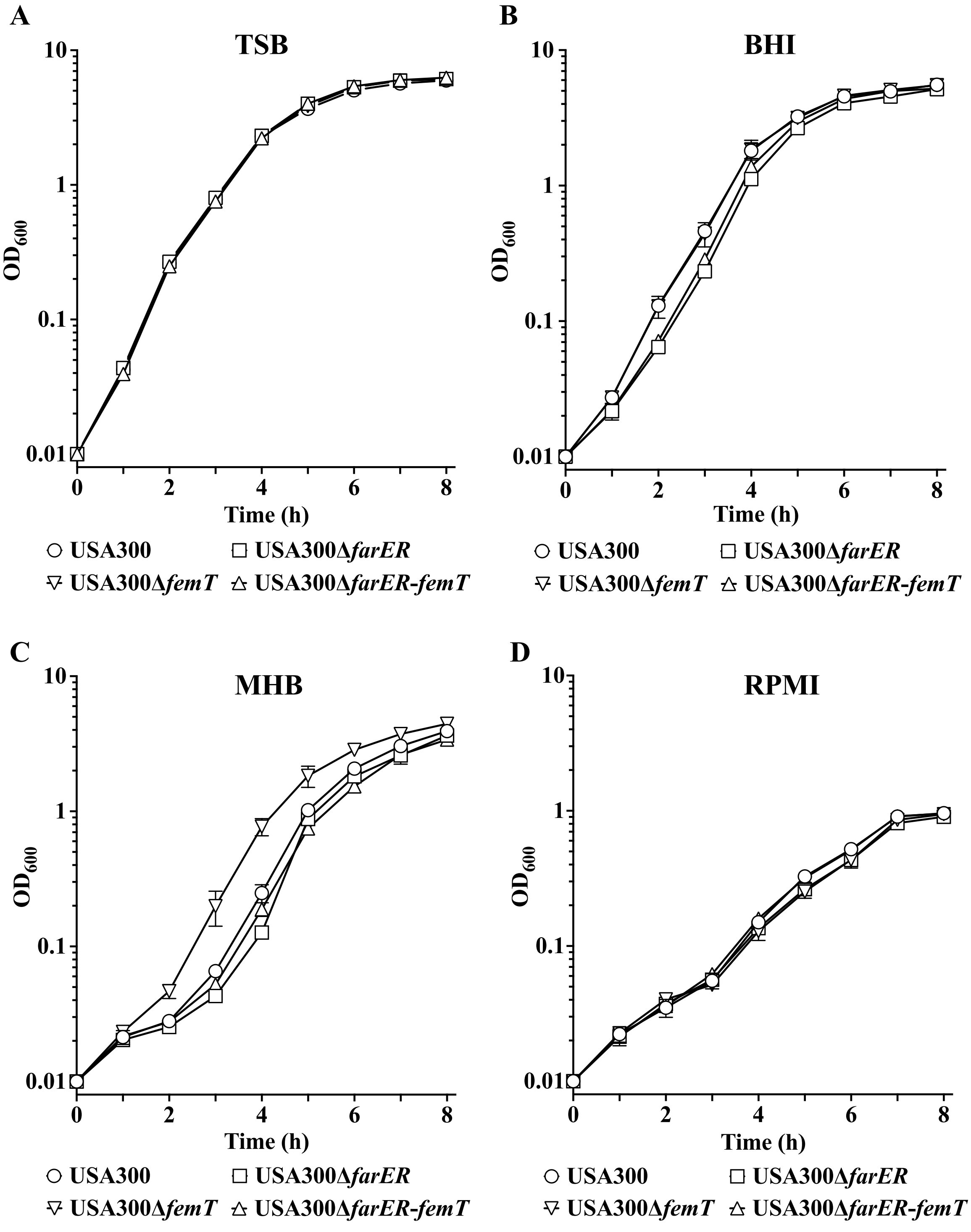

**Figure 3.2 Growth analysis of USA300 and RND pump mutants in TSB, BHI, MHB, and RPMI.** Growth of USA300, USA300Δ*farER*, USA300Δ*femT* and USA300Δ*farER-femT* cultured in (A) TSB, (B) BHI, (C) MHB, and (D) RPMI. Each data point represents the mean value of triplicate cultures; error bars represent the standard error of the mean.

### 3.1.3 USA300Δ*femT* is more susceptible to lysostaphin

To test our hypothesis of FemT involvement in cell wall synthesis, we investigated the potential effect of two cell wall stressors on lysis of USA300 and USA300Δ*femT*. Cells were incubated with the metalloendopeptidase lysostaphin, which cleaves the cross-linking $Gly_5$ bridges in the cell wall, or incubated with the glycoside hydrolase lysozyme, which catalyzes the hydrolysis of 1,4-β-linkages between MurNAc and GlcNAc residues in peptidoglycan. The lytic activity of lysostaphin was compared between USA300 and USA300Δ*femT* to determine if the Gly–Gly bond in the $Gly_5$ crossbridge was altered in the mutant. Gründling *et al.* have demonstrated that truncations in staphylococcal cross bridges, of either one glycine or three glycine units, causes the observed increase in lysostaphin resistance of staphylococci (155). Additionally, Morikawa and co-workers using *S. aureus* N315 showed that cell wall thickness also plays important roles in lysostaphin sensitivity, whereby *S. aureus* cells with thinner envelopes demonstrated increased sensitivity to lysostaphin (156). Although *S. aureus* peptidoglycan is completely resistant to the hydrolytic activity of lysozyme, this is a function of a number of factors, including the wall teichoic acid composition, the degree of peptidoglycan cross-linking, and the degree of peptidoglycan acetylation (157). Therefore, sensitivity to lysozyme was also investigated as a potential marker of the influence of *femT* on cell wall integrity. To evaluate the sensitivity of USA300 and USA300Δ*femT* in both conditions, the decline in $OD_{600}$ of triplicate cultures was measured following the addition of 1 mg/mL lysozyme, or 50 ng/mL lysostaphin. USA300 and USA300Δ*femT* were first grown in MHB to an $OD_{600}$ of ~1.0, and cells were then resuspended in PBS as a control, or PBS containing one of the two stressors.

Although previous research has indicated that 0.8 mg/ml lysozyme is sufficient to differentiate lysozyme sensitive mutants from wild type *S. aureus* (158), USA300 and USA300Δ*femT* exhibited little to no lysis after 2 hours of incubation in 1 mg/ml lysozyme, as illustrated by a similar decline in their ODs over time (Figure 3.3A). However, when cell lysis was determined in the presence of lysostaphin, USA300Δ*femT* cells lysed significantly more at indicated time points compared to USA300, as illustrated by a more rapid decline in $OD_{600}$, graphed as percent of initial OD (Figure 3.3B). This indicates that USA300Δ*femT* is more susceptible to lysostaphin-induced cell lysis compared to USA300.

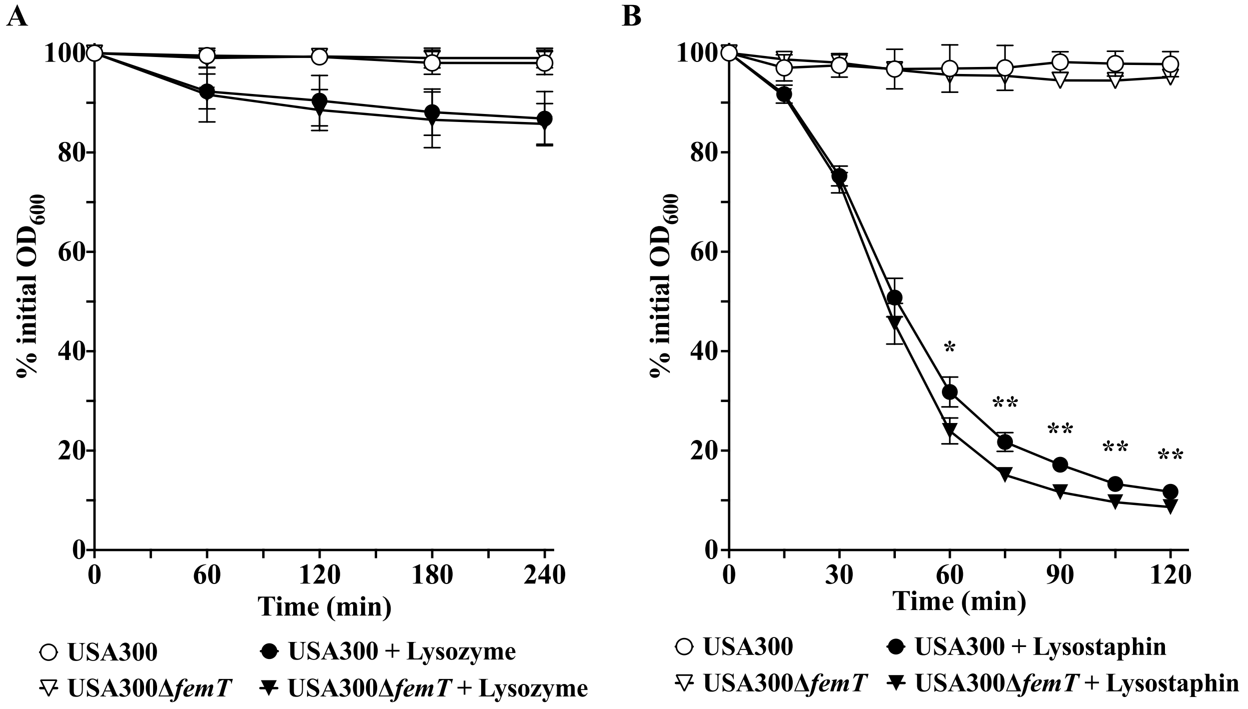

**Figure 3.3 Deletion of femT increases sensitivity of USA300 to lysostaphin.** Lysis assays of USA300 and USA300Δ*femT* were carried out with cells resuspended in PBS alone (open symbols), or in PBS containing (A) 1 mg/mL lysozyme, and (B) 50 ng/mL lysostaphin. $OD_{600}$ measurements were taken at timely intervals and data points were calculated as a percentage of their initial $OD_{600}$. Each data point represents the mean value of triplicate cultures; error bars represent the standard error of the mean. Significant differences in % initial $OD_{600}$ of cultures exposed to lysostaphin were determined by an unpaired one-tailed Student's *t* test (*, $p < 0.05$; **, $p < 0.01$).

### 3.1.4 Deletion of *femT* slightly increases sensitivity of USA300 to select antibiotics

To test our hypothesis that FemT contributes to cell wall synthesis and integrity, we evaluated the sensitivity of USA300 and the RND pump mutants USA300Δ*farER*, USA300Δ*femT* and USA300Δ*farER-femT* to various antibiotics. Sensitivity to daptomycin was tested, as this membrane-active antibiotic has been shown to induce *fem*T transcription 2.0-fold (159). Vancomycin, a glycopeptide antibiotic, and oxacillin, a β-lactam, were also evaluated, as they both inhibit cell wall synthesis. Specifically, vancomycin binds to the stem peptide of the membrane-anchored lipid II precursor at its dipeptide moiety, Lys-D-Ala-D-Ala residue, and thus prevents the precursor from being incorporated into the nascent peptidoglycan chain (160–162). Oxacillin, as a β-lactam antibiotic, inhibits cell wall synthesis through binding and inactivating PBPs.

To assess the sensitivity of USA300 and RND mutants to these antibiotics, MIC evaluations were performed using E-test strips, as described in the Materials and Methods section. When plated on Mueller-Hinton agar plates with a daptomycin E-test, all four cultures were shown to be equally sensitive to daptomycin, with an MIC of 1 µg/mL (Figure 3.4A). USA300 was slightly less susceptible to vancomycin, with an MIC of 2 µg/mL, compared to the three RND pump mutants, which all had the same MIC of 1 µg/mL (Figure 3.4B). Interestingly, USA300 and USA300Δ*farER* were equally sensitive to oxacillin, with an MIC of 0.12 µg/mL (Figure 3.4C). However, the *femT* mutants, USA300Δ*femT* and USA300Δ*farER-femT*, were visibly more sensitive to oxacillin, with an MIC of 0.06 µg/mL. Antibiotic MIC results of each strain are summarized in Table 3.1.

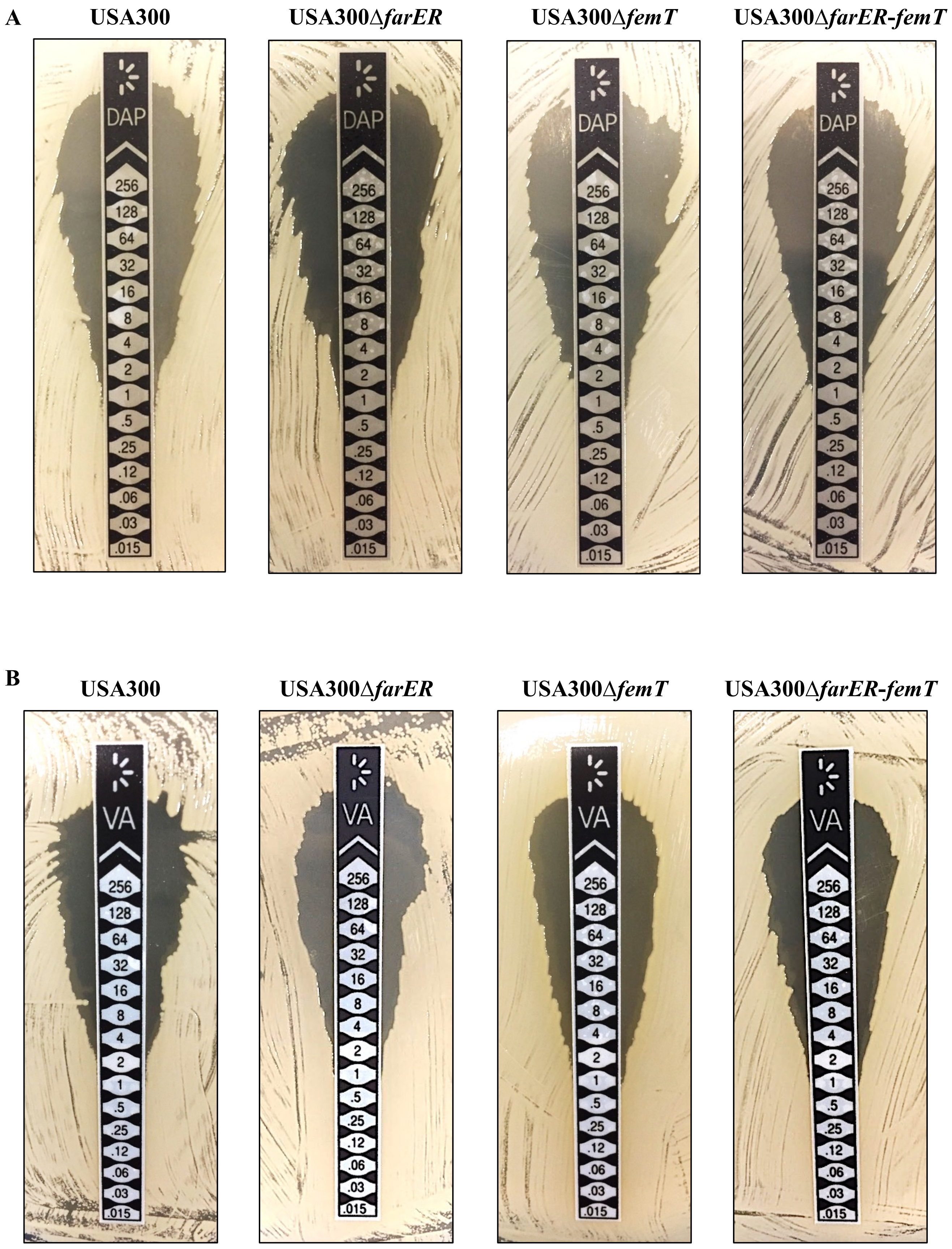
A
USA300
USA300Δ*farER*
USA300Δ*femT*
USA300Δ*farER-femT*
DAP
256
128
64
32
16
8
4
2
1
.5
.25
.12
.06
.03
.015
B
USA300
USA300Δ*farER*
USA300Δ*femT*
USA300Δ*farER-femT*
VA

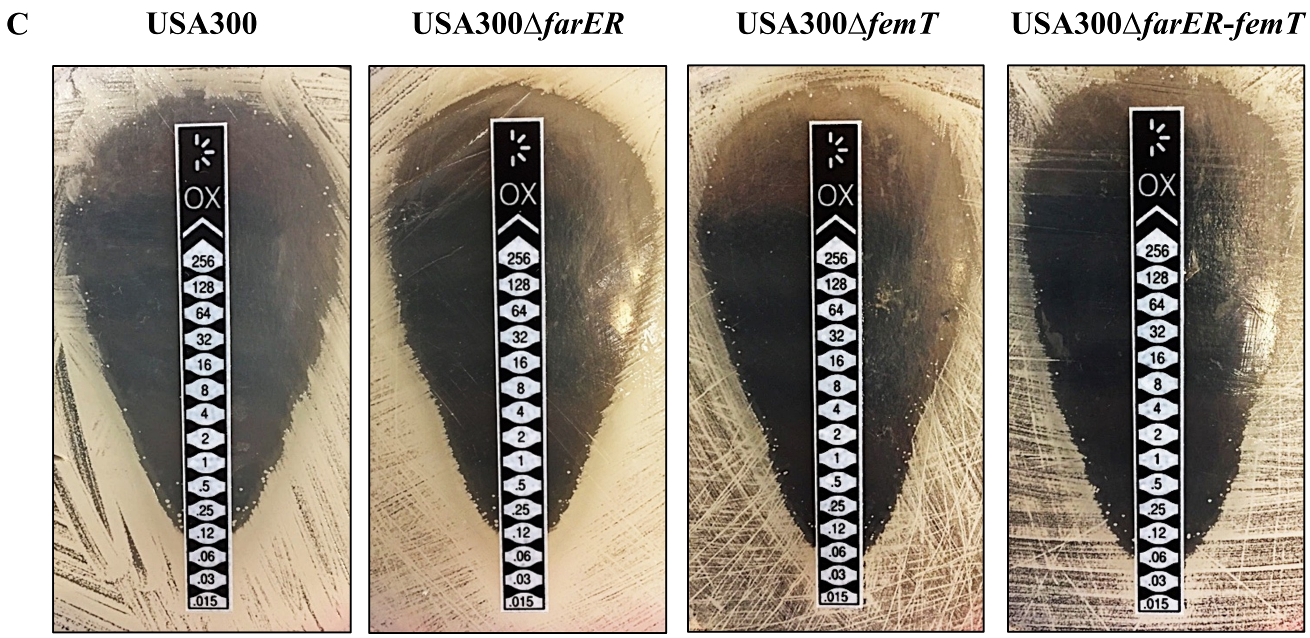

USA300　USA300Δ*farER*　USA300Δ*femT*　USA300Δ*farER-femT*

**Figure 3.4 E-test results for determination of antibiotic sensitivity.** Cultures of USA300, USA300Δ*farER*, USA300Δ*femT*, and USA300Δ*farER-femT* were spread onto Mueller-Hinton agar plates with (A) daptomycin, (B) vancomycin, and (C) oxacillin E-tests. MICs (µg/mL) were read directly from the test strip, where the elliptical zone of inhibition intersected with the MIC scale on the test strip.

**Table 3.1 Resistance profiles of *S. aureus* strains USA300, USA300Δ*farER*, USA300Δ*femT*, and USA300Δ*farER-femT***

| **Antibiotic** | **MIC [µg/mL]** | | | |
|---|---|---|---|---|
| | **USA300** | **USA300Δ*farER*** | **USA300Δ*femT*** | **USA300Δ*farER-femT*** |
| Daptomycin | 1 | 1 | 1 | 1 |
| Vancomycin | 2 | 1 | 1 | 1 |
| Oxacillin | 0.12 | 0.12 | 0.06 | 0.06 |

## 3.2 Evaluation of Substrate Redundancy between FemT and FarE

### 3.2.1 *femT* expression is not upregulated in USA300Δ*farER*

To test for redundancy in substrate efflux between the two RND transporters in *S. aureus*, the expression of *femT* was evaluated in the USA300Δ*farER* deletion background, to observe whether the deletion of *farE* would cause increased expression of *femT*. To evaluate *femT* expression, a promoter-reporter expression system was utilized. *femT* is partially co-transcribed with *femX*, and the genetic organization of *femX-femT* is conserved among all published annotated staphylococcal species (12). Both *femX* and *femT* lie on the negative strand of the *S. aureus* chromosome, and are separated by a 116 bp intergenic segment. In addition to the promoter upstream of *femX*, an additional predicted promoter in the intergenic region between *femX* and *femT* has been identified (163). To evaluate whether the predicted promoter in this region is active, the entire 116 bp segment between *femX* and *femT* was amplified and cloned into the pGY*lux* expression vector, creating pGY*femT::lux.* This construct was then introduced into *E. coli* DH5α, where luciferase activity was monitored at different time points in growth and compared to the activity of the *farE* promoter (Figure 3.5A). Although the *femT* promoter is not expressing to the same level as the *farE* promotor, the pGY*femT::lux* construct is active, and the promoter is driving detectable levels of luminescence in *E. coli* DH5α.

Once promoter activity was confirmed in *E. coli*, *femT* expression was measured in USA300 and USA300Δ*farER*. Since *farE* is known to be induced in LA, *femT* expression was measured in USA300Δ*farER* in the presence of LA to determine if LA, in the absence of *farE*, would induce expression of *femT* as a compensatory mechanism. Therefore, USA300 and USA300Δ*farER* harboring pGY*femT::lux* were cultured into triplicate flasks containing either TSB or TSB supplemented 20 μM LA (Figure 3.5B). Luminescence measurements suggest that the deletion of *farER* does not cause an increase in *femT* expression when exposed to TSB alone, or TSB supplemented with LA. Although the predicted *femT* promoter was shown to be highly active when monitored in *E. coli*, expression in *S. aureus* could only be briefly observed at a low level during early exponential growth in USA300 grown in TSB. Time points earlier than 1 hour were not measured, as the $OD_{600}$ readings would be too low for standardization with RLU measurements.

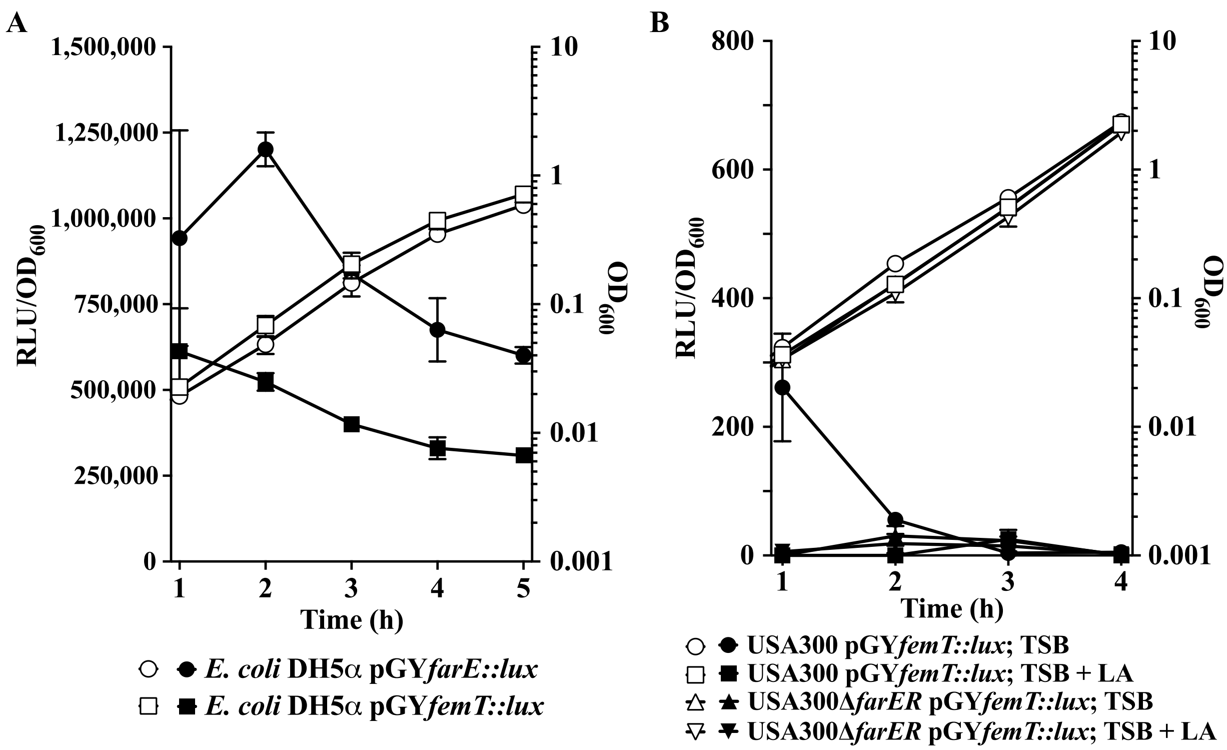

**Figure 3.5 Assay of *femT* expression in *E. coli*, USA300, and USA300Δ*farER*.** Growth ($OD_{600}$; open symbols) and relative luminescence units normalized by $OD_{600}$ ($RLU/OD_{600}$; closed symbols) of (A) *E. coli* DH5α carrying pGY*farE::lux* or pGY*femT::lux*, and (B) USA300 and USA300Δ*farER* with the pGY*femT::lux* reporter vector grown in TSB or TSB with 20 μM LA. Each value represents the mean and standard deviation of four separate cultures, and each culture was subjected to quadruplicate luminescence readings at each time point.

### 3.2.2 *farE* exhibits loss of inducible expression in USA300Δ*femT*

To test whether the deletion of FemT causes a change in *farE* expression, a promoter gene assay was performed measuring *farE* expression in a USA300Δ*femT* mutant background. To accomplish this, the putative promoter of *farE* was cloned in front of the luciferase operon on the pGY*lux* plasmid and transformed into USA300 and USA300Δ*femT*. Expression of *farE* was then monitored during growth in TSB in the presence and absence of sub-inhibitory (20 μM) concentrations of LA and AA (Figure 3.6). As expected from previous experiments, the expression of *farE* is inducible in USA300 when cultured in 20 μM LA and AA, compared to TSB in which *farE* is not expressed (99). Interestingly, inducible expression of *farE* was lost in the USA300Δ*femT* background when cultured in both LA and AA, and expression remained minimal. This is illustrated as a decrease in *farE* expression, measured as RLU/$OD_{600}$, in USA300Δ*femT* compared to its expression in wild-type USA300, when grown in LA and AA. The data, therefore, do not support the contention that increased expression of *farE* compensates for inactivation of *femT*. However, *farE* expression is significantly reduced in USA300Δ*femT* compared to USA300, suggesting perhaps that another mechanism is involved. To confirm this phenotype, Western blot analysis of USA300, *femT* mutants, and complemented *femT* mutants was also performed with specific antibodies generated against FarE, as described in the Materials and Methods section. However, attempts of this Western blot have been unsuccessful due to a low concentration FarE recovered from the immunized rabbit.

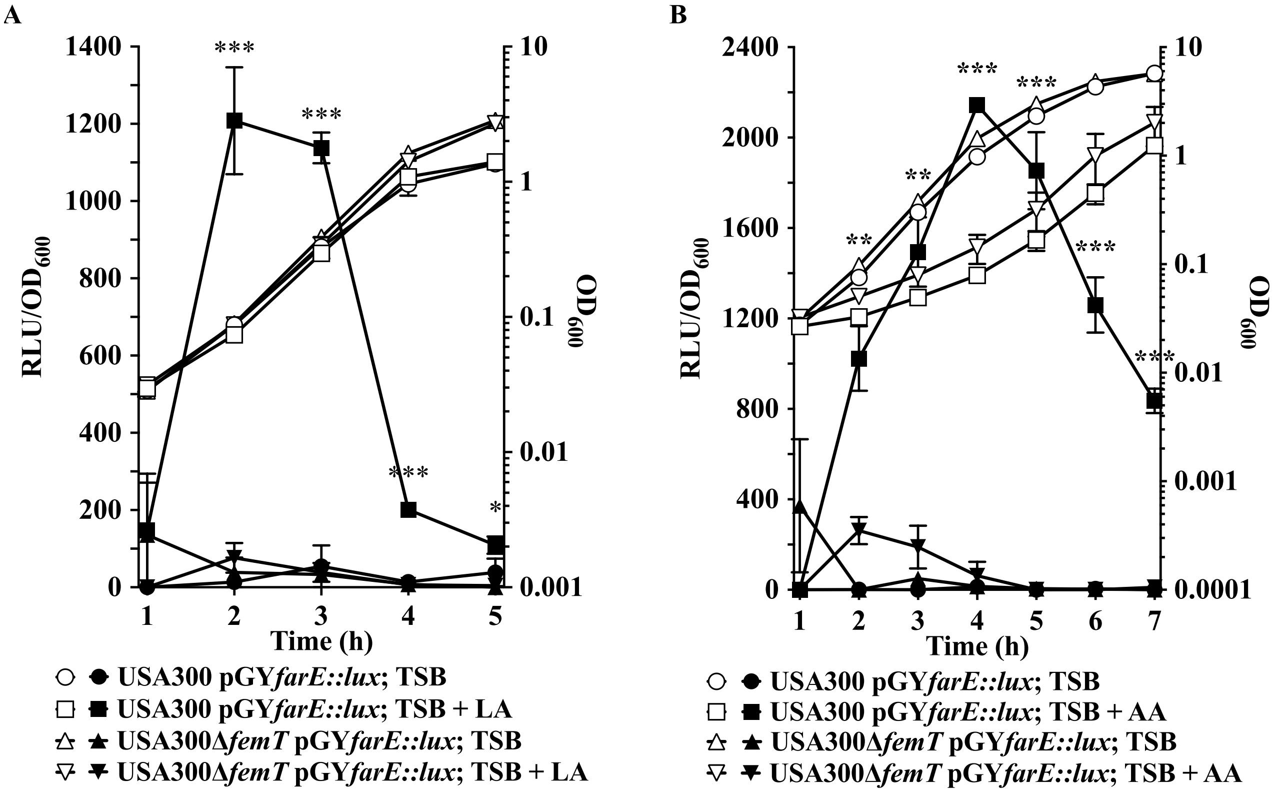

**Figure 3.6 *farE* loses inducible expression in USA300Δ*femT*.** Growth (OD$_{600}$; open symbols) and relative luminescence units normalized by OD$_{600}$ (RLU/OD$_{600}$; closed symbols) of USA300 and USA300Δ*femT* harboring the pGY*farE::lux* reporter vector. (A) Cultures were grown in TSB in the presence and absence of (A) 20 μM linoleic acid (LA); and (B) 20 μM arachidonic acid (AA). Each value represents the mean and standard deviation of triplicate cultures, and each culture was subjected to quadruplicate luminescence readings at each time point. Significance values of RLU/OD$_{600}$ are shown between (A) USA300 pGY*farE::lux* in TSB + LA and USA300Δ*femT* pGY*farE::lux* in TSB + LA; and (B) USA300 pGYf*arE::lux* in TSB + AA and USA300Δ*femT pGYfarE::lux* in TSB + AA, as determined by unpaired one-tailed Student's t tests (*, $p < 0.05$; **, $p < 0.01$; ***, $p < 0.001$).

### 3.2.3 USA300Δ*femT* is more susceptible to killing by bactericidal concentration of linoleic acid

To further investigate the reduced expression of *farE* in USA300Δ*femT*, we investigated the hypothesis that the cell wall of USA300Δ*femT* is altered in such a way that does not allow fatty acids to enter the cell and induce *farE* expression. To accomplish this, a bactericidal assay was performed to assess bactericidal activity of LA on USA300, USA300Δ*femT*, and USA300Δ*femT* containing pALC*femT* for complementation. Cultures were grown to exponential phase in TSB supplemented with a sub-inhibitory concentration (20 μM) of LA, and then inoculated into flasks containing 100 μM LA, a bactericidal concentration. Control curves of USA300 and USA300Δ*femT* grown in TSB without LA were not included as both strains grow similarly in TSB, which is demonstrated in Figure 1. Interestingly, when grown in bactericidal concentrations of LA, the USA300Δ*femT* pALC2073 mutant demonstrated significantly lower survival every hour after initial inoculation compared to wild-type USA300 and the USA300Δ*femT* complement (Figure 3.6). This data shows that mutants that are deficient in *femT* are more susceptible to killing by bactericidal unsaturated free fatty acids, such as LA. Notably, complementation of *femT* restored cell killing to levels not significantly different from wild-type USA300.

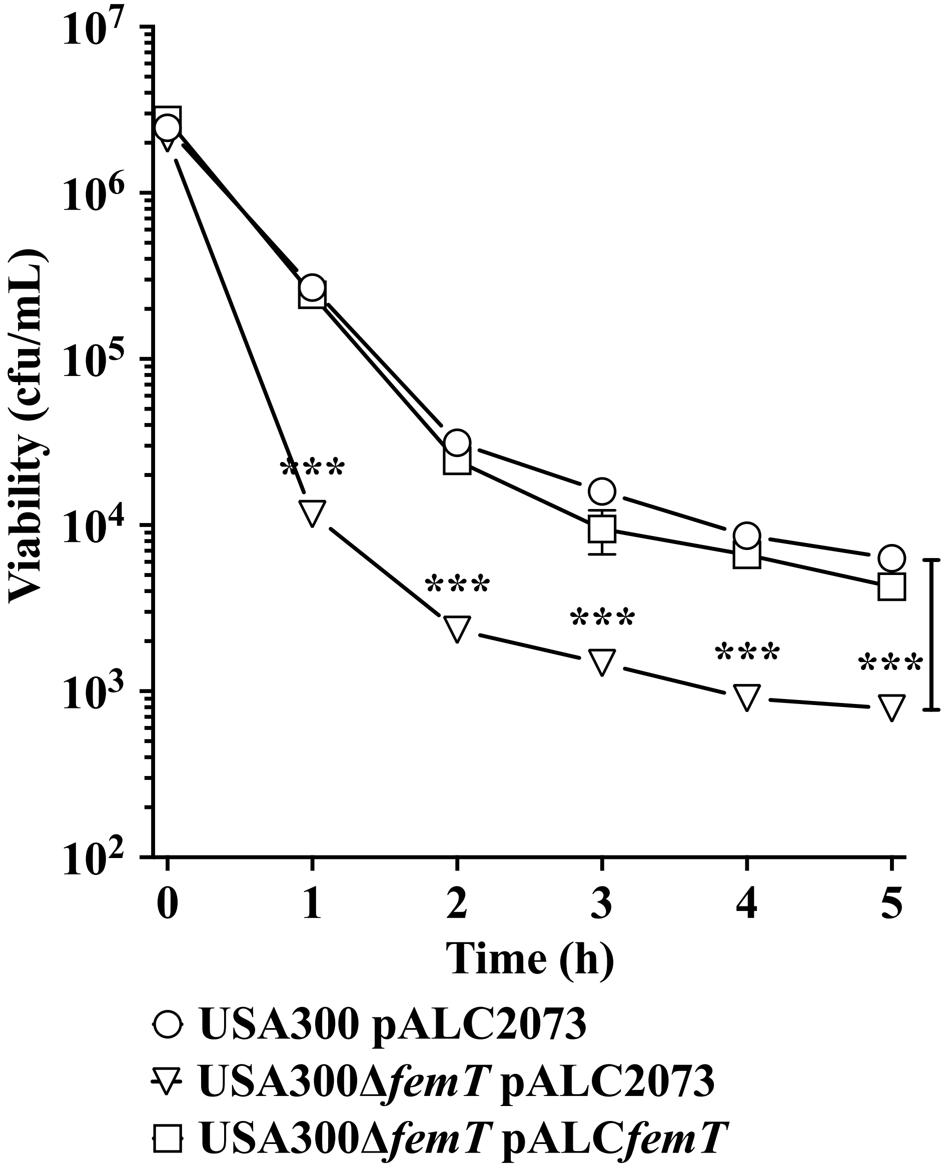

**Figure 3.7 Sensitivity of USA300 and USA300Δ*femT* to the bactericidal activity of linoleic acid.** Cultures of USA300 pALC2073, USA300Δ*femT* pALC2073, and USA300Δ*femT* pALC*femT* were exposed to 100 µM LA after growth to mid-exponential phase in TSB–20 µM LA. Each data point represents the mean value of quadruplicate cultures. Significant differences in viability between USA300 pALC2073 and USA300Δ*femT* pALC2073 were determined by unpaired one-tailed Student's t tests (***, $p < 0.001$).

### 3.2.4 Failure to express *farER* is responsible for increased sensitivity of *femT* deficient strains to killing by linoleic acid

Upon determining that USA300Δ*femT* had significantly reduced survival in bactericidal concentrations of LA compared to wild-type USA300, we wanted to investigate if this phenotype was due to loss of *farE* expression in the *femT* mutant. To evaluate the role of *farE* in the increased susceptibility of USA300Δ*femT*, the mutant strain USA300Δ*farER-femT* was utilized, along with the *femT*-complemented version USA300Δ*farER-femT* pALC*femT*. Bactericidal assays with USA300 pALC2073, USA300Δ*farER-femT* pALC2073, and USA300Δ*farER-femT* pALC*femT* were carried out under the same conditions tested previously; cells were grown to mid-exponential phase in TSB–20 μM LA and then inoculated into flasks containing 100 μM LA.

As expected, the USA300Δ*farER-femT* mutant demonstrated notably lower survival compared to wild-type USA300 (Figure 3.7), but when the USA300Δ*farER-femT* mutant was complemented with pALC*femT*, viability was not restored and remained significantly lower than USA300 at all time points after initial inoculation. Therefore, USA300Δ*femT* and USA300Δ*farER-femT* both exhibit reduced viability in the bactericidal assay, and viability can be restored by complementing with pALC*femT* in USA300Δ*femT*, but not in USA300Δ*farER-femT*. Taken together, these data indicate that that *farER* is not inducible in USA300Δ*femT*, leading to reduced viability when challenged with bactericidal levels of LA.

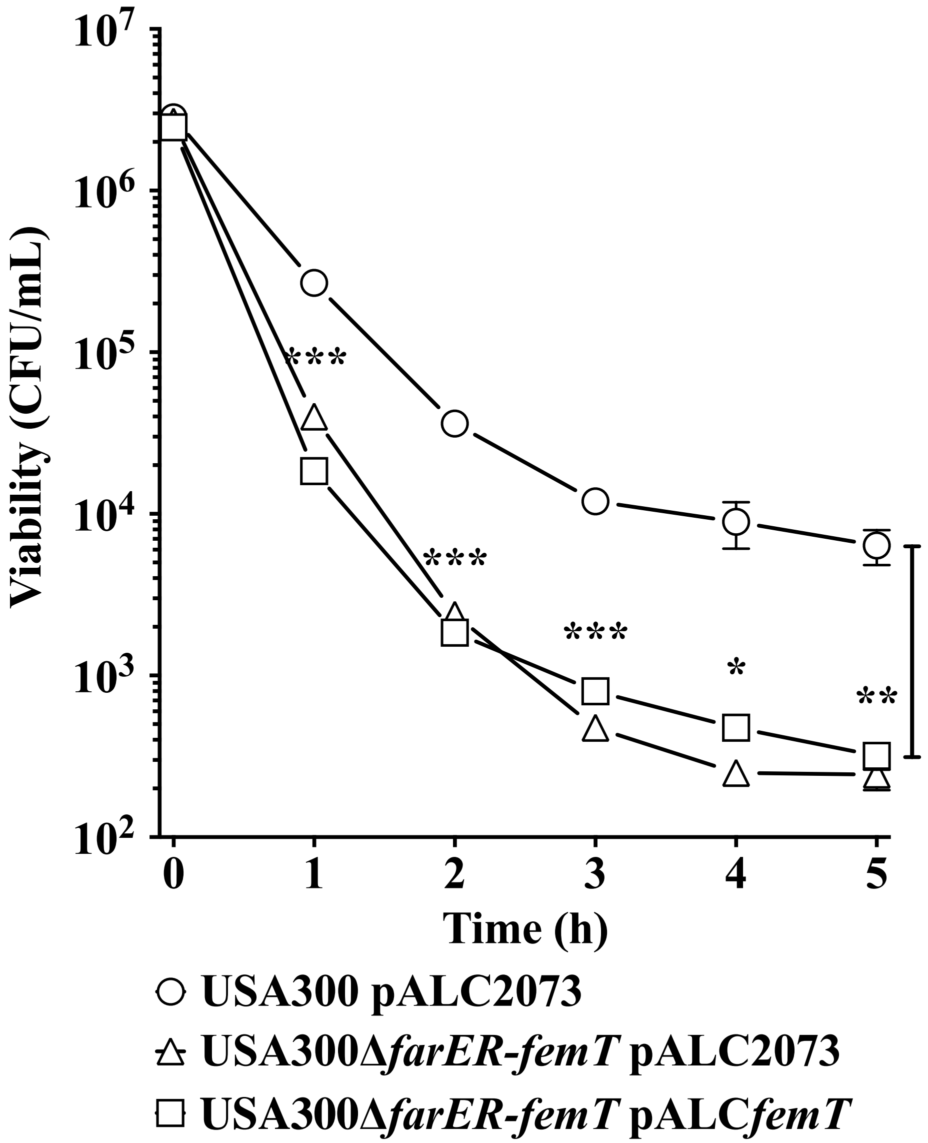

**Figure 3.8 Sensitivity of USA300Δ*farER-femT* to killing by linoleic acid occurs in a *farER*-dependent manner**. Cultures of USA300 pALC2073, USA300Δ*farER-femT* pALC2073, and USA300Δ*farER-femT* complemented with pALC*femT* were exposed to 100 μM LA after growth to mid-exponential phase in TSB–20 μM LA. Each data point represents the mean value of quadruplicate cultures. Significant differences in viability between USA300 pALC2073 and USA300Δ*farER-femT* pALCf*emT* were determined by unpaired one-tailed Student's t tests (*, $p < 0.05$; **, $p < 0.01$; ***, $p < 0.001$).

# 4 Discussion

The emergence of MRSA has become a significant disease burden worldwide, and *S. aureus* USA300 is a prominent strain of CA-MRSA responsible for severe invasive infections in humans. However, to colonize successfully and establish infection, USA300 must overcome host defense mechanisms, including antimicrobial unsaturated free fatty acids that are encountered on the skin and in soft tissue abscesses. A contributing factor known to play a vital role in the intrinsic defense mechanisms of bacterial pathogens is the RND superfamily of efflux pumps, which are ubiquitous among bacteria. In addition to their diverse roles in drug resistance, virulence, and promoting key physiological processes, RND efflux pumps in many bacterial pathogens are required for causing infection. Although the structure and functions of RND transporters are being extensively studied in both Gram negative and Gram positive bacteria, many outstanding questions remain regarding the characterization of this family of transporters in *S. aureus*.

In addition to our own work, which identifies mild phenotypes of the RND transporter mutant USA300Δ*femT* in conditions that impose stress on the cell wall, Quiblier *et al.* using a different approach with *S. aureus* Newman demonstrated that FemT (SA2056) interacted with some of the FemABX factors and the PBPs, suggesting a subsidiary role in peptidoglycan synthesis (163). Despite the extensively characterized roles of RND family efflux pumps as mediators of multidrug resistance, we proposed that the function of FemT is to contribute to the basic biology of *S. aureus*, namely to cell wall synthesis. This is consistent with the role of RND transporters in *M. tuberculosis*, where the primary role of most MmpL RND proteins appears to be the transport of lipids to be incorporated on the cell envelope (164). To elucidate the role of FemT in *S. aureus* USA300, analysis of the markerless *femT* knock-out mutant was extended to various growth and stress conditions.

First, once *femT* deletions in USA300 and USA300Δ*farER* were created, growth of the mutants was analyzed in four different types of media. Typically, a range of different media are used for cultivating *S. aureus* in studies from different laboratories; these are mostly complex media such as TSB, BHI broth, MHB, and LB broth (165). Evaluating the growth of mutants in different media is important, as previous research has indicated that different media have major effects on the expression of selected target virulence and regulatory genes (165, 166). Interestingly, the *femT* deletion mutant grew at a slightly faster rate during mid-exponential growth compared to wild-type in MHB. In comparison, all strains grew at approximately equal rates in the other media tested. MHB is composed of beef extract powder (2 g/L), acid digest of casein (17.5 g/L), and soluble starch (1.5 g/L). Thus, by far the major component of this medium is acid digest of casein, and this is expected to be high in free amino acids, and may have an impact on bacterial cell properties. Indeed, Sen *et al.* have demonstrated that the balance of branched-chain fatty acids and straight-chain fatty acids in the membranes of USA300 strains JE2 and SH1000 was affected considerably by growth in different media; in particular, MHB resulted in high branched-chain and low straight-chain fatty acids, whereas growth in TSB and BHI broth led to a reduction in branched-chain and an increase in straight-chain fatty acids (167). In addition, the membranes of MHB- and serum-grown cells were significantly less fluid compared to cells grown in other media, possibly due to the higher carotenoid contents of cells grown in MHB, which rigidifies the membrane (167). Taken together, these altered membrane characteristics of MHB-grown cells suggest that the ratio of components in MHB differ from TSB, BHI broth, and RPMI broth in such a way that enhances growth of USA300Δ*femT* in MHB, which perhaps is attributable to membrane perturbations of cells grown in this media. Glucose, for example, is absent in MHB, but present in TSB, BHI broth, and RPMI broth, and may possibly account for this phenotype. When *S. aureus* cultures are grown in media lacking glucose, cells are forced to utilize secondary sources of carbon, such as amino acids (168). Under these conditions, perhaps the *femT*-deficient mutant is better able to accommodate the metabolic changes, and thus, can grow at a faster rate compared to wild-type. Growing these cultures in TSB without glucose, or in MHB supplemented with glucose, would prove valuable to examine the role of glucose in this phenotype. Interestingly, Huang *et al.* found the opposite effect, where the deletion of the RND pump *smeIJK* in *Stenotrophomonas maltophilia* mediated growth retardation in MHB, which was reversible when the cultured environment was changed from MHB to LB broth (169). The mechanism behind the growth perturbation remains as a future area of study; for example, it may be useful to examine the membrane properties of USA300Δ*femT* when grown in each media.

Hypothesizing that FemT plays a role in cell wall synthesis, it is noteworthy that the *femT* mutant was more susceptible to lysis with lysostaphin compared to wild type USA300, as this phenotype may suggest that FemT contributes to biosynthetic pathways for cell wall assembly. Lysostaphin is a endopeptidase produced by *Staphylococcus simulans* biovar *staphylolyticus* and lyses staphylococcal cells by hydrolyzing the $Gly_5$ bridges that cross-link the peptidoglycan of several members of this genus, including *S. aureus* (170). Although mutants defective in either the *femA* or *femB* genes are more resistant to lysostaphin due to shortened $Gly_5$ interpeptides, Morikawa *et al.* using *S. aureus* N315 showed that cell wall thickness also plays important roles in lysostaphin sensitivity, whereby cells with thinner envelopes demonstrated increased sensitivity to lysostaphin (156). Based on these findings, it is possible that the glycine-glycine bond of the crossbridge is not altered in the *femT* mutant, but it may be possible that the cell wall of USA300Δ*femT* is marginally thinner than wild-type, contributing to increased lysostaphin sensitivity. This alleged phenotype of the mutant could also explain its increased sensitivity to antibiotics that target the cell wall.

Research by Cui and colleagues demonstrated a significant statistical correlation between the cell wall thickness of 48 *S. aureus* strains and vancomycin MICs; specifically, the thickening of the cell wall is closely associated with the mechanism of vancomycin resistance in resistant strains (171). In this mechanism proposed by several researchers, trapping of vancomycin molecules in the cell wall peptidoglycan would be the essential contributor; the thicker the cell wall, the more vancomycin molecules trapped within the cell wall, thus allowing fewer molecules to reach the cytoplasmic membrane where the real functional targets of vancomycin are present (171–174). Vancomycin binds to the stem peptide of the membrane-anchored lipid II precursor at its dipeptide moiety, Lys-D-Ala-D-Ala residue, and thus prevents the precursor from being incorporated into the nascent peptidoglycan chain (160–162). In addition, a thicker peptidoglycan layer also significantly reduces the time that vancomycin completely inhibits peptidoglycan synthesis. This theory holds true of glycopeptide antibiotics, including vancomycin and teicoplanin, and also of β-lactams, including imipenem and oxacillin, although to a lesser extent (171). Conversely, the opposite could hold true for strains with a thinner cell wall, as a thinner peptidoglycan layer may allow vancomycin to more readily reach the cytoplasmic membrane and completely inhibit peptidoglycan synthesis. In *E. coli*, cells with reduced peptidoglycan content were more sensitive to β-lactam antibiotics, including penicillin and other damaging agents, and cells withstood this drastic reduction in the amount of peptidoglycan without detectable alterations in their morphology, growth, division, and viability in the stationary phase (175). Based on these findings, if the cell wall of USA300Δ*femT* is slightly thinner than wild-type, it seems likely that this would contribute to the increased sensitivity of the mutant to both vancomycin and oxacillin, without affecting growth in culture.

Additionally, while the *femT* mutant showed an increased sensitivity to lysostaphin, vancomycin and oxacillin, the deletion mutant was not found to be differentially affected by lysozyme compared to wild-type. Lysozyme is one of the most important enzymes of the innate immune system, as it is a component of neutrophil granules, the major secretory product of macrophages, and it is also found in mammalian secretions and tissues (176, 177). Although lysozyme preferentially hydrolyzes the β-1,4-glycosidic linkages between MurNAc and GlcNAc, it does not recognize peptidoglycan modified with O-acetyl groups, which enables pathogenic bacteria such as *S. aureus* to overcome this innate defense mechanism (178). *S. aureus* acetylates its cell wall at the C-6 position of MurNAc, producing the 2,6-N,O-diacetylmuramic acid derivative (158). This modification acts as a steric hindrance and inhibits the binding of the lysozyme to the polysaccharide substrate. Bera *et al.* have previously provided evidence that the O-acetylation of peptidoglycan correlates with the observed high lysozyme resistance by *S. aureus*, which is mediated by a peptidoglycan-specific, membrane-bound O-acetyltransferase (OatA) (158). In this study, researchers show that OatA is widespread among pathogenic staphylococci, whereas nonpathogenic staphylococci are lysozyme sensitive and possess no O-acetylated peptidoglycan (158). Therefore, to investigate whether FemT played a role in the acetylation of peptidoglycan, we tested the growth of the *femT* mutant compared to wild-type USA300 when exposed to lysozyme. However, both appeared to be equally resistant to lysozyme, which suggests that peptidoglycan acetylation was not altered in USA300Δ*femT*.

Although a striking phenotype of USA300Δ*femT* was not found upon exposure to several of the conditions tested, the mutant was identified to grow faster in MHB, and is slightly more sensitive to vancomycin, oxacillin, and lysostaphin compared to wild-type; however, *femT* was not required for *S. aureus* growth or stress tolerance when grown in culture and upon exposure to lysozyme and daptomycin. However, the increased sensitivity of USA300Δ*femT* to lysostaphin and cell wall-targeting antibiotics may implicate an accessory role for FemT in cell wall biosynthesis. It is possible that FemT and other proteins share redundancy in substrate efflux, as cell wall synthesis genes are especially redundant, and that deletion of *femT* alone does not impair *S. aureus* sufficiently to produce a striking phenotype. Interestingly, *S. aureus* can survive with minimal peptidoglycan synthesis genes, and Reed *et al.* demonstrated that as many as seven of the nine genes encoding synthesis enzymes can be deleted without affecting normal growth or cell morphology; however, virulence and antibiotic resistance are sacrificed in these mutants (179).

Therefore, future research should be directed at examining the virulence of USA300Δ*femT* and USA300Δ*farER-femT* in a murine colonization model to extend the evaluation of FemT *in vivo*.

A common feature of bacterial pathogens encoding multiple RND pumps is that their functions in substrate efflux tend to be redundant. For example, *P. aeruginosa* has more than ten RND family transporters, of which nine transport multiple, often the same, antibiotic substrates (180). Due to the redundancy of RND pumps, potential exists for the loss of certain pump components to be compensated by increased expression of a homologous pump that could accomplish, at least to some extent, the same function. For example, Eaves *et al.* demonstrated that when *acrB* or *acrF* of *Salmonella* was inactivated, the expression of *acrD* increased (181). Similarly, Blair *et al.* have shown that the expression of all RND efflux pump genes in *S. typhimurium* can be altered when single or multiple *acr* genes are inactivated (182). Comparably, RND transporters MmpL4 and MmpL5 in *M. tuberculosis* have redundant functions in siderophore export, whereby inactivation of either pump increases expression of the other, but a double MmpL4/5 mutant is lethal (183). Since these transporters efflux a wide range of substrates, inactivation of one transporter may alter the balance of metabolites in the cell, and expression of other RND transporters may be adjusted accordingly. Therefore, the redundancy feature of RND transporters contributes to bacterial resilience in many different growth conditions.

Interestingly, when testing for substrate redundancy between FemT and the fatty acid resistance transporter, FarE, our results show that *femT* expression via the predicted promoter is unchanged in the *farER*-deletion mutant. Conversely, we observed a loss of inducible *farE* expression in the *femT*-deletion mutant. In wild-type, *farE* is only expressed in TSB supplemented with LA and AA, but in USA300Δ*femT*, *farE* is not expressed under these conditions. The data, therefore, do not support the contention that increased expression of *farE* compensates for inactivation of *femT*. These results suggest that perhaps another mechanism is involved, or that the cell of USA300Δ*femT* is altered in such a way that does not allow LA or AA to induce *farE* expression. One simple solution could be that FemT acts as both an efflux pump and a portal of entry for certain molecules, such as fatty acids. If this was the case, it would explain why *farE* loses inducible expression in the *femT* deletion mutant, as fatty acids are unable to enter the cell and induce expression. It would also explain why the USA300Δ*femT* mutant is more susceptible to LA in a bactericidal assay, and when introducing *femT* back *in trans*, viability is restored. However, this idea still raises some questions as to specificity of fatty acid entry over other metabolites, and the mechanism by which this process would occur.

Although the mechanism by which *farE* is induced by LA and AA remains to be determined, it is probable that exogenous fatty acids must enter the cell to induce *farE* expression. Therefore, it seems likely that the *femT* mutant is altered in such a way that does not allow entry of fatty acids. Alternatively, it is possible that the regulation of *farE* requires specific forms of phosphorylated fatty acids, and not free fatty acids, to promote *farE* expression. As discovered by Parsons *et al.*, fatty acid kinase A (FakA) is an integral part of the fatty acid kinases, which carries out the first step of incorporating fatty acids into the cell membrane by phosphorylating them into acyl-$PO_4$ (184). If *farE* does indeed require the phosphorylated forms of fatty acids, perhaps the fatty acid kinase pathway is altered in USA300Δ*femT*, and is therefore unable to induce expression of *farE*. First, an altered cell membrane will be considered.

Extracellular fatty acids translocate to the inner leaflet of the cell membrane by spontaneous flipping via the membrane pH gradient, and once inside the cell, they are phosphorylated by the fatty acid kinases (184, 185). Since fatty acids must insert into the membrane to exert their effects, the ability of some bacteria to change their cell surface hydrophobicity may explain why certain strains of the same species differ with respect to their susceptibility to antimicrobial fatty acids (97, 186). For example, the *femT* mutant may contain fewer proteins in its cell membrane, which makes the cell surface less charged and more hydrophobic. Thus, free fatty acids are more attracted to the cell and are more likely to insert into the membrane, exerting their toxic effects (97, 186, 187). This is consistent with our observation that USA300Δ*femT* is more susceptible to killing by bactericidal concentrations of LA compared to wild-type. An example of such a component in the membrane that contributes to this phenotype is the membrane-located carotenoids. Carotenoids are antioxidants that also stabilize the cell membrane by decreasing fluidity and, if they are increased in number, their presence may counteract the effects of free fatty acid degradation products or fatty acid-induced increases in membrane fluidity (188). Indeed, strains of *S. aureus* containing high levels of carotenoids are less susceptible to the antibacterial effects of unsaturated fatty acids than strains with lower quantities of carotenoids in their membranes (95, 188). Therefore, it seems likely that if *S. aureus* strains such as USA300Δ*femT* contain reduced amounts of membrane carotenoids or other large membrane proteins, these cells would be more susceptible to fatty acids. Interestingly, in some species, RND family transporters are thought to be utilized to replace fatty acids from membranes as part of maintaining homeostasis (189). Although this mechanism is not currently understood, this phenomenon, along with a decrease in other membrane proteins, could explain why, when *femT* is deleted, the membrane may be more fluid and more susceptible to the insertion of fatty acids. In addition, a more fluid membrane of *femT*-deficient cells could explain its enhanced growth in MHB, as this media promotes a higher proportion of branched-chain fatty acids and carotenoids in the cell membrane, which may aid the growth of USA300Δ*femT* compared to cells with a naturally more rigid membrane.

Increased susceptibility of the *femT* mutant to LA may also be due to the proposed thinner cell wall. In addition to altered membrane properties of the cell, differential susceptibility of bacterial species to the action of fatty acids is also likely to be due to the ability of exogenous fatty acids to permeate the cell wall, which will enable access to the sites of action on the membrane (187). Interestingly, *S. aureus* appears to upregulate the expression of genes encoding cell wall synthesis proteins upon exposure to unsaturated free fatty acids, a strategy that serves as a protective measure, as a thicker cell wall makes it more difficult for fatty acids to penetrate and exert their antibacterial effects at the membrane (185). An altered cell membrane and/or cell wall provides a reasonable interpretation of the increased susceptibility of USA300Δ*femT* to LA. However, it does not explain the loss of inducible *farE* expression. Before a definitive explanation for this phenotype can be determined, the mechanism by which *farE* is induced by LA and AA needs to be investigated. One possible theory that will be discussed further is the disruption of the fatty acid kinase pathway.

In the USA300 genome, *farE* is divergently transcribed with *farR*, a regulator of fatty acid resistance, and expression of *farE* is induced in a *farR*-dependent mechanism in response to exogenous fatty acids (99). It is believed that FarR may function as a repressor of *farE* in the absence of inducer, and in the presence of exogenous fatty acids, may serve to promote expression of *farE* (99). While *farE* was found to be induced by exposure to fatty acids, it is unknown whether the induction requires free fatty acids or if it requires specific forms of phosphorylated acyl-$PO_4$ fatty acids that have been incorporated into *S. aureus* by the fatty acid kinases. Interestingly, when *farE* expression was measured in a *fakA*-deficient mutant (USA300Δ*fakA*), *farE* expression, in media alone and media supplemented with LA, was significantly reduced compared to its expression in USA300 grown in LA (147). Moreover, *farE* loses its inducible expression in LA in the *fakA* mutant. These results are very similar to the expression of *farE* in the *femT*-deficient mutant, where *farE* loses its inducible expression in both LA and AA. Taken together, these results are consistent with the notion that the regulation of *farE* requires specific forms of acyl-$PO_4$ and not free fatty acids to promote *farE* expression. Therefore, if the fatty acid kinase pathway was disrupted in the USA300Δ*femT* mutant, it would explain the lack of change in *farE* expression between USA300Δ*femT* grown in TSB or in fatty acids. Although the mechanism is not currently understood, what is known is that *farE* expression is significantly reduced in *femT* deficient mutants. This is consistent with the observation that USA300Δ*femT* and USA300Δ*farER-femT* both exhibit reduced viability in the bactericidal assay, and viability can be restored by complementing with pALC*femT* in USA300Δ*femT*, but not in USA300Δ*farER-femT*. To confirm this phenotype is due to loss of *farE*, complementing USA300Δ*farER-femT* with pALC*farE* would prove valuable. Identifying why fatty acid kinase activity might be altered in USA300Δ*femT* and identifying specific regulation of *farE* remains a future area of study. Since the inactivation of the fatty acid kinases severely attenuates virulence factor production in *S. aureus*, it would prove highly valuable to examine the virulence of USA300Δ*femT* (184).

In summary, we have examined the involvement of FemT in cell wall synthesis and the relationship between FemT and FarE transporters in *S. aureus* resistance to unsaturated free fatty acids. Results of this study implicate a possible involvement of FemT in cell wall biosynthesis, and identified a multifactorial relationship between RND transporters FemT and FarE. Notably, *farE* loses inducible expression in mutants lacking FemT. The USA300Δ*femT* mutant was also significantly more susceptible to bactericidal concentrations of unsaturated free fatty acids compared to wild-type. Cumulatively, these findings represent the first description of both RND efflux systems operating in *S. aureus*. Detailed evaluation of RND transporter function will provide novel insight into the biology of staphylococci and further our understanding of this ubiquitous family of proteins in Gram positive pathogens.

# 5 References

1. Brugger SD, Bomar L, Lemon KP, Brown LW, Martin J, Mitreva M. 2016. Commensal–pathogen interactions along the human nasal passages. PLOS Pathog 12:e1005633.

2. Williams R. 1963. Healthy carriage of *Staphylococcus aureus*: its prevalence and importance. Bacteriol Rev 27:56–71.

3. Kluytmans J, van Belkum A, Verbrugh H. 1997. Nasal carriage of *Staphylococcus aureus*: epidemiology, underlying mechanisms, and associated risks. Clin Microbiol Rev 10:505–520.

4. Ogston A. 1881. Report upon micro-organisms in surgical diseases. Br Med J 1:369–375.

5. Ogston A. 1984. On abscesses. Clin Infect Dis 6:122–128.

6. Ogston A. 1882. Micrococcus poisoning. J Anat Physiol 17:24–58.

7. Licitra G. 2013. Etymologia: Staphylococcus. Emerg Infect Dis 19:1553.

8. Clauditz A, Resch A, Wieland K-P, Peschel A, Götz F. 2006. Staphyloxanthin plays a role in the fitness of *Staphylococcus aureus* and its ability to cope with oxidative stress. Infect Immun 74:4950–4953.

9. Smith W, Hale JH. 1944. The nature and mode of action of *Staphylococcus* coagulase. Br J Exp Pathol 25:101.

10. Młynarczyk G, Kochman M, Lawrynowicz M, Fordymacki P, Młynarczyk A, Jeljaszewicz J. 1998. Coagulase-negative variants of methicillin-resistant *Staphylococcus aureus* subsp. *aureus* strains isolated from hospital specimens. Zentralbl Bakteriol 288:373–381.

11. Otto M. 2010. Basis of virulence in community-associated methicillin-resistant *Staphylococcus aureus*. Annu Rev Microbiol 64:143–162.

12. Wertheim HF, Melles DC, Vos MC, van Leeuwen W, van Belkum A, Verbrugh HA, Nouwen JL. 2005. The role of nasal carriage in *Staphylococcus aureus* infections. Lancet Infect Dis 5:751–762.

13. Williams RE, Jevons MP, Shooter RA, Hunter CJ, Girling JA, Griffiths JD, Taylor GW. 1959. Nasal staphylococci and sepsis in hospital patients. Br Med J 2:658–62.

14. von Eiff C, Becker K, Machka K, Stammer H, Peters G. 2001. Nasal carriage as a source of *Staphylococcus aureus* bacteremia. N Engl J Med 344:11–16.

15. Bekeredjian-Ding I, Stein C, Uebele J. 2015. The innate immune response against *Staphylococcus aureus*. Curr Top Microbiol Immunol.

16. Kobayashi SD, Malachowa N, DeLeo FR. 2015. Pathogenesis of *Staphylococcus aureus* abscesses. Am J Pathol 185:1518–27.

17. Koziel J, Potempa J. 2013. Protease-armed bacteria in the skin. Cell Tissue Res 351:325–37.

18. Coleman G. 1983. The effect of glucose on the differential rates of extracellular protein and alpha-toxin formation by *Staphylococcus aureus*. Arch Microbiol 134:208–11.

19. Bronner S, Monteil H, Prévost G. 2004. Regulation of virulence determinants in *Staphylococcus aureus*: complexity and applications. FEMS Microbiol Rev 28:183–200.

20. Donlan RM, Costerton JW. 2002. Biofilms: survival mechanisms of clinically relevant microorganisms. Clin Microbiol Rev 15:167–93.

21. McCormick JK, Yarwood JM, Schlievert PM. 2001. Toxic shock syndrome and bacterial superantigens: an update. Annu Rev Microbiol 55:77–104.

22. Flannagan RS, Heit B, Heinrichs DE. 2016. Intracellular replication of *Staphylococcus aureus* in mature phagolysosomes in macrophages precedes host cell death, and bacterial escape and dissemination. Cell Microbiol 18:514–535.

23. Hamza T, Li B. 2014. Differential responses of osteoblasts and macrophages upon *Staphylococcus aureus* infection. BMC Microbiol 14:207.

24. Tomasz A. 2006. The staphylococcal cell wall, p. 443–455. *In* Gram-Positive Pathogens, Second Edition. American Society of Microbiology.

25. Weidel W, Pelzer H. 1964. Bagshaped macromolecules - a new outlook on bacterial cell walls. Adv Enzym Relat Subj Biochem 26:193–232.

26. Snowden MA, Perkins HR, Wyke AW, Hayes M V., Ward JB. 1989. Cross-linking and O-acetylation of newly synthesized peptidoglycan in *Staphylococcus aureus*. Microbiology 135:3015–3022.

27. Gally D, Archibald AR. 1993. Cell wall assembly in *Staphylococcus aureus*: proposed absence of secondary crosslinking reactions. J Gen Microbiol 139:1907–1913.

28. Gally DL, Hancock IC, Harwood CR, Archibald AR. 1991. Cell wall assembly in *Bacillus megaterium*: incorporation of new peptidoglycan by a monomer addition process. J Bacteriol 173:2548–55.

29. Schneider T, Senn MM, Berger-Bächi B, Tossi A, Sahl H-G, Wiedemann I. 2004. *In vitro* assembly of a complete, pentaglycine interpeptide bridge containing cell wall precursor (lipid II-Gly5) of *Staphylococcus aureus*. Mol Microbiol 53:675–685.

30. Ton-That H, Labischinski H, Berger-Bächi B, Schneewind O. 1998. Anchor structure of staphylococcal surface proteins. III. Role of the FemA, FemB, and FemX factors in

anchoring surface proteins to the bacterial cell wall. J Biol Chem 273:29143–9.

31. Ling B, Berger-Bächi B. 1998. Increased overall antibiotic susceptibility in *Staphylococcus aureus femAB* null mutants. Antimicrob Agents Chemother 42:936–8.

32. Hubscher J, Jansen A, Kotte O, Schafer J, Majcherczyk PA, Harris LG, Bierbaum G, Heinemann M, Berger-Bochi B. 2007. Living with an imperfect cell wall: compensation of *femAB* inactivation in *Staphylococcus aureus*. BMC Genomics 8:307.

33. Rohrer S, Ehlert K, Tschierske M, Labischinski H, Berger-Bächi B. 1999. The essential *Staphylococcus aureus* gene *fmhB* is involved in the first step of peptidoglycan pentaglycine interpeptide formation. Proc Natl Acad Sci U S A 96:9351–6.

34. Murakami K, Tomasz A. 1989. Involvement of multiple genetic determinants in high-level methicillin resistance in *Staphylococcus aureus*. J Bacteriol 171:874–9.

35. Brown S, Santa Maria JP, Walker S, Walker S. 2013. Wall teichoic acids of Gram-positive bacteria. Annu Rev Microbiol 67:313–36.

36. Park JT, Shaw DR, Chatterjee AN, Mirelman D, Wu T. 1974. Mutants of staphylococci with altered cell walls. Ann N Y Acad Sci 236:54–62.

37. Campbell J, Singh AK, Santa Maria JP, Kim Y, Brown S, Swoboda JG, Mylonakis E, Wilkinson BJ, Walker S. 2011. Synthetic lethal compound combinations reveal a fundamental connection between wall teichoic acid and peptidoglycan biosyntheses in *Staphylococcus aureus*. ACS Chem Biol 6:106–116.

38. Kohler T, Weidenmaier C, Peschel A. 2009. Wall teichoic acid protects *Staphylococcus aureus* against antimicrobial fatty acids from human skin. J Bacteriol 191:4482–4.

39. Brown S, Xia G, Luhachack LG, Campbell J, Meredith TC, Chen C, Winstel V, Gekeler C, Irazoqui JE, Peschel A, Walker S. 2012. Methicillin resistance in *Staphylococcus aureus* requires glycosylated wall teichoic acids. Proc Natl Acad Sci U S A 109:18909–14.

40. Pinho MG, Kjos M, Veening J-W. 2013. How to get (a)round: mechanisms controlling growth and division of coccoid bacteria. Nat Rev Microbiol 11:601–614.

41. Chambers HF, Deleo FR. 2009. Waves of resistance: *Staphylococcus aureus* in the antibiotic era. Nat Rev Microbiol 7:629–41.

42. Kirby WMM. 1944. Extraction of a highly potent penicillin inactivator from penicillin resistant staphylococci. Science (80- ) 99:452–453.

43. Bondi A, Dietz CC. 1945. Penicillin resistant staphylococci. Exp Biol Med 60:55–58.

44. Jevons MP. 1961. Celbenin-resistant staphylococci. Br Med J 1:124.

45. Hartman BJ, Tomasz A. 1984. Low-affinity penicillin-binding protein associated with beta-lactam resistance in *Staphylococcus aureus*. J Bacteriol 158:513–6.

46. Wu SW, de Lencastre H, Tomasz A. 2001. Recruitment of the *mecA* gene homologue of *Staphylococcus sciuri* into a resistance determinant and expression of the resistant phenotype in *Staphylococcus aureus*. J Bacteriol 183:2417–24.

47. Katayama Y, Ito T, Hiramatsu K. 2000. A new class of genetic element, staphylococcus cassette chromosome mec, encodes methicillin resistance in *Staphylococcus aureus*. Antimicrob Agents Chemother 44:1549–55.

48. Tenover FC, Goering R V. 2009. Methicillin-resistant *Staphylococcus aureus* strain USA300: origin and epidemiology. J Antimicrob Chemother 64:441–446.

49. Tenover FC, McDougal LK, Goering R V, Killgore G, Projan SJ, Patel JB, Dunman PM. 2006. Characterization of a strain of community-associated methicillin-resistant *Staphylococcus aureus* widely disseminated in the United States. J Clin Microbiol 44:108–18.

50. Hageman JC, Patel J, Franklin P, Miscavish K, McDougal L, Lonsway D, Khan FN. 2008. Occurrence of a USA300 vancomycin-intermediate *Staphylococcus aureus*. Diagn Microbiol Infect Dis 62:440–442.

51. Moran GJ, Krishnadasan A, Gorwitz RJ, Fosheim GE, McDougal LK, Carey RB, Talan DA. 2006. Methicillin-resistant *S. aureus* infections among patients in the emergency department. N Engl J Med 355:666–674.

52. McDougal LK, Steward CD, Killgore GE, Chaitram JM, McAllister SK, Tenover FC. 2003. Pulsed-field gel electrophoresis typing of oxacillin-resistant *Staphylococcus aureus* isolates from the United States: establishing a national database. J Clin Microbiol 41:5113–20.

53. Li M, Diep BA, Villaruz AE, Braughton KR, Jiang X, DeLeo FR, Chambers HF, Lu Y, Otto M. 2009. Evolution of virulence in epidemic community-associated methicillin-resistant *Staphylococcus aureus*. Proc Natl Acad Sci 106:5883.

54. Centers for Disease Control and Prevention. 2001. Methicillin-resistant *Staphylococcus aureus* skin or soft tissue infections in a state prison - Mississippi, 2000. MMWR Morb Mortal Wkly Rep 2001.

55. Kazakova S V., Hageman JC, Matava M, Srinivasan A, Phelan L, Garfinkel B, Boo T, McAllister S, Anderson J, Jensen B, Dodson D, Lonsway D, McDougal LK, Arduino M, Fraser VJ, Killgore G, Tenover FC, Cody S, Jernigan DB. 2005. A clone of methicillin-resistant *Staphylococcus aureus* among professional football players. N Engl J Med 352:468–475.

56. Nimmo GR. 2012. USA300 abroad: global spread of a virulent strain of community-associated methicillin-resistant *Staphylococcus aureus*. Clin Microbiol Infect 18:725–734.

57. Carvalho KS, Mamizuka EM, Gontijo Filho PP. 2010. Methicillin/Oxacillin-resistant *Staphylococcus aureus* as a hospital and public health threat in Brazil. Brazilian J Infect Dis 14:71–76.

58. Ender M, McCallum N, Adhikari R, Berger-Bächi B. 2004. Fitness cost of SCC*mec* and methicillin resistance levels in *Staphylococcus aureus*. Antimicrob Agents Chemother 48:2295–7.

59. Diep BA, Stone GG, Basuino L, Graber CJ, Miller A, Etages S des, Jones A, Palazzolo-Ballance AM, Perdreau-Remington F, Sensabaugh GF, DeLeo FR, Chambers HF. 2008. The Arginine Catabolic Mobile Element and Staphylococcal Chromosomal Cassette *mec* linkage: Convergence of virulence and resistance in the USA300 clone of methicillin-resistant *Staphylococcus aureus*. J Infect Dis 197:1523–1530.

60. Planet PJ, LaRussa SJ, Dana A, Smith H, Xu A, Ryan C, Uhlemann A-C, Boundy S, Goldberg J, Narechania A, Kulkarni R, Ratner AJ, Geoghegan JA, Kolokotronis S-O, Prince A. 2013. Emergence of the epidemic methicillin-resistant *Staphylococcus aureus* strain USA300 coincides with horizontal transfer of the arginine catabolic mobile element and *speG*-mediated adaptations for survival on skin. MBio 4:e00889-13.

61. Thurlow LR, Joshi GS, Clark JR, Spontak JS, Neely CJ, Maile R, Richardson AR, Bayles KW, Horswill AR, Kielian T, Al. E. 2013. Functional modularity of the arginine catabolic mobile element contributes to the success of USA300 methicillin-resistant *Staphylococcus aureus*. Cell Host Microbe 13:100–107.

62. Wang C-H, Lin C-Y, Luo Y-H, Tsai P-J, Lin Y-S, Lin MT, Chuang W-J, Liu C-C, Wu J-J. 2005. Effects of oligopeptide permease in group a streptococcal infection. Infect Immun 73:2881–90.

63. Satriano J. 2004. Arginine pathways and the inflammatory response: interregulation of nitric oxide and polyamines: review article. Amino Acids 26:321–329.

64. Gantwerker EA, Hom DB. 2012. Skin: Histology and physiology of wound healing. Clin Plast Surg 39:85–97.

65. Diep BA, Gill SR, Chang RF, Phan TH, Chen JH, Davidson MG, Lin F, Lin J, Carleton HA, Mongodin EF, Sensabaugh GF, Perdreau-Remington F. 2006. Complete genome sequence of USA300, an epidemic clone of community-acquired meticillin-resistant *Staphylococcus aureus*. Lancet 367:731–739.

66. Chambers HF. 2005. Community-associated MRSA — resistance and virulence Converge. N Engl J Med 352:1485–1487.

67. de Haas CJC, Veldkamp KE, Peschel A, Weerkamp F, Van Wamel WJB, Heezius ECJM, Poppelier MJJG, Van Kessel KPM, van Strijp JAG. 2004. Chemotaxis inhibitory protein of *Staphylococcus aureus*, a bacterial antiinflammatory agent. J Exp Med 199:687–95.

68. Li M, Cheung GYC, Hu J, Wang D, Joo H-S, Deleo FR, Otto M. 2010. Comparative

analysis of virulence and toxin expression of global community-associated methicillin-resistant *Staphylococcus aureus* strains. J Infect Dis 202:1866–76.

69. Montgomery CP, Boyle-Vavra S, Adem P, Lee J, Husain A, Clasen J, Daum R. 2008. Comparison of virulence in community-associated methicillin-resistant *Staphylococcus aureus* pulsotypes USA300 and USA400 in a rat model of pneumonia. J Infect Dis 198:561–570.

70. Vandenesch F, Naimi T, Enright MC, Lina G, Nimmo GR, Heffernan H, Liassine N, Bes M, Greenland T, Reverdy M-E, Etienne J. 2003. Community-acquired methicillin-resistant *Staphylococcus aureus* carrying Panton-Valentine leukocidin genes: worldwide emergence. Emerg Infect Dis 9:978–84.

71. Tseng CW, Kyme P, Low J, Rocha MA, Alsabeh R, Miller LG, Otto M, Arditi M, Diep BA, Nizet V, Doherty TM, Beenhouwer DO, Liu GY. 2009. *Staphylococcus aureus* Panton-Valentine leukocidin contributes to inflammation and muscle tissue injury. PLoS One 4:e6387.

72. Cribier B, Prévost G, Couppie P, Finck-Barbançon V, Grosshans E, Piémont Y. 1992. *Staphylococcus aureus* leukocidin: a new virulence factor in cutaneous infections? An epidemiological and experimental study. Dermatology 185:175–80.

73. Wilke GA, Bubeck Wardenburg J. 2010. Role of a disintegrin and metalloprotease 10 in *Staphylococcus aureus* alpha-hemolysin-mediated cellular injury. Proc Natl Acad Sci U S A 107:13473–8.

74. Bantel H, Sinha B, Domschke W, Peters G, Schulze-Osthoff K, Jänicke RU. 2001. alpha-Toxin is a mediator of *Staphylococcus aureus*-induced cell death and activates caspases via the intrinsic death pathway independently of death receptor signaling. J Cell Biol 155:637–48.

75. Bubeck Wardenburg J, Bae T, Otto M, DeLeo FR, Schneewind O. 2007. Poring over pores: α-hemolysin and Panton-Valentine leukocidin in *Staphylococcus aureus* pneumonia. Nat Med 13:1405–1406.

76. Wang R, Braughton KR, Kretschmer D, Bach T-HL, Queck SY, Li M, Kennedy AD, Dorward DW, Klebanoff SJ, Peschel A, DeLeo FR, Otto M. 2007. Identification of novel cytolytic peptides as key virulence determinants for community-associated MRSA. Nat Med 13:1510–1514.

77. Lauderdale KJ, Boles BR, Cheung AL, Horswill AR. 2009. Interconnections between Sigma B, *agr*, and proteolytic activity in *Staphylococcus aureus* biofilm maturation. Infect Immun 77:1623–35.

78. Shaw L, Golonka E, Potempa J, Foster SJ. 2004. The role and regulation of the extracellular proteases of *Staphylococcus aureus*. Microbiology 150:217–228.

79. Massimi I, Park E, Rice K, Müller-Esterl W, Sauder D, McGavin MJ. 2002. Identification

of a novel maturation mechanism and restricted substrate specificity for the SspB cysteine protease of *Staphylococcus aureus*. J Biol Chem 277:41770–41777.

80. Prokešová L, Potužníková B, Potempa J, Zikán J, Radl J, Hachová L, Baran K, Porwit-Bobr Z, John C. 1992. Cleavage of human immunoglobulins by serine proteinase from *Staphylococcus aureus*. Immunol Lett 31:259–265.

81. Potempa J, Dubin A, Korzus G, Travis J. 1988. Degradation of elastin by a cysteine proteinase from *Staphylococcus aureus*. J Biol Chem 263:2664–7.

82. McGavin MJ, Zahradka C, Rice K, Scott JE. 1997. Modification of the *Staphylococcus aureus* fibronectin binding phenotype by V8 protease. Infect Immun 65:2621–8.

83. Karlsson A, Saravia-Otten P, Tegmark K, Morfeldt E, Arvidson S. 2001. Decreased amounts of cell wall-associated protein A and fibronectin-binding proteins in *Staphylococcus aureus sarA* mutants due to up-regulation of extracellular proteases. Infect Immun 69:4742–8.

84. Arsic B, Zhu Y, Heinrichs DE, McGavin MJ. 2012. Induction of the staphylococcal proteolytic cascade by antimicrobial fatty acids in community acquired methicillin resistant *Staphylococcus aureus*. PLoS One 7:e45952.

85. Lindsay JA, Foster SJ. 1999. Interactive regulatory pathways control virulence determinant production and stability in response to environmental conditions in *Staphylococcus aureus*. Mol Gen Genet 262:323–31.

86. Joshi GS, Spontak JS, Klapper DG, Richardson AR. 2011. Arginine catabolic mobile element encoded *speG* abrogates the unique hypersensitivity of *Staphylococcus aureus* to exogenous polyamines. Mol Microbiol 82:9–20.

87. Baze P, Milano G, Verrando P, Renee N, Ortonne JP. 1985. Distribution of polyamines in human epidermis. Br J Dermatol 112:393–396.

88. Elias PM. 2007. The skin barrier as an innate immune element. Semin Immunopathol 29:3–14.

89. Chikakane K, Takahashi H. Measurement of skin pH and its significance in cutaneous diseases. Clin Dermatol 13:299–306.

90. Anderson DS. The acid-base balance of the skin. Br J Dermatol 63:283–96.

91. Wille JJ, Kydonieus A. Palmitoleic acid isomer (C16:1delta6) in human skin sebum is effective against gram-positive bacteria. Skin Pharmacol Appl Skin Physiol 16:176–87.

92. Stefaniak AB, Harvey CJ. 2006. Dissolution of materials in artificial skin surface film liquids. Toxicol In Vitro 20:1265–83.

93. Takigawa H, Nakagawa H, Kuzukawa M, Mori H, Imokawa G. 2005. Deficient

production of hexadecenoic acid in the skin is associated in part with the vulnerability of atopic dermatitis patients to colonization by *Staphylococcus aureus*. Dermatology 211:240–8.

94. Do TQ, Moshkani S, Castillo P, Anunta S, Pogosyan A, Cheung A, Marbois B, Faull KF, Ernst W, Chiang SM, Fujii G, Clarke CF, Foster K, Porter E. 2008. Lipids including cholesteryl linoleate and cholesteryl arachidonate contribute to the inherent antibacterial activity of human nasal fluid. J Immunol 181:4177–87.

95. Xiong Z, Ge S, Chamberlain NR, Kapral FA. 1993. Growth cycle-induced changes in sensitivity of *Staphylococcus aureus* to bactericidal lipids from abscesses. J Med Microbiol 39:58–63.

96. Shryock TR, Kapral FA. 1992. The production of bactericidal fatty acids from glycerides in staphylococcal abscesses. J Med Microbiol 36:288–292.

97. Clarke SR, Mohamed R, Bian L, Routh AF, Kokai-Kun JF, Mond JJ, Tarkowski A, Foster SJ. 2007. The *Staphylococcus aureus* surface protein IsdA mediates resistance to innate defenses of human skin. Cell Host Microbe 1:199–212.

98. King NP, Sakinc T, Ben Zakour NL, Totsika M, Heras B, Simerska P, Shepherd M, Gatermann SG, Beatson SA, Schembri MA. 2012. Characterisation of a cell wall-anchored protein of *Staphylococcus saprophyticus* associated with linoleic acid resistance. BMC Microbiol 12:8.

99. Alnaseri H, Arsic B, Schneider JET, Kaiser JC, Scinocca ZC, Heinrichs DE, McGavin MJ. 2015. Inducible expression of a resistance-nodulation-division-type efflux pump in *Staphylococcus aureus* provides resistance to linoleic and arachidonic acids. J Bacteriol 197:1893–905.

100. Peters JS, Chin C-K. 2003. Inhibition of photosynthetic electron transport by palmitoleic acid is partially correlated to loss of thylakoid membrane proteins. Plant Physiol Biochem 41:117–124.

101. Parsons JB, Yao J, Frank MW, Jackson P, Rock CO. 2012. Membrane disruption by antimicrobial fatty acids releases low-molecular-weight proteins from *Staphylococcus aureus*. J Bacteriol 194:5294–5304.

102. Kapral FA, Smith S, Lal D. 1992. The esterification of fatty acids by *Staphylococcus aureus* fatty acid modifying enzyme (FAME) and its inhibition by glycerides. J Med Microbiol 37:235–237.

103. Piddock LJ V. 2006. Multidrug-resistance efflux pumps - not just for resistance. Nat Rev Microbiol 4:629–636.

104. Fernando DM, Kumar A. 2013. Resistance-nodulation-division multidrug efflux pumps in Gram-negative bacteria: role in virulence. Antibiot (Basel, Switzerland) 2:163–81.

105. Bailo R, Bhatt A, Aínsa JA. 2015. Lipid transport in *Mycobacterium tuberculosis* and its implications in virulence and drug development. Biochem Pharmacol 96:159–167.

106. Li X-Z, Nikaido H. 2009. Efflux-mediated drug resistance in bacteria: an update. Drugs 69:1555–623.

107. Tseng TT, Gratwick KS, Kollman J, Park D, Nies DH, Goffeau A, Saier MH. 1999. The RND permease superfamily: an ancient, ubiquitous and diverse family that includes human disease and development proteins. J Mol Microbiol Biotechnol 1:107–25.

108. Nies DH. 2003. Efflux-mediated heavy metal resistance in prokaryotes. FEMS Microbiol Rev 27:313–39.

109. Ma D, Cook DN, Alberti M, Pon NG, Nikaido H, Hearst JE. 1995. Genes *acrA* and *acrB* encode a stress-induced efflux system of *Escherichia coli*. Mol Microbiol 16:45–55.

110. Poole K, Gotoh N, Tsujimoto H, Zhao Q, Wada A, Yamasaki T, Neshat S, Yamagishi J, Li XZ, Nishino T. 1996. Overexpression of the *mexC-mexD-oprJ* efflux operon in *nfxB*-type multidrug-resistant strains of *Pseudomonas aeruginosa*. Mol Microbiol 21:713–24.

111. Shafer WM, Qu X, Waring AJ, Lehrer RI. 1998. Modulation of *Neisseria gonorrhoeae* susceptibility to vertebrate antibacterial peptides due to a member of the resistance/nodulation/division efflux pump family. Proc Natl Acad Sci USA 95:1829–33.

112. Piddock LJ, White DG, Gensberg K, Pumbwe L, Griggs DJ. 2000. Evidence for an efflux pump mediating multiple antibiotic resistance in *Salmonella* enterica serovar *Typhimurium*. Antimicrob Agents Chemother 44:3118–21.

113. Goel AK, Rajagopal L, Nagesh N, Sonti R V. 2002. Genetic locus encoding functions involved in biosynthesis and outer membrane localization of xanthomonadin in *Xanthomonas oryzae pv. oryzae*. J Bacteriol 184:3539–48.

114. Du D, Wang Z, James NR, Voss JE, Klimont E, Ohene-Agyei T, Venter H, Chiu W, Luisi BF. 2014. Structure of the AcrAB-TolC multidrug efflux pump. Nature 509:512–5.

115. Du D, Voss J, Wang Z, Chiu W, Luisi BF. 2015. The pseudo-atomic structure of an RND-type tripartite multidrug efflux pump. Biol Chem 396:1073–82.

116. Nikaido H. 2011. Structure and mechanism of RND-type multidrug efflux pumps. Adv Enzymol Relat Areas Mol Biol 77:1–60.

117. Eswaran J, Koronakis E, Higgins MK, Hughes C, Koronakis V. 2004. Three's company: component structures bring a closer view of tripartite drug efflux pumps. Curr Opin Struct Biol 14:741–747.

118. Murakami S, Nakashima R, Yamashita E, Yamaguchi A. 2002. Crystal structure of bacterial multidrug efflux transporter AcrB. Nature 419:587–593.

119. Nakashima R, Sakurai K, Yamasaki S, Hayashi K, Nagata C, Hoshino K, Onodera Y, Nishino K, Yamaguchi A. 2013. Structural basis for the inhibition of bacterial multidrug exporters. Nature 500:102–106.

120. Pak JE, Ekendé EN, Kifle EG, O'Connell JD, De Angelis F, Tessema MB, Derfoufi K-M, Robles-Colmenares Y, Robbins RA, Goormaghtigh E, Vandenbussche G, Stroud RM. 2013. Structures of intermediate transport states of ZneA, a Zn(II)/proton antiporter. Proc Natl Acad Sci U S A 110:18484–9.

121. Seeger MA, Schiefner A, Eicher T, Verrey F, Diederichs K, Pos KM. 2006. Structural asymmetry of AcrB trimer suggests a peristaltic pump mechanism. Science (80- ) 313:1295–1298.

122. Murakami S, Nakashima R, Yamashita E, Matsumoto T, Yamaguchi A. 2006. Crystal structures of a multidrug transporter reveal a functionally rotating mechanism. Nature 443:173–179.

123. Seeger MA, von Ballmoos C, Verrey F, Pos KM. 2009. Crucial role of Asp408 in the proton translocation pathway of multidrug transporter AcrB: evidence from site-directed mutagenesis and carbodiimide labeling. Biochemistry 48:5801–5812.

124. Eicher T, Seeger MA, Anselmi C, Zhou W, Brandstatter L, Verrey F, Diederichs K, Faraldo-Gomez JD, Pos KM. 2014. Coupling of remote alternating-access transport mechanisms for protons and substrates in the multidrug efflux pump AcrB. Elife 3.

125. Hobbs EC, Yin X, Paul BJ, Astarita JL, Storz G. 2012. Conserved small protein associates with the multidrug efflux pump AcrB and differentially affects antibiotic resistance. Proc Natl Acad Sci 109:16696–16701.

126. Seeger M, Diederichs K, Eicher T, Brandstatter L, Schiefner A, Verrey F, Pos K. 2008. The AcrB efflux pump: conformational cycling and peristalsis lead to multidrug resistance. Curr Drug Targets 9:729–749.

127. Yen MR, Chen JS, Marquez JL, Sun EI, Saier MH. 2010. Multidrug resistance: phylogenetic characterization of superfamilies of secondary carriers that include drug exporters. Methods Mol Biol 637:47–64.

128. King G, Sharom FJ. 2012. Proteins that bind and move lipids: MsbA and NPC1. Crit Rev Biochem Mol Biol 47:75–95.

129. Chim N, Torres R, Liu Y, Capri J, Batot G, Whitelegge J, Goulding C. 2015. The structure and interactions of periplasmic domains of crucial MmpL membrane proteins from *Mycobacterium tuberculosis*. Chem Biol 22:1098–1107.

130. Sandhu P, Akhter Y. 2015. The internal gene duplication and interrupted coding sequences in the MmpL genes of *Mycobacterium tuberculosis*: Towards understanding the multidrug transport in an evolutionary perspective. Int J Med Microbiol 305:413–423.

131. Bernut A, Viljoen A, Dupont C, Sapriel G, Blaise M, Bouchier C, Brosch R, de Chastellier C, Herrmann J-L, Kremer L. 2016. Insights into the smooth-to-rough transitioning in *Mycobacterium bolletii* unravels a functional Tyr residue conserved in all mycobacterial MmpL family members. Mol Microbiol 99:866–883.

132. Su C-C, Li M, Gu R, Takatsuka Y, McDermott G, Nikaido H, Yu EW. 2006. Conformation of the AcrB multidrug efflux pump in mutants of the putative proton relay pathway. J Bacteriol 188:7290–6.

133. Wells RM, Jones CM, Xi Z, Speer A, Danilchanka O, Doornbos KS, Sun P, Wu F, Tian C, Niederweis M. 2013. Discovery of a siderophore export system essential for virulence of *Mycobacterium tuberculosis*. PLoS Pathog 9:e1003120.

134. Kobayashi K, Tsukagoshi N, Aono R. 2001. Suppression of hypersensitivity of *Escherichia coli acrB* mutant to organic solvents by integrational activation of the *acrEF* operon with the IS1 or IS2 element. J Bacteriol 183:2646–2653.

135. Nishino K, Latifi T, Groisman EA. 2006. Virulence and drug resistance roles of multidrug efflux systems of *Salmonella enterica* serovar Typhimurium. Mol Microbiol 59:126–141.

136. Deshayes C, Bach H, Euphrasie D, Attarian R, Coureuil M, Sougakoff W, Laval F, Av-Gay Y, Daffe M, Etienne G, Reyrat J-M. 2010. MmpS4 promotes glycopeptidolipids biosynthesis and export in *Mycobacterium smegmatis*. Mol Microbiol 78:989–1003.

137. Domenech P, Reed MB, Barry CE, III. 2005. Contribution of the *Mycobacterium tuberculosis* MmpL protein family to virulence and drug resistance. Infect Immun 73:3492–501.

138. Pacheco SA, Hsu F-F, Powers KM, Purdy GE. 2013. MmpL11 protein transports mycolic acid-containing lipids to the mycobacterial cell wall and contributes to biofilm formation in *Mycobacterium smegmatis*. J Biol Chem 288:24213–24222.

139. Seeliger JC, Holsclaw CM, Schelle MW, Botyanszki Z, Gilmore SA, Tully SE, Niederweis M, Cravatt BF, Leary JA, Bertozzi CR. 2012. Elucidation and chemical modulation of sulfolipid-1 biosynthesis in *Mycobacterium tuberculosis*. J Biol Chem 287:7990–8000.

140. Carel C, Nukdee K, Cantaloube S, Bonne M, Diagne CT, Laval F, Daffé M, Zerbib D. 2014. *Mycobacterium tuberculosis* proteins involved in mycolic acid synthesis and transport localize dynamically to the old growing pole and septum. PLoS One 9:e97148.

141. Fernández-Moreno MA, Caballero JL, Hopwood DA, Malpartida F. 1991. The *act* cluster contains regulatory and antibiotic export genes, direct targets for translational control by the *bldA* tRNA gene of *Streptomyces*. Cell 66:769–80.

142. Kearns DB, Chu F, Rudner R, Losick R. 2004. Genes governing swarming in *Bacillus subtilis* and evidence for a phase variation mechanism controlling surface motility. Mol Microbiol 52:357–369.

143. Quiblier C, Zinkernagel AS, Schuepbach RA, Berger-Bächi B, Senn MM. 2011. Contribution of SecDF to *Staphylococcus aureus* resistance and expression of virulence factors. BMC Microbiol 11:72.

144. Quiblier C, Seidl K, Roschitzki B, Zinkernagel AS, Berger-Bachi B, Senn MM. 2013. Secretome analysis defines the major role of SecDF in *Staphylococcus aureus* virulence. PLoS One 8:e63513.

145. Kelley LA, Mezulis S, Yates CM, Wass MN, Sternberg MJE. 2015. The Phyre2 web portal for protein modeling, prediction and analysis. Nat Protoc 10:845–858.

146. Novick RP. 1991. Genetic systems in staphylococci. Methods Enzymol 204:587–636.

147. Schneider JET. 2015. Investigating the regulation of a fatty acid efflux pump in methicillin resistant *Staphylococcus aureus*. Electron Thesis Diss Repos 3298.

148. Mesak LR, Yim G, Davies J. 2009. Improved lux reporters for use in *Staphylococcus aureus*. Plasmid 61:182–187.

149. Bae T, Schneewind O. 2006. Allelic replacement in *Staphylococcus aureus* with inducible counter-selection. Plasmid 55:58–63.

150. Bateman BT, Donegan NP, Jarry TM, Palma M, Cheung AL. 2001. Evaluation of a tetracycline-inducible promoter in *Staphylococcus aureus in vitro* and *in vivo* and its application in demonstrating the role of *sigB* in microcolony formation. Infect Immun 69:7851–7.

151. Maniatis T, Fritsch EF, Sambrook J. 1983. Molecular Cloning. A Laboratory Manual. Cold Spring Harbor Laboratory, New York.

152. Cleveland DW, Fischer SG, Kirschner MW, Laemmli UK. 1977. Peptide mapping by limited proteolysis in sodium dodecyl sulfate and analysis by gel electrophoresis. J Biol Chem 252:1102–6.

153. Towbin H, Staehelin T, Gordon J. 1979. Electrophoretic transfer of proteins from polyacrylamide gels to nitrocellulose sheets: procedure and some applications. Proc Natl Acad Sci U S A 76:4350–4.

154. Sen S, Sirobhushanam S, Johnson SR, Song Y, Tefft R, Gatto C, Wilkinson BJ. 2016. Growth-environment dependent modulation of *Staphylococcus aureus* branched-chain to straight-chain fatty acid ratio and incorporation of unsaturated fatty acids. PLoS One 11:e0165300.

155. Gründling A, Missiakas DM, Schneewind O. 2006. *Staphylococcus aureus* mutants with increased lysostaphin resistance. J Bacteriol 188:6286–97.

156. Morikawa K, Maruyama A, Inose Y, Higashide M, Hayashi H, Ohta T. 2001. Overexpression of sigma factor, sigma(B), urges *Staphylococcus aureus* to thicken the cell

wall and to resist β-lactams. Biochem Biophys Res Commun 288:385–389.

157. Bera A, Biswas R, Herbert S, Kulauzovic E, Weidenmaier C, Peschel A, Götz F. 2007. Influence of wall teichoic acid on lysozyme resistance in *Staphylococcus aureus*. J Bacteriol 189:280–3.

158. Bera A, Herbert S, Jakob A, Vollmer W, Gotz F. 2005. Why are pathogenic staphylococci so lysozyme resistant? The peptidoglycan O-acetyltransferase OatA is the major determinant for lysozyme resistance of *Staphylococcus aureus*. Mol Microbiol 55:778–787.

159. Muthaiyan A, Silverman JA, Jayaswal RK, Wilkinson BJ. 2008. Transcriptional profiling reveals that daptomycin induces the *Staphylococcus aureus* cell wall stress stimulon and genes responsive to membrane depolarization. Antimicrob Agents Chemother 52:980–90.

160. Reynolds PE, Somner EA. 1990. Comparison of the target sites and mechanisms of action of glycopeptide and lipoglycodepsipeptide antibiotics. Drugs Exp Clin Res 16:385–9.

161. Walsh C. 1999. Deconstructing vancomycin. Science 284:442–3.

162. Howden BP, Davies JK, Johnson PDR, Stinear TP, Grayson ML. 2010. Reduced vancomycin susceptibility in *Staphylococcus aureus*, including vancomycin-intermediate and heterogeneous vancomycin-intermediate strains: resistance mechanisms, laboratory detection, and clinical implications. Clin Microbiol Rev 23:99–139.

163. Quiblier C, Luczak-Kadlubowska A, Holdener E, Alborn D, Schneider T, Wiedemann I, Pinho M, Sahl H-G, Rohrer S, Berger-Bächi B, Senn M. 2013. The *Staphylococcus aureus* membrane protein SA2056 interacts with peptidoglycan synthesis enzymes. Antibiotics 2:11–27.

164. Alvarez-Ortega C, Olivares J, Martínez JL. 2013. RND multidrug efflux pumps: what are they good for? Front Microbiol 4:7.

165. Ray B, Ballal A, Manna AC. 2009. Transcriptional variation of regulatory and virulence genes due to different media in *Staphylococcus aureus*. Microb Pathog 47:94–100.

166. Oogai Y, Matsuo M, Hashimoto M, Kato F, Sugai M, Komatsuzawa H. 2011. Expression of virulence factors by *Staphylococcus aureus* grown in serum. Appl Environ Microbiol 77:8097–8105.

167. Sen S, Sirobhushanam S, Johnson SR, Song Y, Tefft R, Gatto C, Wilkinson BJ. 2016. Growth-environment dependent modulation of *Staphylococcus aureus* branched-chain to straight-chain fatty acid ratio and incorporation of unsaturated fatty acids. PLoS One 11:e0165300.

168. Halsey CR, Lei S, Wax JK, Lehman MK, Nuxoll AS, Steinke L, Sadykov M, Powers R, Fey PD. 2017. Amino acid catabolism in *Staphylococcus aureus* and the function of carbon catabolite repression. MBio 8:e01434-16.

169. Huang Y-W, Liou R-S, Lin Y-T, Huang H-H, Yang T-C. 2014. A linkage between SmeIJK efflux Pump, cell envelope integrity, and σE-mediated envelope stress response in *Stenotrophomonas maltophilia*. PLoS One 9:e111784.

170. Browder HP, Zygmunt WA, Young JR, Tavormina PA. 1965. Lysostaphin: Enzymatic mode of action. Biochem Biophys Res Commun 19:383–9.

171. Cui L, Ma X, Sato K, Okuma K, Tenover FC, Mamizuka EM, Gemmell CG, Kim M-N, Ploy M-C, El-Solh N, Ferraz V, Hiramatsu K. 2003. Cell wall thickening is a common feature of vancomycin resistance in *Staphylococcus aureus*. J Clin Microbiol 41:5–14.

172. Breukink E, Wiedemann I, van Kraaij C, Kuipers OP, Sahl HG, de Kruijff B. 1999. Use of the cell wall precursor lipid II by a pore-forming peptide antibiotic. Science 286:2361–4.

173. Sieradzki K, Pinho MG, Tomasz A. 1999. Inactivated *pbp4* in highly glycopeptide-resistant laboratory mutants of *Staphylococcus aureus*. J Biol Chem 274:18942–6.

174. Hiramatsu K. 2001. Vancomycin-resistant *Staphylococcus aureus*: a new model of antibiotic resistance. Lancet Infect Dis 1:147–155.

175. Prats R, de Pedro MA. 1989. Normal growth and division of *Escherichia coli* with a reduced amount of murein. J Bacteriol 171:3740–5.

176. Keshav S, Chung P, Milon G, Gordon S. 1991. Lysozyme is an inducible marker of macrophage activation in murine tissues as demonstrated by in situ hybridization. J Exp Med 174:1049–58.

177. Fahlgren A, Hammarström S, Danielsson A, Hammarström M-L. 2003. Increased expression of antimicrobial peptides and lysozyme in colonic epithelial cells of patients with ulcerative colitis. Clin Exp Immunol 131:90–101.

178. Blake CC, Johnson LN, Mair GA, North AC, Phillips DC, Sarma VR. 1967. Crystallographic studies of the activity of hen egg-white lysozyme. Proc R Soc London Ser B, Biol Sci 167:378–88.

179. Reed P, Atilano ML, Alves R, Hoiczyk E, Sher X, Reichmann NT, Pereira PM, Roemer T, Filipe SR, Pereira-Leal JB, Ligoxygakis P, Pinho MG. 2015. *Staphylococcus aureus* survives with a minimal peptidoglycan synthesis machine but sacrifices virulence and antibiotic resistance. PLOS Pathog 11:e1004891.

180. Poole K. 2008. Bacterial multidrug efflux pumps serve other functions. Microbe 3:179–185.

181. Eaves DJ, Ricci V, Piddock LJ V. 2004. Expression of *acrB, acrF, acrD, marA*, and *soxS* in *Salmonella enterica* serovar Typhimurium: role in multiple antibiotic resistance. Antimicrob Agents Chemother 48:1145–50.

182. Blair JMA, Smith HE, Ricci V, Lawler AJ, Thompson LJ, Piddock LJ V. 2015.

Expression of homologous RND efflux pump genes is dependent upon AcrB expression: implications for efflux and virulence inhibitor design. J Antimicrob Chemother 70:424–31.

183. Wells RM, Jones CM, Xi Z, Speer A, Danilchanka O, Doornbos KS, Sun P, Wu F, Tian C, Niederweis M. 2013. Discovery of a siderophore export system essential for virulence of *Mycobacterium tuberculosis*. PLoS Pathog 9:e1003120.

184. Parsons JB, Broussard TC, Bose JL, Rosch JW, Jackson P, Subramanian C, Rock CO. 2014. Identification of a two-component fatty acid kinase responsible for host fatty acid incorporation by *Staphylococcus aureus*. Proc Natl Acad Sci 111:10532–10537.

185. Garlid KD, Orosz DE, Modrianský M, Vassanelli S, Jezek P. 1996. On the mechanism of fatty acid-induced proton transport by mitochondrial uncoupling protein. J Biol Chem 271:2615–20.

186. Kenny JG, Ward D, Josefsson E, Jonsson I-M, Hinds J, Rees HH, Lindsay JA, Tarkowski A, Horsburgh MJ. 2009. The *Staphylococcus aureus* response to unsaturated long chain free catty acids: Survival mechanisms and virulence implications. PLoS One 4:e4344.

187. Desbois AP, Smith VJ. 2010. Antibacterial free fatty acids: activities, mechanisms of action and biotechnological potential. Appl Microbiol Biotechnol 85:1629–1642.

188. Chamberlain NR, Mehrtens BG, Xiong Z, Kapral FA, Boardman JL, Rearick JI. 1991. Correlation of carotenoid production, decreased membrane fluidity, and resistance to oleic acid killing in *Staphylococcus aureus* 18Z. Infect Immun 59:4332–7.

189. Adebusuyi AA, Foght JM. 2011. An alternative physiological role for the EmhABC efflux pump in *Pseudomonas fluorescens* cLP6a. BMC Microbiol 11:834–843.

# Curriculum Vitae

| | |
|---|---|
| **Name:** | Jamie N. Halucha |
| **Post-secondary Education and Degrees:** | M.Sc. in Microbiology and Immunology, 2017<br>Western University, London, ON Canada<br>B.Sc. (Honours), 2015<br>Brock University, St. Catharines, ON Canada |
| **Honours and Awards:** | Dr. FW Luney Graduate Travel Award in Microbiology and Immunology, 2017<br>Dr. RGE Murray Graduate Scholarship in Microbiology and Immunology, 2016-2017<br>Infection and Immunity Research Forum Poster Presentation Award (Graduate <6 months), 2015<br>Dr. FW Luney Graduate Entrance Scholarship in Microbiology and Immunology, 2015 |
| **Related Work Experience:** | Teaching Assistant, 2016-2017<br>Western University, London ON Canada |
| **Committee Memberships:** | Infection and Immunity Research Forum Organizing Committee, 2015-2016 |

**Presentations:**

Functional relationships of RND efflux pumps in *Staphylococcus aureus*. Canadian Society of Microbiologists 67th Annual Conference. Oral Presentation. June 22, 2017. London, ON Canada

Functional relationships of RND efflux pumps in *Staphylococcus aureus*. Canadian Society of Microbiologists 67th Annual Conference. Poster Presentation. June 22, 2017. London, ON Canada

Functional relationships of RND efflux pumps in *Staphylococcus aureus*. London Health Research Day. Poster Presentation. March 28, 2017. London, ON Canada

Structure-function relationships of RND efflux pumps in *Staphylococcus aureus*. 11th Annual Infection and Immunity Research Forum. Poster Presentation. September 23, 2016. London, ON Canada

Function and cellular localization of RND efflux pumps in *Staphylococcus aureus*. London Health Research Day. Poster Presentation. March 29, 2016. London, ON Canada

Function and cellular localization of RND efflux pumps in *Staphylococcus aureus*. 10th Annual Infection and Immunity Research Forum. Poster Presentation. November 6, 2015. London, ON Canada